

# **HSP90-MEDIATED MATURATION OF KINASES AND NUCLEAR STEROID HORMONE RECEPTORS**

A Dissertation Presented

By

NATALIE WAYNE PURSELL

Submitted to the Faculty of the  
University of Massachusetts Graduate School of Biomedical Sciences, Worcester  
in partial fulfillment of the requirements for the degree of

DOCTOR OF PHILOSOPHY

APRIL 28, 2011

BIOCHEMISTRY AND MOLECULAR PHARMACOLOGY

**HSP90-MEDIATED MATURATION OF KINASES AND NUCLEAR  
STEROID HORMONE RECEPTORS**

A Dissertation Presented

By

NATALIE WAYNE PURSELL

The signatures of the Dissertation Defense Committee signifies  
completion and approval as to style and content of the Dissertation

Daniel Bolon, Ph.D., Thesis Advisor

Reid Gilmore, Ph.D., Member of Committee

C. Robert Matthews, Ph.D., Member of Committee

Peter Pryciak, Ph.D., Member of Committee

Jeffrey Brodsky, Ph.D., Member of Committee

The signature of the Chair of the Committee signifies that the written dissertation meets  
the requirements of the Dissertation Committee

Anthony Carruthers, Ph.D., Chair of Committee

The signature of the Dean of the Graduate School of Biomedical Sciences signifies  
that the student has met all graduation requirements of the school.

Anthony Carruthers, Ph.D.,  
Dean of the Graduate School of Biomedical Sciences

Biochemistry and Molecular Pharmacology

April 28, 2011

## **DEDICATION**

To my family for their unconditional love and support always.

## **ACKNOWLEDGMENTS**

First, I would like to thank my thesis advisor, Dan Bolon, for his support, encouragement, and patience. His direction guided this work and helped me develop critical thinking, writing and presentation skills during my time in his lab. I would also like to thank members of my committee Tony Carruthers, Reid Gilmore, Bob Matthews, Peter Pryciak, and Mary Munson for their feedback and suggestions through the duration of my thesis research and Jeff Brodsky for serving as external committee member for my thesis defense.

I would also like to thank the members of the Department of Biochemistry as a whole for helpful suggestions and support throughout my thesis work. This is a great department to work in and has made for an educational and enjoyable graduate experience.

Finally, I would like to thank my friends and family for their love, patience, and support during my graduate years. To my parents, Chuck and Judy Wayne, and my sister Nancy thank you for always supporting and believing in me. To my husband Bryan, thank you for your love and constant support.

## ABSTRACT

Among heat shock proteins, Hsp90 is unusual because it is not required for the proper folding of most cellular proteins but rather is disproportionally linked to the activation of signal transduction proteins including over forty kinases and many steroid hormone receptors. Mutated forms of many Hsp90 clients are causative agents in cancer, making Hsp90 a promising pharmacological target. Many small molecular inhibitors have been identified that competitively bind to the ATP binding site of Hsp90, some of which are in clinical trials as anticancer agents. Although the activation of kinase and hormone receptor clients by Hsp90 and its co-chaperones has been extensively studied, the molecular mechanism of client protein activation is poorly understood.

Hsp90 is a dimeric chaperone containing three domains: the N-terminal (N) and middle (M) domains contribute directly to ATP binding and hydrolysis and the C-terminal (C) domain mediates dimerization. At physiological concentration, Hsp90 predominantly forms dimers, but the possibility that full-length monomers might also function in cells has not been tested. In Chapter 3, we used a single-chain strategy to design a full-length Hsp90 monomer (NMCC). The resulting construct was predominantly monomeric at physiological concentration and did not function to support yeast viability as the sole Hsp90. NMCC Hsp90 was also defective at ATP hydrolysis and the activation of kinase and steroid hormone receptor clients in yeast cells. The ability to support yeast growth was rescued by the addition of a coiled-coil dimerization

domain, indicating that the parental single-chain construct is functionally defective because it is monomeric.

After finding that a full-length Hsp90 monomer containing only one ATPase site was unable to support yeast viability or activate Hsp90 clients, we set out to further explore the role of ATPase activity in client protein activation. Approximately 10 % of the yeast proteome binds to Hsp90 making it important to study Hsp90 function in the cellular environment where all binding partners are present. In Chapter 4, we observed that co-expression of different Hsp90 subunits in *Saccharomyces cerevisiae* caused unpredictable synthetic growth defects due to cross-dimerization. We engineered super-stabilized Hsp90 dimers that resisted cross-dimerization with endogenous Hsp90 and alleviated the synthetic growth defect. We utilized these super-stabilized dimers to analyze the ability of ATPase mutant homodimers to activate known Hsp90 client proteins in yeast cells. We found that ATP binding and hydrolysis by Hsp90 are both required for the efficient maturation of the glucocorticoid hormone receptor (GR) and v-src confirming the critical role of ATP hydrolysis in the maturation of steroid hormone receptors and kinases *in vivo*.

In addition to its role in the activation of signal transduction client proteins, Hsp90 has been shown to suppress the *in vitro* aggregation of numerous hard-to-fold proteins. In Chapter 5, we examine the role of charge in Hsp90 anti-aggregation activity.

The charge on Hsp90 is largely concentrated in two highly acidic regions. We found that deletion of both charge-rich regions dramatically impaired Hsp90 anti-aggregation activity. Addition of an acid-rich region with a distinct amino acid sequence to our double-deleted Hsp90 construct rescued the anti-aggregation activity of Hsp90 indicating that the net charge contributes to its anti-aggregation activity.

The *in vitro* anti-aggregation activity of Hsp90 studied in Chapter 5 occurs in the absence of ATP. However, all of the biologically important functions of Hsp90 in cells identified to date, including the maturation of kinases and nuclear steroid hormone receptors, clearly require ATP hydrolysis. Why does Hsp90 robustly hinder the aggregation of hard-to-fold proteins without ATP *in vitro*, but *in vivo* uses ATP hydrolysis for all of its essential functions? By utilizing separation of function Hsp90 variants (that specifically lack *in vitro* anti-aggregation activity) we have begun to address this question. We find that anti-aggregation deficient Hsp90 is unable to support yeast growth under stressful conditions, potentially due to reduced cellular expression. Interestingly, the ATP-independent anti-aggregation activity of Hsp90 has no measureable impact on cellular function. Thus, hindering the aggregation of most hard-to-fold proteins by Hsp90 (independent of ATP hydrolysis) does not appear to be important for cell function. These results suggest a cellular model where the Hsp40/60/70 machinery is responsible for hindering the aggregation of most hard-to-fold proteins

while Hsp90 assists in the maturation of a select set of clients in an ATP-dependent fashion, potentially aided by its inherent anti-aggregation properties.



## TABLE OF CONTENTS

Dedication	iii
Acknowledgements	iv
Abstract	v
Table of Contents	ix
List of Tables	xii
List of Figures	xiii
List of Abbreviations	xvi
 CHAPTER I: Introduction	 1
Steroid hormone receptor Hsp90 clients	13
Kinase clients of Hsp90	15
Non-signal transduction Hsp90 clients	19
Questions addressed in this thesis	22
 CHAPTER II: Methods	 27
Plasmid construction	28
Protein production	29
Circular dichroism	30
Urea denaturation	31
Analytical ultracentrifugation	32
Analytical size exclusion chromatography	33
Enzymatically coupled ATPase assay	33
Subunit mixing analysis	34
Fluorescent GA binding	34
Sole Hsp90 in yeast	35
v-src assay	37
GR assay	38
Sequence-based analysis of charge conservation	39
<i>In vitro</i> aggregation assays	40
Analysis of protein aggregates	42
Cellular accumulation of yeast kinases	42
Identification of peptide substrates for yeast kinases	43
Kinase assays	45

CHAPTER III: Dimerization of Hsp90 is required for <i>in vivo</i> function	46
Abstract	47
Introduction	48
Results	52
<i>C domain has marginal stability to urea denaturation.</i>	52
<i>Isolated single-chain C domain is stable and monomeric.</i>	55
<i>Full-length NMCC monomer design is deficient for ATP hydrolysis.</i>	59
<i>Function of NMCC in vivo.</i>	66
<i>Activation of v-src and GR in vivo.</i>	72
<i>NMCC function is rescued by addition of a coiled-coil dimerization motif.</i>	77
Discussion	80
Conclusions	84
CHAPTER IV: Hsp90 ATPase activity is required for <i>in vivo</i> function	85
Abstract	86
Introduction	87
Results	89
<i>Cross-dimers of Hsp90 have unpredictable functions.</i>	89
<i>Super-stabilization strategy to hinder cross-dimerization.</i>	92
<i>The coiled-coil super-stabilizes Hsp90 dimers.</i>	92
<i>The coiled-coil is compatible with Hsp90 function.</i>	95
<i>Super-stabilization leads to preferential homodimer assembly.</i>	98
<i>NMCcoil<sup>D79N</sup> rescues growth when co-expressed with ts NMC<sup>G170D</sup>.</i>	101
<i>ATPase-deficient Hsp90 mutants function at elevated temperature.</i>	102
<i>Maturation of v-src.</i>	105
<i>Glucocorticoid receptor (GR) activation.</i>	108
<i>Hsp90 dimers constitute the essential biological oligomer.</i>	108
Discussion	115
CHAPTER V: Charge-rich regions modulate the anti-aggregation activity of Hsp90	121
Abstract	122
Introduction	123
Results	125

<i>Negative charge is a common feature of molecular chaperones.</i>	125
<i>The charge-rich regions of Hsp90 influence anti-aggregation activity.</i>	133
<i>The anti-aggregation activity of <math>\Delta CL\Delta CX</math> can be rescued by an exogenous acid-rich region.</i>	151
Discussion	151
CHAPTER VI: Investigating the role of Hsp90 anti-aggregation activity <i>in vivo</i>	158
Abstract	159
Introduction	160
Results	161
<i>Hsp90 anti-aggregation activity is required for yeast growth under stressful conditions.</i>	161
<i>ATP-independent anti-aggregation activity of Hsp90 is not sufficient for cell function.</i>	172
Discussion	177
CHAPTER VII: Discussion and Future Directions	184
Conclusion	196
APPENDIX I: Chaperoning of yeast kinsases by Hsp90	197
Introduction	198
Results	199
<i>Hsp90 is important for kinase accumulation in yeast cells.</i>	199
<i>Role of Hsp90 in kinase activation.</i>	203
Discussion and Future Directions	213
BIBLIOGRAPHY	216

## LIST OF TABLES

Table 1.1	Classes of Hsp90 clients.	12
Table 5.1	Charge conservation of select cytoplasmic proteins.	126
Table 5.2	Protein charge analysis of select cytoplasmic proteins.	127
Table 5.3	Midpoint concentrations of urea required to denature Hsp90.	143
Table 7.1	Protein charge analysis of select Hsp90 anti-aggregation substrates.	190
Table 7.2	Protein charge analysis of small heat shock proteins.	192
Table 7.3	Protein charge analysis of Hsp110 chaperone.	193
Table A.1	Yeast kinases used in this study.	200
Table A.2	Yeast kinase domain constructs.	204
Table A.3	Potential peptide substrates for select <i>S. cerevisiae</i> kinases.	210

## LIST OF FIGURES

Figure 1.1	Crystal Structure of Hsp90 dimer.	5
Figure 1.2	Model of the ATPase driven conformational cycle of Hsp90 that leads to client maturation.	8
Figure 3.1	Design strategy.	51
Figure 3.2	Single-chain C-domains are increased in stability and monomeric.	54
Figure 3.3	Biophysical properties of C domain constructs.	58
Figure 3.4	Full-length NMCC construct is predominantly monomeric and is defective for ATP hydrolysis.	62
Figure 3.5	Equilibrium analytical ultracentrifugation of wild-type Hsp90.	64
Figure 3.6	NMCC protein accumulates to similar levels as wild-type Hsp90 and does not prevent growth when wild-type Hsp90 is present.	69
Figure 3.7	NMCC as the sole Hsp90 does not support yeast viability.	71
Figure 3.8	Experimental setup to analyze client protein activity in Hsp90 <sup>ts</sup> yeast.	74
Figure 3.9	In yeast cells, NMCC does not aid in the activation of v-src or GR.	76
Figure 3.10	Dimerization of NMCCcoil rescues <i>in vitro</i> and <i>in vivo</i> function.	79
Figure 4.1	Co-expression of different NMC Hsp90 variants <i>in vivo</i> leads to the formation of cross-dimers with unpredictable function.	91
Figure 4.2	Superstabilization strategy is compatible with Hsp90 function.	94
Figure 4.3	Superstabilized NMCcoil is dimeric.	97
Figure 4.4	Superstabilization disfavors cross-dimerization.	100
Figure 4.5	Hsp90 ATPase mutants are stable at 37 °C.	104
Figure 4.6	ATPase deficient NMCcoil variants are unable to mature v-src kinase in yeast.	107
Figure 4.7	Hsp90 ATPase mutants do not mature GR in yeast.	110
Figure 4.8	Dimers of Hsp90 constitute the essential biological oligomer whose ATPase function is required for maturation of clients.	112
Figure 4.9	Subunit exchange of Hsp90 dimers.	114

Figure 4.10	Molecular image of the C-domain interface of Hsp90.	118
Figure 5.1	Hsp90 constructs to test the role of charge-rich regions in anti-aggregation activity.	130
Figure 5.2	Hydrophobicity plot for Hsp90.	132
Figure 5.3	Suppression of CFTR-NBD1 and CS aggregation by Hsp90.	135
Figure 5.4	Charge-rich regions influence the anti-aggregation activity of Hsp90.	137
Figure 5.5	Solubility of wild-type and $\Delta\text{CL}\Delta\text{CX}$ Hsp90.	139
Figure 5.6	Deletion of charge-rich regions does not disrupt the Hsp90 dimer or essential function.	142
Figure 5.7	Mechanistic model of charge-dependent anti-aggregation activity of Hsp90.	146
Figure 5.8	Charge-dependent anti-aggregation activity of Hsp90.	149
Figure 5.9	The anti-aggregation activity of $\Delta\text{CL}\Delta\text{CX}$ Hsp90 was rescued by an exogenous acid-rich region.	153
Figure 5.10	Biochemical analysis of CR Hsp90.	155
Figure 6.1	Hsp90 anti-aggregation activity is not required for the essential function of Hsp90 in yeast.	163
Figure 6.2	Hsp90 anti-aggregation activity is required for yeast growth under stressful conditions.	166
Figure 6.3	Reducing cellular expression levels of Hsp90 impairs cell function.	168
Figure 6.4	How does the expression level of $\Delta\text{CL}\Delta\text{CX}$ Hsp90 compare to different expression levels of wild-type Hsp90?	171
Figure 6.5	$\Delta\text{CL}\Delta\text{CX}$ Hsp90 can be expressed at wild-type levels.	174
Figure 6.6	Reduced expression of anti-aggregation deficient $\Delta\text{CL}\Delta\text{CX}$ Hsp90 is not responsible for the growth defect observed at 37 °C.	176
Figure 6.7	The ATP-independent anti-aggregation activity of Hsp90 is not sufficient for cell function.	179
Figure 7.1	R380A Hsp90 can activate GR but not v-src in yeast.	188
Figure A.1	Hsp90 influences the cellular accumulation of numerous yeast kinases.	202
Figure A.2	Identification of peptide substrates for yeast kinases.	206

Figure A.3	Phosphorylation of select peptide substrates for yeast kinases.	208
Figure A.4	Example gel shift experiments to monitor peptide phosphorylation.	212

## LIST OF ABBREVIATIONS

Heat Shock Protein 90	Hsp90
Heat Shock Factor 1	HSF1
N-terminal domain	N domain
Middle domain	M domain
C-terminal	C domain
Geldanamycin	GA
Progesterone Receptor	PR
Glucocorticoid Receptor	GR
Co-immunoprecipitation	co-IP
Cystic Fibrosis Transductance Regulator	CFTR
Nucleotide Binding Domain of CFTR	CFTR-NBD1
Citrate Synthase	CS
Circular dichroism	CD
BODIPY-GA	BDGA
5-Fluoroorotic Acid	5-FOA
$\beta$ -galactosidase	$\beta$ -gal
Deoxycorticosterone	DOCS
Analytical Ultracentrifugation	AUC
Temperature Sensitive	ts
Temperature Sensitive (G170D) Hsp90	Hsp90 <sup>ts</sup>
Glucocorticoid Response Elements	GRE's
Charged linker	CL
C-terminal extension	CX
Charge rescue	CR
Standard Deviation	SD
Standard Error of the Mean	SEM



# CHAPTER I

## Introduction

This work was previously submitted for publication as:

Natalie Wayne<sup>\*</sup>, Parul Mishra<sup>\*</sup>, and Daniel N. Bolon. (Submitted) Hsp90 and Client Protein Maturation. *Methods in Molecular Biology*.

<sup>\*</sup>These authors contributed equally to this work.

Hsp90, as with most heat shock proteins, was initially identified from changes in transcriptional pattern (1) and relative translational rate (2) upon shifting cells to elevated temperature. Hsp90 is named for its induction in response to temperature stress as well as its molecular weight of approximately 90 kilodaltons. Elevated temperature challenges the ability of proteins to fold efficiently, placing an elevated burden on cellular chaperones. In response to elevated temperature and many other stressful conditions, eukaryotes induce expression of the heat shock factor 1 (HSF1) transcription factor that in turn up-regulates expression of chaperones including Hsp90 (3). Many eukaryotes including budding yeast and humans have two genes encoding Hsp90 that encode nearly identical amino-acid sequences, one of which is constitutively expressed, while the other is HSF1 inducible (4). The constitutive expression level of Hsp90 under non-stress conditions is very high and Hsp90 is one of the most abundant proteins in the cell, accumulating primarily in the cytosol (5). The high expression level of Hsp90 in the absence of stress is consistent with its requirement for the activity of many critical signal transduction clients in eukaryotes. Hsp90 is essential for viability in eukaryotes (4). In bacteria, which lack the wealth of signal transduction proteins present in eukaryotes, Hsp90 knockouts are viable (6).

The Hsp90 chaperone is highly conserved in eukaryotes both at the level of amino-acid sequence and biochemical function. The *Saccharomyces cerevisiae* and human Hsp90 proteins are 59 % identical in amino acid sequence alignments. The

conservation of Hsp90 in eukaryotes extends to the functional level as *S. cerevisiae* with both endogenous Hsp90 genes knocked out can be rescued by expression of human Hsp90 (7). Hsp90 serves as a protein interaction hub, binding to about 10 % of the yeast proteome (8) including many co-chaperones necessary for client maturation. The observation that human Hsp90 complements *S. cerevisiae* knockouts indicates that essential elements of this hub are evolutionarily conserved. Consistent with the functional conservation of Hsp90, steroid hormone receptors that are not natural to *S. cerevisiae* function in an Hsp90-dependent manner when introduced into yeast (7).

Hsp90 contains three domains: the N-terminal (N) domain, middle (M) domain, and the C-terminal (C) domain (Figure 1.1). Crystal structure analysis of complexes between the N-domain of yeast Hsp90 and either ADP or ATP identified an adenine nucleotide binding site homologous to the ATP-binding site of the DNA gyrase B (9-11). Although fully able to bind ATP, isolated N-domain Hsp90 constructs have negligible ATPase activity indicating the involvement of other domains in the ATPase cycle. Several conserved amino acids in the N-domain make up a molecular “lid” that closes over the nucleotide-binding pocket in the ATP-bound, but not ADP-bound, state (12). Structural and biochemical studies demonstrate that Hsp90 is a “split” ATPase with catalytic amino acids from both the N (E33) and M (R380) domains in the same molecule contributing to hydrolysis (10, 13, 14). The C-domain forms a stable dimer (15).

**Figure 1.1. Crystal structure of Hsp90 dimer (10).**

Hsp90 is a homodimeric protein consisting of an N-terminal nucleotide binding domain, middle domain, and C-terminal dimerization domain.

## Hsp90 dimer

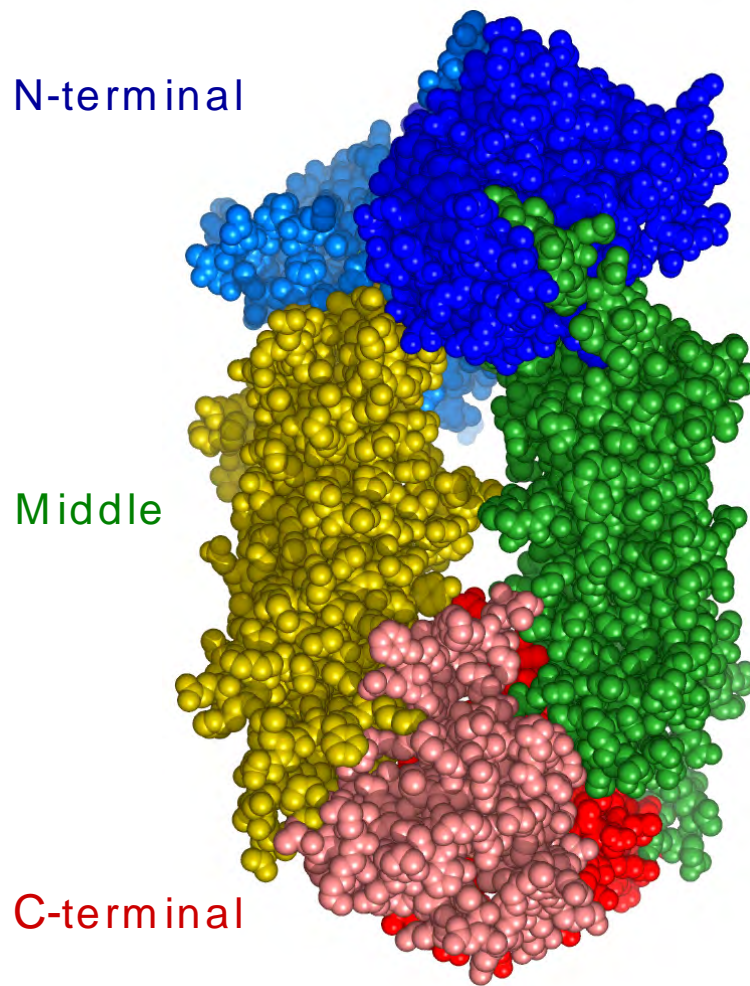


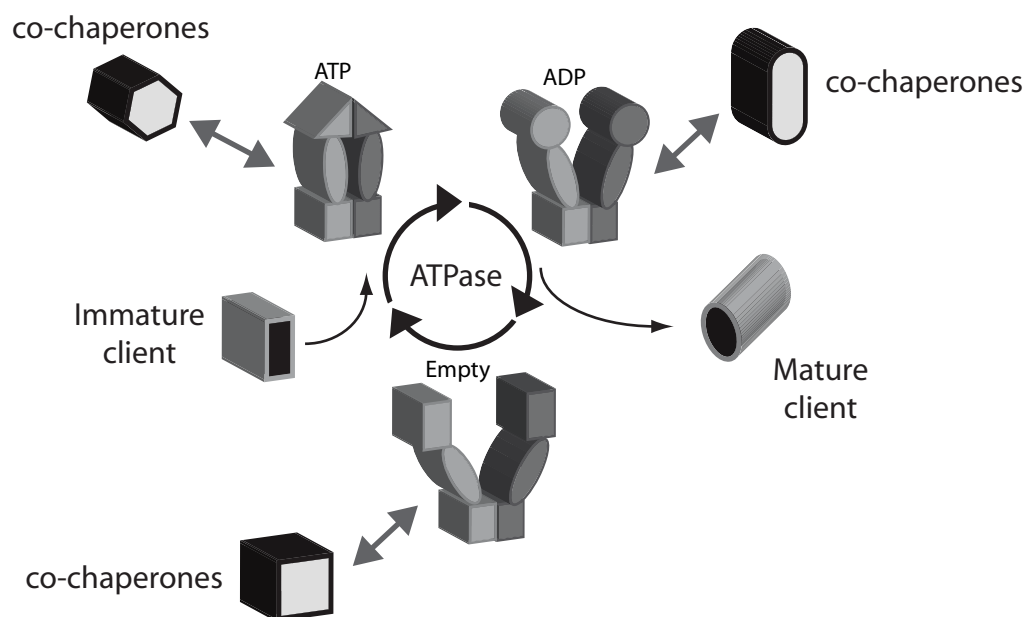
Figure 1.1

The activation of client proteins by Hsp90 relies on the opening and closing of a dimeric “molecular clamp” by transient association of the N-domains (Figure 1.2) and is directly coupled to the ATPase cycle of Hsp90 (16-19). Recent tour-de-force structural studies have revealed that flexible hinges between all three domains enable Hsp90 to adopt dramatically different three-dimensional conformations (10, 17, 20, 21). In the open conformation, Hsp90 first binds ATP in a fast reaction followed by a slow formation of the first intermediate, possibly where the so-called ATP lid is released from contact with the N-terminal segment. The N-domains of Hsp90 can then dimerize and subsequent rearrangements in the N to M domain contacts lead to the closed, ATPase active state. Following the hydrolysis of ATP, the products (ADP and  $P_i$ ) are released and Hsp90 returns to the open state. Importantly, the structural changes are large and are the rate limiting steps in the ATPase cycle (12).

A recent study found that a conformational equilibrium exists between the three-states (ATP, ADP, apo) that is not irreversibly determined by the presence of nucleotide (19). Nucleotide binding was found to provide modest stabilizing energy to bias the equilibrium toward the corresponding conformational state. Comparison between *Escherichia coli*, yeast, and human Hsp90s identifies evolutionary adaptations to the conformational equilibrium between species to meet the particular client protein and metabolic environment of the organism.

**Figure 1.2. Model of the ATPase driven conformational cycle of Hsp90 that leads to client maturation.**

In addition to client and ATP, numerous co-chaperones bind to Hsp90 and influence its chaperone activity. Many of these Hsp90 binding interactions are inter-dependent. The nucleotide-bound state of Hsp90 influences the binding of both co-chaperones and clients.



**Figure 1.2**



Isolated Hsp90 is a slow ATPase, ranging from about  $1 \text{ min}^{-1}$  for yeast Hsp90 to about  $0.1 \text{ min}^{-1}$  for human Hsp90. Mutation of either of the catalytic amino acids of Hsp90 (E33 or R380) impairs ATPase activity and prevents yeast viability when present as the sole copy of Hsp90. However, Hsp90 point mutations that perturb the ATPase activity from 2 to 400 % of the wild-type level can support yeast growth under non-stressful conditions (16). Thus, cell viability can tolerate a wide range of Hsp90 ATPase levels.

The open and closed conformational rearrangements of Hsp90 during the ATPase cycle are coupled to the binding of many co-chaperones (22-24). Hsp90 interacts with more than twenty co-chaperones that coordinate the interplay between Hsp90 and other chaperone systems, regulate the ATPase activity of Hsp90, recruit Hsp90 client proteins, and contribute to the chaperone cycle through their enzymatic activities (12, 25). For example, the co-chaperone p23 and its *S. cerevisiae* homologue Sba1 preferentially bind to Hsp90 in the presence of ATP (26-28). Although not essential for Hsp90-dependent activation of client proteins, the interaction of p23/Sba1 with Hsp90 makes the activation process more efficient by stabilizing the state required for client-protein activation and slowing ATP turnover (23, 29-33). The Hsp90 co-chaperone Sti1 (Hop in mammals) is involved in the recruitment of client proteins to the Hsp90 system and is capable of arresting the ATPase cycle of Hsp90 to allow for client protein loading (34, 35). The kinase-specific Hsp90 co-chaperone Cdc37 also arrests the ATPase cycle of Hsp90 in the

client-loading phase by inhibiting the ATP-dependent N-domain dimerization (22, 24, 36). To date, Aha1 and its homolog Hch1 are the only co-chaperones known to activate the ATPase activity of Hsp90 (23, 37, 38) and therefore most likely interacts with an intermediate conformation of Hsp90 between the open and the closed state (17).

Different co-chaperones preferentially interact with distinct conformations of Hsp90 allowing them to exert temporal control over conformational changes within the Hsp90-client complex (39). Asymmetric complexes between Hsp90 and co-chaperones allowing for interaction with multiple co-chaperones simultaneously have recently been identified (39-41). How the interaction of Hsp90 with its co-chaperones guides its recognition of client proteins and modulates its biochemical activities is an active area of investigation.

Hsp90 has a unique ATP binding site and the discovery of small-molecule inhibitors that specifically inhibit Hsp90 has provided useful research tools that also show promise as anti-cancer therapeutic agents. Hsp90 inhibitors were originally uncovered from a natural product screen for compounds that reversed the transformed phenotype of the v-src oncogenic kinase. One of the natural products from this screen, geldanamycin (GA) was found to bind specifically to Hsp90 and inhibit its ability to chaperone v-src (42). GA binds to the adenine nucleotide binding pocket of Hsp90 suggesting it acts by blocking the binding of nucleotides to Hsp90 (9, 43). While Hsp90 function is essential

for the viability of healthy cells, cancer cells tend to have a higher level of Hsp90-dependent clients and a higher required level of Hsp90 activity. For many types of cancer there appears to be a therapeutic window where cancer cells can be preferentially impacted by Hsp90 inhibition compared to healthy cells. The medical interest in Hsp90 has spurred the synthesis of many small-molecule inhibitors as drug candidates (44).

Hsp90 is a specialized molecular chaperone that is required for the maturation of a limited set of clients. Many newly synthesized proteins require general molecular chaperones including Hsp60 (GroEL in bacteria), Hsp70 and Hsp40 in order to fold properly, but only a small fraction of these rely upon Hsp90. The limited proteins that require Hsp90 to mature to their active state are referred to as Hsp90 clients. These Hsp90 clients fall into three main categories: protein kinases, steroid hormone receptors, and non-signal transduction clients (Table 1.1). Within each greater client class, research has revealed important aspects of the mechanism of Hsp90-mediated client maturation, yet the molecular mechanism by which Hsp90 binds to and activates clients remains largely a mystery.

**Table 1.1. Classes of Hsp90 Clients.**

<b>Client Class</b>	<b>Example Clients</b>	<b>Co-chaperones</b>	<b>References</b>
Steroid Hormone Receptors	Progesterone & Glucocorticoid Receptors	FKBP51, FKBP52, Hop, p23	(45)
Kinase	v-src, B-Raf	Cdc37, Hop, p23	(42, 46)
Non-Signal Transduction			
CFTR	CFTR	Aha1	(47-49)
Telomerase	Telomerase	p23	(50)
Antigen Presentation	MHC peptide loading		(51, 52)

### ***Steroid hormone receptor Hsp90 clients***

Steroid hormone receptors are a class of transcription factors that are activated by binding to steroid agonist and were some of the first proteins actively studied as Hsp90 clients. In 1984, Baulieu and colleagues reported that monoclonal antibodies raised against progesterone receptor (PR) recognized a 90 kilodalton protein that tightly associated with apo-receptor, but not steroid-bound receptor (53), properties that indicated a regulatory role for the 90 kilodalton protein. Soon after, Pratt and colleagues reported that monoclonal antibodies raised against glucocorticoid receptor (GR) were capable of immuno-isolating the receptor as well as a 90 kilodalton protein that cross-reacted with antibodies raised against Hsp90 (54); thus identifying Hsp90 as a steroid hormone receptor chaperone.

Hsp90 was found to bind strongly to the apo-form of many other steroid-hormone receptors including the estrogen and androgen receptors; however some receptors such as those for retinoic acid and thyroid hormone showed little or no affinity for Hsp90 (55-58). Different DNA binding properties in the absence of steroid agonist were noted for Hsp90-dependent and Hsp90-independent receptors in cell-free expression systems (55). In the absence of steroid agonist, Hsp90-independent receptors were found to bind to target DNA in the presence and absence of Hsp90. In contrast, Hsp90-dependent receptors without steroid agonist only bound to DNA when Hsp90 was absent. In the absence of steroid agonist, Hsp90-dependent receptors were found in the cytoplasm while

Hsp90-independent receptors were found in the nucleus. At the time, these results led to the hypothesis that Hsp90 functions to repress steroid hormone receptors by sequestering them in the cytoplasm. However, it is now appreciated that Hsp90-dependent receptors require Hsp90 in order to bind to steroid. Steroid binding controls the activity of all steroid receptors and for Hsp90-dependent receptors this step requires Hsp90 activity.

Co-immunoprecipitation (co-IP) experiments revealed many components of the Hsp90 chaperone complexes involved in receptor maturation and paved the way for *in vitro* reconstitution of the chaperone reaction. Glutaraldehyde cross-linking studies revealed that the stoichiometry of receptor-Hsp90 complexes was 1:2 indicating that a receptor monomer binds to an Hsp90 dimer (59). From immuno-isolation of steroid receptors expressed in cell-free expression systems it was discovered that receptor-Hsp90 complexes contained a number of co-chaperones including Hsp70, p23 and Hop (60, 61). A combination of these three co-chaperones along with the general chaperone Hsp40 and Hsp90 were found to be sufficient to develop a purified chaperone system for the maturation of PR to the steroid-bound active form (62).

Structural and biochemical approaches have shown that steroid hormone receptors bind steroid ligand in an internal cavity and indicate that Hsp90 remodels this cavity to provide a solvent-accessible path for the hormone to enter. X-ray crystal (63, 64) structures clearly show that steroid ligands bind to receptors in an internal cavity that is

completely inaccessible to solvent. Evidence for Hsp90 opening of this cleft comes from chemical modification studies that indicate modestly higher susceptibility of the steroid-binding cavity in the Hsp90-bound form of apo-GR (65). While the mechanism by which Hsp90 opens the steroid binding cleft remains unknown, the data clearly indicates that isolated apo-GR and apo-PR are not able to bind to steroid agonist, but that when complexed with Hsp90 the binding to steroid becomes efficient (45).

While much is understood about Hsp90 mediated steroid receptor maturation, many important aspects of the molecular mechanism remain open questions. It is clear that ATP hydrolysis by Hsp90 is required for efficient PR maturation (66). However, it is not clear how the ATPase driven conformational cycle of Hsp90 leads to opening of the steroid-binding cavity. What are the molecular interactions that cause apo-receptor to bind to Hsp90, Hsp90 to catalyze steroid binding, and steroid-bound receptor to dissociate from the chaperone complex? These questions are challenging to answer because of the dynamic nature of the Hsp90 conformational cycle, but may be addressed by structural and biochemical approaches that trap individual steps in the process.

### ***Kinase clients of Hsp90***

The oncogenic v-src kinase was first shown to bind to Hsp90 through co-IP analysis (67), but it was not clear that Hsp90 was required for v-src kinase activity until it was reported that the natural compound GA prevents v-src activity indirectly by

inhibiting Hsp90 (42). When v-src is expressed in the presence of GA, it accumulates in an inactive form indicating that Hsp90 is required for the maturation of v-src to an active form. In addition, treatment of cells with GA causes an increase in the proteasome mediated degradation rate of v-src and a decrease in the steady-state v-src level (68). Thus, Hsp90 is required for the maturation of v-src kinase to an active form and also protects v-src from degradation.

The maturation of kinases mediated by Hsp90 requires co-chaperones including the kinase-specific co-chaperone Cdc37. Cdc37 was originally identified in a screen for genes required for cell cycle progression (69). Genetic evidence for a functional interaction between Cdc37 and Hsp90 came from studies showing that either mutations in Cdc37 or a reduction in the level of the yeast Hsp90 protein suppresses the lethality of v-src over-expression (70, 71). Mutations in Hsp90 and Cdc37 were also found to exacerbate a defect in the *Drosophila melanogaster* sevenless receptor tyrosine kinase (72). Thus, Hsp90 and Cdc37 are both involved in the maturation of these model kinases. A physical connection between Cdc37 and Hsp90 was first indicated by co-IP analysis with the cyclin dependent kinase CDK4 (73). Both Hsp90 and Cdc37 were found to associate with CDK4 during co-IP analysis with an anti-CKD4 antibody suggesting there may be a direct mechanistic link between Hsp90 and Cdc37 in chaperoning kinases.



The direct interaction between Cdc37 and Hsp90 has recently been confirmed and described in atomic detail through structural analyses. Comparison of full-length yeast Hsp90 to truncated Hsp90 constructs indicated that the isolated Hsp90 N-domain was primarily responsible for mediating binding to the C-terminal domain of human Cdc37 (24). Co-crystallization of these domains revealed the atomic details of this interaction (24). More recently, Pearl and colleagues have successfully purified a homogenous complex of human Cdk4 and Cdc37 along with Hsp90 from the insect *Spodoptera frugiperda* expression system and analyzed the structure of this complex by negative stain electron microscopy (21). This tour de force work indicates that the kinase-loaded complex consists of an Hsp90 dimer bound to single copies of Cdc37 and Cdk4. The observed electron density can be well fit with a structural model where Cdc37 binds to the Hsp90 N-domain and Cdk4 binds to the Hsp90 M-domain. Biochemical analyses of Cdk4-Cdc37 complexes in the absence of Hsp90 indicate a stoichiometry of one kinase to two Cdc37 molecules (21). The biochemical and structural data are consistent with an ordered model where a dimer of Cdc37 initially binds to kinases and subsequent binding of this complex to Hsp90 results in the release of one Cdc37 molecule.

The association of human Cdc37 with yeast Hsp90 observed biochemically and structurally (24) is consistent with the high amino acid conservation of Hsp90 between these two species. This conservation is also apparent at a functional level as metazoan Cdc37 (from flies) is capable of rescuing robust growth of *S. cerevisiae* made unhealthy

by a point mutant in the yeast Cdc37 (72). Unlike Hsp90, the amino acid sequence of Cdc37 is divergent from yeast to humans with only 17 % sequence identity after alignment. Of note, yeast Cdc37 binds to yeast Hsp90 with about 100-fold weaker affinity than human Cdc37 (36), indicating that while qualitative Cdc37 function may be similar across eukaryotes, the interaction details are quantitatively distinct.

The Hsp90 and Cdc37 chaperones stabilize the cellular accumulation of many kinases. Indeed, the observation that Hsp90 inhibition can lead to decreased cellular levels of client kinases has become a convenient screen to identify Hsp90-dependent kinases. In mammalian cells, inhibition of Hsp90 activity resulted in reduced levels of 80 out of 105 kinases analyzed (74). A recent study also found that more than 50 % of the *S. cerevisiae* kinome was affected by the loss of functional Cdc37 (75) confirming the importance of a functional Hsp90:Cdc37 chaperone complex for the stability of cellular protein kinases.

Recent efforts have described the minimum chaperone requirements for the maturation of a kinase *in vitro*. Arlander et al. identified a five protein system for chaperoning the Chk1 kinase *in vitro* that consisted of Hsp90, Hsp70, Hsp40, Cdc37 and CK2 (46). The *in vitro* chaperone systems for kinases and steroid hormone receptors differ in their co-chaperone requirements and sensitivities, indicating the influential role that co-chaperones play in the client maturation process (62, 76). As with steroid

hormone receptors, the *in vitro* chaperone system for kinases provides a promising route to carefully analyze the client maturation process in detail.

### ***Non-signal transduction Hsp90 clients***

Recent evidence indicates that Hsp90 is involved in the maturation of active telomerase. The catalytic core of telomerase consists of a protein component (TERT) and a template RNA (TR). Chaperones were originally implicated in the maturation of telomerase from the observation that reconstitution of active telomerase from isolated TERT and TR was stimulated by increasing concentration of chaperones present in reticulocyte lysates (77). A two-hybrid screen revealed that the Hsp90 co-chaperone p23 interacted with TERT and co-IP analyses revealed that both Hsp90 and p23 are involved in complexes with telomerase in mammalian cells (77). More recent biochemical dissections of telomerase function indicate that the interplay between Hsp90 and p23 influences the dynamics of telomerase binding to telomeres (78). Hsp90 activity *in vivo* is important for the proper maintenance of telomeric DNA length that decreases when Hsp90 activity is impaired or when Hsp90 is over-expressed (50, 79).

Hsp90 can bind to antigenic peptides and has been implicated in the delivery of these peptides to major histocompatibility complexes (MHCs). Hsp90 was first connected with antigen presentation from analyses of antigens in tumors that could confer immunity in syngenic recipients (80). Fractionation studies revealed that Hsp90 from the

tumors was important in the development of immunity (81, 82). Cellular studies indicated that antigenic peptides complexed with Hsp90 are loaded on to MHC class I with much higher efficiency than free peptides (51), which may otherwise be prone to rapid degradation. In addition, the delivery of peptides to MHC class II proteins is reduced upon treatment of cells with Hsp90 inhibitors (52). The molecular details of Hsp90 involvement in antigen presentation are a current area of active investigation.

In addition to soluble proteins, Hsp90 has recently been implicated in the maturation of the Cystic Fibrosis Transductance Regulator (CFTR), an integral membrane protein. Hsp90 was originally implicated in CFTR maturation from the observation that treatment of mammalian cells with the Hsp90-specific inhibitors prevented newly synthesized wild-type CFTR from transitioning to the maturely glycosylated cell-surface form (47). Cystic fibrosis-causing mutations in CFTR, including the most commonly occurring – deletion of a phenylalanine codon ( $\Delta F508$ ), cause defective folding and export of CFTR from the ER (83). Immunoprecipitation of wild-type and  $\Delta F508$  CFTR followed by mass spectrometry revealed that Hsp90 and many co-chaperones exhibited differential binding for wild-type and mutant CFTR (48). RNA interference screening of these co-chaperones demonstrated that silencing of the Hsp90 co-chaperone Aha1 rescued cell-surface expression and chloride ion transport of  $\Delta F508$  CFTR (48). Recent biochemical analyses indicate that Aha1 associates with  $\Delta F508$  CFTR nearly twice as much as with wild-type CFTR (49). The observation that

reducing the association of  $\Delta F508$  CFTR with Aha1 corrects the function of this anion channel provides a promising avenue for the development of therapeutics to treat cystic fibrosis.

Hsp90 can function as a promiscuous anti-aggregation chaperone *in vitro* for a large variety of hard-to-fold proteins, but it appears that Hsp90 is not required for the folding and solubility of most proteins in cells (84). Following the discovery that Hsp90 expression increased in response to conditions that stress protein folding, a number of studies examined the capacity of Hsp90 to assist in the folding of proteins that were difficult to fold on their own including citrate synthase (CS), amyloid beta, p53, and the nucleotide binding domain of CFTR (CFTR-NBD1) (85-88). The ability of Hsp90 to suppress protein aggregation *in vitro* often does not require ATP (88-90). In contrast both steroid hormone receptors and kinase clients of Hsp90 are dramatically impaired by mutations that destroy ATPase activity or by competitive inhibition of the ATP binding site with drugs (42, 66). Thus, the anti-aggregation properties of Hsp90 do not seem to require the same ATPase driven Hsp90 conformational cycle that is implicated in the maturation of kinases and steroid hormone receptors. Multiple chaperones in addition to Hsp90 are capable of providing anti-aggregation properties in cells providing a possible explanation for the observation that the general anti-aggregation properties of Hsp90 do not appear to be important in cells.

### ***Questions addressed in this thesis***

Molecular chaperones are involved in many different cellular pathways including: 1) the folding and maturation of client proteins 2) the prevention of protein mis-folding and aggregation 3) the destruction and proteolysis of proteins that are unable to reach their mature state. As mentioned previously, Hsp90 is required for the maturation of numerous kinases (8) and steroid hormone receptors (91). Hsp90 has also been shown to function as a promiscuous anti-aggregation chaperone *in vitro* (85-88). More recently, Hsp90 has been shown to play a role in proteasome-mediated degradation of abnormal proteins through interactions with quality-control ubiquitin ligases such as CHIP (92). This thesis focuses on the role of Hsp90 in the maturation of client proteins and in the prevention of protein mis-folding and aggregation.

In the subsequent chapters, I will address the following questions: 1) How does Hsp90 dimerization contribute to its function in cells? 2) Is the ATPase activity of Hsp90 required for maturation of kinases and steroid hormone receptors *in vivo*? 3) Is net charge required for chaperone-mediated protein solubility? 4) Why does Hsp90 anti-aggregation activity *in vitro* function in the absence of ATP, but *in vivo* function demonstrates absolute requirement for ATPase activity?

Hsp90 is predominately dimeric at physiological concentrations but can dissociate into monomers on the same time-scale as ATP hydrolysis. While the chaperone cycle of

Hsp90 has been examined extensively, the role dimerization in Hsp90 function in cells was previously unknown. Truncation of the C-terminal dimerization domain of Hsp90 results in monomeric Hsp90 constructs that do not support yeast viability (93, 94). However, the C-domain may contribute other functional properties to Hsp90 in addition to dimerization. NM constructs of yeast Hsp90 that lack the C-domain were found to have a concentration-dependent specific ATPase activity suggesting they can mediate weak dimerization in the absence of the C-domain (93, 95). These studies suggest that Hsp90 monomers may be inactive for ATP hydrolysis. Yet heterodimers made up of one full-length Hsp90 subunit and one C-domain were found to have about 30 % of wild-type ATPase activity (93) which is within the range of reduced Hsp90 ATPase activity previously found to support yeast viability (16). These observations indicate that a full-length Hsp90 monomer is required to test the role of dimerization in Hsp90 function in cells.

In Chapter III, I designed and analyzed the function of a full-length monomer (NMCC) in yeast cells. NMCC Hsp90 had significantly reduced ATPase activity and was unable to support yeast viability as the sole copy of Hsp90. It was also unable to activate the Hsp90 client proteins GR and v-Src in yeast cells indicating that dimerization of Hsp90 is required for *in vivo* function. By forcing NMCC Hsp90 to dimerize by adding a C-terminal coiled-coil dimerization domain to the C-terminus, I was able to rescue the

ATPase and growth defects of monomeric Hsp90. This indicates that NMCC Hsp90 is defective purely because it is monomeric.

Homo-oligomeric proteins have numerous functions in cells; however, co-expression of homo-oligomeric proteins often results in the formation of cross-oligomers with unanticipated activity. The ability to restrict cross-oligomerization is crucial for the investigation of homo-oligomeric proteins, such as Hsp90, in cells. Chapter IV presents a modular approach to control cross-oligomerization using an additional coiled-coil dimerization domain fused to the C-terminus of Hsp90 (referred to as NMCcoil). This super-stabilization strategy prevented cross-oligomerization and was compatible with Hsp90 function in yeast cells. Contrary to previous models of Hsp90 function, the C-domain dimer was recently found to open and close with fast kinetics with the C- and N-domain dimerizations being anticorrelated (18). The ability of super-stabilized NMCcoil dimers to function fully *in vivo* suggests that any opening and closing of the C-domain dimer is not required for Hsp90 function.

Super-stabilized NMCcoil Hsp90 was then used to investigate the role of ATP hydrolysis in Hsp90 function in yeast cells. Hsp90 mutations that prevent ATP binding (D79N) or hydrolysis (E33A) were previously identified *in vitro* and found to be incapable of supporting yeast viability (11, 96). While these results suggest that ATP hydrolysis by Hsp90 is critical for *in vivo* function, the role of ATP hydrolysis in client



protein maturation by Hsp90 had not previously been determined. In Chapter IV, I tested the ability of super-stabilized ATPase-deficient dimers to support that maturation of an Hsp90 client kinase (v-src) and steroid hormone receptor (GR). Both binding and hydrolysis of ATP by Hsp90 were found to be required for efficient maturation of kinase and steroid hormone receptor client proteins in yeast cells.

In Chapter V, I describe one mechanism by which Hsp90 can prevent protein misfolding and aggregation. In mis-folded states, hydrophobic side-chains become increasingly exposed to solvent. Mis-folded proteins frequently aggregate in an energetic effort to bury these exposed hydrophobic surfaces. In contrast to hydrophobic effects, charged amino acids have been shown to increase proteins solubility (97). Analysis of net charge of three chaperones with anti-aggregation activity (Hsp90, Hsp70, and Hsp33) indicates they are all characterized by a high net charge that is evolutionarily conserved. In Hsp90, the negative charge is concentrated in the acid-rich charged linker (CL) and C-terminal extension (CX). The combined deletion of the CL and CX ( $\Delta\text{CL}\Delta\text{CX}$ ) dramatically impaired the ability of Hsp90 to suppress the aggregation of CFTR-NBD1 and CS. Importantly, addition of an acid-rich region with a distinct amino acid sequence to  $\Delta\text{CL}\Delta\text{CX}$  Hsp90 efficiently rescued anti-aggregation activity. These results indicate that the net charge of Hsp90, and not sequence-specific features, contributes to its anti-aggregation activity *in vitro*.

Why does Hsp90 anti-aggregation activity *in vitro* function in the absence of ATP, but *in vivo* function demonstrates absolute requirement for ATPase activity? In Chapter VI, I discuss preliminary experiments attempting to address this apparent contradiction. Anti-aggregation deficient  $\Delta\text{CL}\Delta\text{CX}$  Hsp90 which maintains wild-type ability to hydrolyze ATP provides a useful separation of function mutant to address this controversy *in vivo*. I have shown that  $\Delta\text{CL}\Delta\text{CX}$  Hsp90 is able to support yeast growth at 25 °C but not under stressful conditions (37 °C). However,  $\Delta\text{CL}\Delta\text{CX}$  accumulation is reduced compared to wild-type under stressful conditions. At this time, I cannot distinguish growth defects from expression level defects. In an effort to determine whether Hsp90 anti-aggregation activity is ATP-independent *in vivo*, I co-expressed  $\Delta\text{CL}\Delta\text{CX}$  Hsp90 with an ATP-binding deficient Hsp90 mutant (D79N) that was found to maintain *in vitro* anti-aggregation activity. D79N Hsp90 was unable to rescue the growth defect of  $\Delta\text{CL}\Delta\text{CX}$  Hsp90 indicating that the ATP-independent anti-aggregation activity is not sufficient to support yeast growth. Importantly, the growth defect observed for  $\Delta\text{CL}\Delta\text{CX}$  is not a dominant effect as co-expression of wild-type Hsp90 was able to efficiently rescue cell growth. My findings thus far are consistent with a model where Hsp90 assists in the maturation of select clients in an ATP-dependent fashion aided by its inherent anti-aggregation properties.

## **CHAPTER II**

### **Methods**

### ***Plasmid construction***

All Hsp90 constructs used in these studies were generated from the yeast *HSP82* gene. To aid in protein purification and Western blot detection, a 6xHis tag (GGHHHHHHGGH) was appended to the N terminus of Hsp90 constructs. Constructs were cloned into pACYC for bacterial expression and into p414GPD for expression in yeast. In Chapter 6, NMCcoil and D79Ncoil were cloned into p413GPD for co-expression with  $\Delta$ CL $\Delta$ CX 414GPD. Standard PCR techniques were used to generate all Hsp90 mutants. To generate super-stabilized Hsp90 dimers, a *GCN4*-based coiled-coil computationally optimized for stability (98) was inserted after amino acid 678 of the *HSP82* gene resulting in the following protein sequence (I<sup>678</sup>GGGTSSVKELEDKNEELLSEIAHLKNEVARLKKLVGERTGD<sup>679</sup>). We refer to constructs containing this coiled-coil with the suffix coil. In addition, we refer to full-length Hsp90 containing the N, M and C-domains as NMC to distinguish it from truncations containing only the C-domain. Thus, Ccoil refers to the C-domain appended with the coiled-coil and NMCcoil represents full-length constructs with the coiled-coil appended.

The C-domain of Hsp90 contains amino acids 542-709. Single chain constructs of the C-domain were constructed with amino acids 537-680 from *HSP82* followed by the glycine-rich linkers outlined in Figure 3.2 then by amino acids 542-709 from *HSP82*. The NMCC construct (Figure 3.1) contains amino acids 1-680 from *HSP82* followed by the

15 amino acid linker in Figure 3.2 then amino acids 542-709 from *HSP82*. The NMCCcoil construct contains the coiled-coil sequence described above inserted after amino acid 678 of the second C domain of NMCC (Figure 3.10).

Yeast kinases tested in Appendix I were generously provided by Michael Snyder (Stanford University) in a high copy *URA3* expression vector, pEG(KG), that produces GST fusion proteins under the control of the galactose-inducible *GALI* promoter (99). pEG(KG) also contains an N-terminal 6xH tag to make the resulting GST-6xH-kinase fusion protein. The kinase Kin28 was amplified from yeast lysates and cloned into pEG(KG). For generating isolated kinase domain constructs, kinase domains were amplified from the full-length construct and cloned into pEG(KG).

### ***Protein production***

All Hsp90 constructs were expressed in BLR(DE3) cells induced with 1 mM isopropyl  $\beta$ -D-1-thiogalactopyranoside at 30 °C for five hours. Cells were harvested by centrifugation and resuspended in Wash Buffer (50 mM potassium phosphate pH 8.0, 300 mM potassium chloride, 20 mM imidazole). Cell lysis was accomplished by treatment with lysozyme and sonication in the presence of DNase1. After pelleting cell debris, lysates were incubated with Ni<sup>2+</sup>NTA agarose (Qiagen). After rinsing the nickel resin extensively with Wash Buffer, Hsp90 protein was competitively eluted with Elution

Buffer (200 mM imidazole, pH 7.5). Ethylenedinitrilotetraacetic acid (EDTA) was added to 10 mM to eluates which were subsequently dialyzed into Buffer A (20 mM potassium phosphate pH 6.8, 1 mM EDTA) for proteins in Chapters 3 and 4 or Buffer B (20 mM potassium phosphate pH 7.0, 1 mM EDTA) for proteins in Chapter 5. Protein samples were further purified by anion exchange chromatography using a Q sepharose HP column (GE) eluted with a linear gradient from 0 to 1 M potassium chloride in Buffer A or Buffer B. Protein samples in Chapter 3 were subjected to a final purification step of size exclusion chromatography using a Sephacryl S300 column (GE) in Buffer C (20 mM potassium phosphate, pH 6.8, 1 mM EDTA, 100 mM potassium chloride). Proteins were concentrated using Amicon Ultra concentrators (Millipore). Protein concentrations were determined spectroscopically using extinction coefficients ( $M^{-1}cm^{-1}$ ) based on amino acid composition using the program Sednterp (Amgen) at 280 nm. Purified wild-type human CFTR-NBD1 encompassing amino acids 388-673 was a kind gift from the lab of Phil Thomas (University of Texas Southwestern – CFTR Folding Consortium). Purified citrate synthase from porcine heart was purchased from Sigma-Aldrich.

### ***Circular dichroism***

CD measurements were made on a Jasco A-810 spectropolarimeter equipped with a Peltier temperature control unit in a 1 mm pathlength cuvette. C domain spectra were acquired from 280 to 200 nm at a subunit concentration of 20  $\mu$ M in 20 mM potassium

phosphate, pH 7.0 at 25 °C while all other spectra were obtained at a concentration of 5  $\mu$ M in Buffer A or Buffer B.

### ***Urea denaturation***

Equilibrium urea titrations in Chapters 3 and 4 were performed in Buffer C at 25 °C. Protein denaturation was followed by monitoring the loss of ellipticity at 222 nm. Measurements at a subunit concentration of 2  $\mu$ M were made in a cuvette with a 1 cm pathlength using an autotitrator with a mixing time of 600 seconds (determined to be more than three times greater than the time constant for unfolding at the  $C_m$ ). For urea titrations at a subunit concentration of 20  $\mu$ M, samples were manually mixed, allowed to equilibrate for 30 minutes and measurements made in a 1 mm cuvette.

Urea denaturation experiments in Chapter 5 were performed with 3  $\mu$ M protein samples in a 0.3 cm pathlength cuvette. Samples were manually mixed, equilibrated for one hour, and changes in tryptophan fluorescence measured using a PTI QM-4SE spectrofluorometer with excitation set to 290 nm and emission scanned from 300 to 380 nm at 1 nm/second.

For all urea denaturation experiments, both the pre- and post-transition regions were fit to linear equations and used to replot the data as fraction unfolded or fraction folded using center-of-mass fluorescence ( $C_m$ ) after correction for the fluorescence of the folded and unfolded states. The fraction unfolded or fraction folded plots were fit to two

state models with or without dimerization as appropriate and previously described (100, 101) using the program Kaleidograph (Synergy Software).

### ***Analytical ultracentrifugation***

Equilibrium experiments were performed at 20 °C on a Beckman XLI instrument using absorbance optics and a Ti60 rotor. Absorbance profiles were taken at 12 hour intervals, and overlapping profiles were used as a criterion for equilibration. For the C domain constructs in Chapter 3, samples were analyzed at a subunit concentration of 50  $\mu$ M in Buffer A with a rotor speed of 15,000 RPM and an equilibration time of 36 hours. For full-length constructs, samples were analyzed at a subunit concentration of 12  $\mu$ M in Buffer C (Chapter 3), Buffer D (50 mM Tris pH 7.5, 50 mM potassium chloride, 10 mM magnesium chloride – Chapter 4) or Buffer E (20 mM potassium phosphate pH 6.8, 150 mM potassium chloride, 5 mM magnesium chloride – Chapter 5) with a rotor speed of 8,000 RPM and an equilibration time of 36 hours. Absorbance profiles were fit to a single species model as previously described (102):

$$c_2(x) = c_2(x_0)\exp\left[\frac{M(1-V\rho)\omega^2}{2RT}(x^2-x_0^2)\right]$$

where  $c_2(x)$  is the concentration at a radial distance of  $x$ ,  $x_0$  is a reference point,  $M$  is the molecular weight,  $V$  is the partial specific volume,  $\rho$  is the buffer density,  $\omega$  is the angular velocity,  $R$  is the universal gas constant, and  $T$  is the temperature. Data were fit in Kaleidograph using buffer density and  $V$ -bar values based on the buffer and amino acid composition and determined using the Sednterp program.



### ***Analytical size exclusion chromatography***

100  $\mu$ L samples ranging in subunit concentration from 5-50  $\mu$ M were analyzed using Buffer C and a Superdex200 column (GE). Absorbance at 280 nm was used to monitor the elution profile.

### ***Enzymatically coupled ATPase assay***

ATP hydrolysis was enzymatically linked to NADH oxidation that was monitored spectroscopically (103). Hsp90 catalyzed ATP hydrolysis to generate ADP. Pyruvate kinase was used to convert ADP and phosphoenolpyruvate to ATP and pyruvate. Lactate dehydrogenase was used to convert pyruvate and NADH to lactate and NAD with a corresponding drop in absorbance at 340 nm ( $\Delta\epsilon_{340} = 6220 \text{ M}^{-1}\text{cm}^{-1}$ ). ATPase assays were performed at 37 °C. Both Hsp90 protein samples (3  $\mu$ M) and ATPase components were pre-warmed then mixed. Using a Bio50 Spectrophotometer equipped with a Peltier temperature control unit (Cary) and a 1 cm pathlength cuvette, absorbance at 340 nm was measured at 15 second intervals (avoids photobleaching of NADH) for 10 minutes. Final concentration of ATPase components was 20 mM Tris pH 7.5, 5 mM magnesium chloride, 100 mM KCl, 1 mM ATP (Sigma), 0.17 mM NADH (Sigma), 0.67 mM phosphoenolpyruvate (Sigma), 0.01 mg/ml pyruvate kinase (Sigma), and 0.02 mg/ml lactate dehydrogenase (EMD Biosciences). The rate of NADH oxidation with 0.3 mM ADP was more than an order of magnitude greater than the highest rate observed with

Hsp90 demonstrating that ATPase components are not rate limiting. Rates were determined by fitting the change in absorbance versus time to a linear model, converting absorbance units to amount of NADH oxidized and normalizing to the concentration of Hsp90.

### ***Subunit mixing analysis***

Before measuring ATPase activity, mixtures of full-length and truncated Hsp90 proteins were equilibrated in a volume of 90  $\mu$ L for 24 hours in Buffer A at 30  $^{\circ}$ C. After equilibration, 60  $\mu$ L of ATPase components were added and ATPase measurements made over 10 minutes at 37  $^{\circ}$ C. Final concentrations were: 5  $\mu$ M full-length Hsp90, 0-30  $\mu$ M truncated Hsp90. To determine the kinetics of NMCcoil and Ccoil subunit exchange, the equimolar experiment was repeated and ATPase activity measured as a function of pre-equilibration time. The resulting data were fit to an exponential decay model:

$$V=A+B*e^{-kt}.$$

For isolated full-length NMCcoil incubated at 30  $^{\circ}$ C, we found no detectable decay in ATPase rate after 48 hours.

### ***Fluorescent GA binding***

BODIPY-GA (BDGA) was synthesized as described (104). BDGA concentration was determined by absorbance in methanol using an extinction coefficient of 80,000  $M^{-1}$

$^1\text{cm}^{-1}$  at 506 nm (105) and was in close agreement with the weighed mass of BDGA used. 3  $\mu\text{M}$  BDGA was pre-incubated in assay buffer (20 mM Tris pH 7.5, 5 mM magnesium chloride, 100 mM potassium chloride, 0.01 % NP-40) with 10 mM dithiothreitol (DTT) for four hours at room temperature to convert GA to the high-affinity hydroquinone form (106). Samples were prepared in assay buffer with 5 mM DTT containing 1  $\mu\text{M}$  reduced BDGA and wild type or NMCC Hsp90 ranging from 0.1 to 3.3  $\mu\text{M}$ . These concentrations of Hsp90 and BDGA are both well above the 5 nM  $K_d$  determined for human Hsp90 and BDGA (106). Samples were equilibrated for 10 minutes at room temperature and fluorescence anisotropy measurements were made in a 0.3 cm pathlength cuvette on a PTI QM-4SE spectrofluorometer with excitation set to 488 nm and emission at 510 nm.

### ***Sole Hsp90 in yeast***

The haploid *S. cerevisiae* strains iG170Da (84) and ECU82a (107) are derivatives of W303 in which both endogenous Hsp90 genes, *HSP82* and *HSC82*, are knocked out. In strain iG170Da, the temperature sensitive G170D mutant of *HSP82* is chromosomally integrated and expressed from a GPD promoter. In strain ECU82a, wild type *HSC82* is constitutively expressed from pKAT6, a *URA3* marked 2 micron (high copy) plasmid that is amenable to negative selection. To test the ability of our Hsp90 constructs to support yeast viability, we generated them in p414GPD (108), a *TRP1* marked CEN plasmid with a strong constitutive promoter. Lithium acetate was used to introduce our Hsp90

constructs into iG170Da and ECU82a and plating in the absence of tryptophan was used to select for transformants. For the iG170Da strain transformed with NMC<sup>D79N</sup>, it took six days for colonies to grow (for all other strains colonies were apparent after two days). Transformants were grown in liquid media lacking tryptophan to an OD600 of 0.7, serially diluted and plated under permissive or non-permissive conditions. All samples were grown and plated in synthetic media lacking tryptophan and with 2 % dextrose as a sugar source. For strain iG170Da, 25 °C was permissive and 37 °C was non-permissive. Strain ECU82a was grown at 25 °C, in the absence or presence of 5-fluoroorotic acid (5-FOA) which selects for loss of the pKAT6 plasmid.

For monitoring yeast growth at elevated temperature in Chapter 6, single colonies of ECU82a strains were selected from plates containing 5-FOA where the only copy of Hsp82 is the 414GPD plasmid-borne copy of interest. Liquid cultures were grown to an OD600 of approximately 0.5, serially diluted and plated on synthetic media lacking tryptophan with 2 % dextrose as a sugar source. Strains were then grown at the indicated temperature for 3-5 days. For monitoring growth at 37 °C in liquid culture, ECU82a strains containing only our plasmid-borne Hsp82 of interest (post-FOA swap), were grown for 48 hours with frequent dilution to sustain log-phase growth. Cell growth over time was measured using a Victor X5 multilabel plate reader (Perkin Elmer). The cell density once the cells had fully equilibrated to growth at 37 °C (after 24 hours) was fit to a linear curve to determine growth rate.

To determine the expression level of our Hsp90 constructs in ECU82a, liquid cultures in minimal media were grown to a cell density of  $5 \times 10^7$  cells/ml determined with a hemacytometer. Cells were lysed by vortexing with glass beads and resuspension in SDS. Proteins from the lysis of  $10^7$  cells were separated by SDS-PAGE and the expression level quantified by Western blotting against the 6xH epitope tag. A standard curve was generated using purified Hsp90 added to lysates from cells that did not express any epitope tagged Hsp90.

#### ***v-src assay***

Plasmid p316Galv-srcv5 was generated from p316v-src (107) and contains v-src with a C-terminal v5 epitope tag (GKPIPPLLGLDST) under a galactose regulated promoter on a *URA3* marked CEN plasmid. To analyze galactose induced expression of a non-Hsp90 client, the gene encoding the SspB protein (109) from *Escherichia coli* was cloned in place of v-src to create p316GalSspBv5. Lithium acetate was used to introduce p316Galv-srcv5 and p316GalSspBv5 into iG170Da cells and plating in the absence of uracil was used to select for transformants. To these cells we introduced our Hsp90 constructs on p414GPD plasmids. On plates, cells were grown with dextrose as the sugar source to prevent v-src expression. Liquid cultures were grown in synthetic raffinose media without uracil and tryptophan at 25 °C to a cell density of about  $5 \times 10^6$  cells/ml. Cells were pelleted and resuspended in media with either 2 % raffinose or galactose as the sugar source. After 15 minutes at 38 °C (Chapter 3) or 39 °C (Chapter 4) (to

inactivate G170D Hsp90), cells were grown in a shaking incubator at 36 °C for five hours (Chapter 3) or 37 °C for six hours (Chapter 4). Cell pellets were collected by centrifugation, washed once with water and frozen at -80 °C. The frozen cell pellets were lysed by vortexing with glass beads in Src Lysis Buffer (50 mM Tris, pH 7.5, 5 mM EDTA, 0.2 mM sodium orthovanadate to inhibit dephosphorylation, 1 mM phenylmethanesulfonylfluoride) followed by addition of SDS to 2 %. Protein concentration in these SDS lysates was assessed using the BCA assay (Pierce). Samples (2 µg protein) were subject to SDS-PAGE and phosphotyrosine levels quantified by Western blot analysis with antibody 4G10 (Upstate) in the presence of 0.1 % TWEEN20. The level of v-src was quantified (20 µg protein/lane) with  $\alpha$ -v5 antibody (Invitrogen) and the level of Hsp90 was quantified (20 µg protein/lane) with  $\alpha$ -HisG antibody (Invitrogen) by Western blot analysis.

### ***GR assay***

P2A/GRGZ (107) is a 2 micron *ADE2* plasmid that contains rat glucocorticoid receptor expressed from the constitutive GPD promoter and the  $\beta$ -galactosidase ( $\beta$ -gal) reporter under the control of three glucocorticoid response elements. We introduced P2A/GRGZ together with our p414GPD Hsp90 constructs into iG170Da cells. Cells were grown in synthetic dextrose media lacking tryptophan and adenine at 25 °C to a cell density of about  $5 \times 10^6$  cells/ml. Cells were pelleted by centrifugation. Cultures were grown in a shaking incubator at 38 °C (Chapter 3) or 39 °C (Chapter 4) for fifteen

minutes (to inactivate G170D Hsp90) and then split in half. Deoxycorticosterone (DOCS) dissolved in ethanol was added to final concentrations of 0, 0.08, 0.4, 2, 10, or 50  $\mu\text{M}$  (final concentration of ethanol was 0.1 % in all cases). Cells were grown for a further 60 minutes at 36 °C or 37 °C and collected by centrifugation. After washing once with water, cell pellets were frozen at -80 °C. Cells were lysed by vortexing with glass beads in  $\beta\text{Gal}$  Lysis Buffer (100 mM potassium phosphate, pH 7.3, 2 mM magnesium acetate, 1 mM PMSF). After removing cell debris, protein concentration in the lysates was determined using the BCA assay (Pierce). A total of 10  $\mu\text{g}$  of lysate was reacted for 15 minutes in a total volume of 80  $\mu\text{L}$  of 1 mg/ml o-nitrophenyl-beta-D-galactoside (Sigma) in  $\beta\text{Gal}$  Lysis Buffer. The reaction was stopped by adding 80  $\mu\text{L}$  of 1 M sodium carbonate. Reporter activity was quantified by monitoring the absorbance at 420 nm. GR assays were repeated three times starting from fresh yeast colonies. One-tailed student T-tests were used to compare the no-insert strain to the Hsp90 strains. To analyze GR levels, a FLAG epitope was introduced into P2A/GRGZ at the Nco site that is preceded by a polyglutamine repeat in GR. GR-FLAG levels were analyzed by Western blotting with  $\alpha\text{-FLAG}$  antibody (Sigma). GR-FLAG responded to DOCS stimulation in all of the mutants indistinguishable from untagged GR.

### ***Sequence-based analysis of charge conservation***

For the eukaryotic proteins Hsp90, Hsp70, Hsp60, and triosephosphate isomerase, protein sequences from the same six species were analyzed (Table 5.2). Predicted net

charge of the proteins at pH 7 was determined based on the amino acid composition using the program SEDNTERP (Amgen). For the bacterial heat shock protein Hsp33, protein sequences from six species representing three distinct phyla were analyzed (Table 5.2). To ensure that the charge analysis was not affected by the diversity of bacterial genomes, only sequences that maintained at least 20 % sequence identity to the remaining sequences were analyzed.

### ***In vitro aggregation assays***

CFTR-NBD1 experiments were performed essentially as previously described (88) except that native protein was used as the starting material. Right-angle light scattering was measured in a PTI QM-4SE spectrofluorometer in a temperature controlled 0.3 cm pathlength cuvette. Protein samples were degassed for twenty minutes at room temperature and aggregation was initiated by transfer to a cuvette prewarmed at 37°C. Measurements were made as a function of time at a wavelength of 400 nm (excitation and emission) in CFTR buffer (100 mM Tris-hydrochloride pH 7.4, 0.385 M L-arginine, 10 mM DTT, 200 mM potassium chloride, 20 mM magnesium chloride) (88). Protein concentrations were 5  $\mu$ M Hsp90 and 1  $\mu$ M CFTR NBD1. CFTR-NBD1 aggregation experiments were also attempted at varying concentrations of salt. However, CFTR-NBD1 aggregation in low salt buffers was too rapid to interpret data obtained under these conditions. All data were normalized to the light-scattering intensity for CFTR-NBD1 aggregation after twenty minutes at 45 °C.



The solubility of Hsp90 constructs was monitored by light scattering under the same conditions, in the absence of CFTR-NBD1. The aggregation of Hsp90 variants on their own was also monitored by Native PAGE. Samples of 5  $\mu$ M protein in Buffer B were heated in a PCR machine for 5 minutes, cooled to room temperature, run on native PAGE (6 % acrylamide, 30 mM Hepes, 30 mM imidazole) and stained with Sypro Ruby gel stain (Invitrogen).

Mixing experiments were performed by mixing 2.5  $\mu$ M NMCcoil Hsp90 (110) and 2.5  $\mu$ M  $\Delta$ CL $\Delta$ CX Hsp90. Light scattering from the mixed sample was compared to that of CFTR-NBD1 in the presence or absence of 2.5  $\mu$ M NMCcoil Hsp90 or 2.5  $\mu$ M  $\Delta$ CL $\Delta$ CX Hsp90.

Aggregation of 0.075  $\mu$ M CS was measured in the presence of 0.6  $\mu$ M Hsp90 as described previously (85). Protein samples were degassed for forty minutes at room temperature and then right angle light scattering at a wavelength of 500nm was measured at 43 °C in CS Buffer (40 mM HEPES pH 7.5, 1 mM MgCl<sub>2</sub>). The solubility of the Hsp90 constructs was monitored under the same conditions, in the absence of CS. Mixing experiments were performed by mixing 0.3  $\mu$ M NMCcoil Hsp90 and 0.3  $\mu$ M  $\Delta$ CL $\Delta$ CX Hsp90. Light scattering from the mixed sample was compared to that of CS in the presence or absence of 0.3  $\mu$ M NMCcoil Hsp90 or 0.3  $\mu$ M  $\Delta$ CL $\Delta$ CX Hsp90. All data

were normalized to the light-scattering intensity for CS aggregation after forty minutes at 43 °C.

### ***Analysis of protein aggregates***

To monitor the content of the aggregates formed by mis-folded CFTR-NBD1, 200  $\mu$ L samples of CFTR-NBD1 in the presence and absence of Hsp90 were heated to 45 °C for 20 minutes in a water bath. Polycarbonate centrifuge tubes (Beckman) were pre-blocked with 10 mg/mL gelatin to prevent non-specific sticking then samples were pelleted at 17,000 rpm in a Beckman Optima TL Ultracentrifuge for 10 minutes. Pellets were washed with CFTR buffer and resuspended in SDS Loading Buffer. Samples were separated by SDS-PAGE, transferred to nitrocellulose, and analyzed by western blot for Hsp90 or CFTR-NBD1 (antibody was graciously provided by William Balch, Scripps Research Institute – CFTR Folding Consortium). To compare protein levels on the Hsp90 and CFTR-NBD1 western blots, 10 % or 100 % load samples were added.

### ***Cellular accumulation of yeast kinases***

Yeast kinase pEG(KG) constructs were transformed into the haploid *S. cerevisiae* strain iG170Da wild-type Hsp90 414GPD or an empty 414GPD vector. Liquid cultures were grown in synthetic raffinose media without uracil and tryptophan at 25 °C to a cell density of about  $5 \times 10^6$  cells/ml. Cells were pelleted and resuspended in media with 2 % galactose as the sugar source. After 15 minutes at 39 °C (to inactivate G170D Hsp90),

cells were grown in a shaking incubator at 37 °C for six hours. Cell pellets were collected by centrifugation, washed once with water and frozen at -80 °C.

Frozen cell pellets were lysed by vortexing with glass beads in Kinase Lysis Buffer (50 mM potassium phosphate, pH 8.0, 300 mM potassium chloride, 0.5 % Tween-20, 10 mM PMSF) followed by addition of SDS to 2 %. Protein concentration in these SDS lysates was assessed using the BCA assay (Pierce). The level of each kinase was quantified (20 µg protein/lane) with  $\alpha$ -GST antibody (Santa Cruz Biotechnology) by Western blot analysis.

### ***Identification of peptide substrates for yeast kinases***

GST-6xH-tagged kinases were expressed in iG170D cells at 25 °C. Cells were grown in synthetic raffinose media in the absence of uracil to a cell density of  $1 \times 10^7$  cells/mL then pelleted and used to inoculate one liter of synthetic galactose media. After kinases were expressed at 25 °C for six hours, cell pellets were collected by centrifugation and frozen at -80 °C. Cell lysis was accomplished by nitrogen decompression in Kinase Lysis Buffer. After pelleting cell debris, lysates were incubated with  $\text{Co}^{2+}$ NTA agarose. After rinsing the cobalt resin extensively with Kinase Wash Buffer (50 mM potassium phosphate pH 8.0, 300 mM potassium chloride, 20 mM imidazole), kinases were competitively eluted with Kinase Elution Buffer (50 mM potassium phosphate pH 8.0, 300 mM potassium chloride, 250 mM imidazole). Purified

protein was dialyzed into Kinase Dialysis Buffer (50 mM Tris pH 7.5, 150 mM potassium chloride, 2 mM DTT). As a purification control, a non-kinase yeast protein (YIR027C, Dal1) was also purified as a GST-6xH fusion protein.

Potential peptide substrates for each kinase were synthesized on amino-PEG cellulose membranes (MIT Biopolymers Laboratory). Membranes were first blocked with 1 % bovine serum albumin in phosphate buffered saline (PBS) for one hour at 30 °C. Membranes were washed with PBS then incubated with 10 mL purified Dal1, 500  $\mu$ Ci  $\gamma$ - $^{32}$ P[ATP], and 200  $\mu$ L 1 mM ATP at 30 °C for 30 minutes. Membranes were washed for thirty minutes in PBS then exposed to a phosphor screen and scanned using a Typhoon FLA-9000 (GE). Signal was quantified using Multi Gauge (Fujifilm).

Membranes were dephosphorylated at 30 °C for two hours using 400 units/mL Lambda Protein Phosphatase (NEB) with 1 mM manganese chloride in Kinase Dephosphorylation Buffer (50 mM HEPES pH 7.5, 100 mM sodium chloride, 2 mM DTT, 0.01% Triton X-100). After washing for 20 minutes in PBS, membranes were incubated with 10 mL purified kinase, 500  $\mu$ Ci  $\gamma$ - $^{32}$ P[ATP], and 200  $\mu$ L 1 mM ATP at 30 °C for 30 minutes, washed for thirty minutes in PBS then exposed to a phosphor screen and scanned using a Typhoon FLA-9000 (GE). Signal was quantified using Multi Gauge (Fujifilm).

***Kinase assays***

To monitor phosphorylation of peptide substrates identified for each kinase, 200  $\mu$ M fluorescently-labeled peptide was mixed with 2 mM ATP, 0.2 mg/mL creatine kinase, 100 mM creatine phosphate in Kinase Assay Buffer (20 mM Tris pH 7.5, 100 mM potassium chloride, 5 mM magnesium chloride, 10 mM DTT). The peptide mixture was then mixed with an equal volume of yeast lysate or purified kinase and incubated at 30 °C for 30 minutes. An equal volume of Native Gel Loading Buffer (5 mM HEPES, pH 7.5 and 20 % sucrose) was added and samples separated by native PAGE (6 % acrylamide, 30 mM Hepes, 30 mM imidazole). Gels were scanned using a Typhoon FLA-9000 (GE) and the signal quantified with Multi Gauge (Fujifilm).

## CHAPTER III

### **Dimerization of Hsp90 is required for *in vivo* function**

This work was previously published as:

Natalie Wayne and Daniel N. Bolon. (2007) Dimerization of Hsp90 is Required for *In Vivo* Function: Design and Analysis of Monomers and Dimers. *The Journal of Biological Chemistry*. **282**(48), 35386-35395.

Experiments in this chapter were primarily conducted by Daniel Bolon. I designed and completed the experiment to determine the stoichiometry of Hsp90 (wild-type and NMCC) binding to BDGA (Figure 3.4C).

## **Abstract**

Heat shock protein 90 (Hsp90) plays a central role in signal transduction and has emerged as a promising target for anti-cancer therapeutics, but its molecular mechanism is poorly understood. At physiological concentration, Hsp90 predominantly forms dimers, but the function of full-length monomers in cells is not clear. Hsp90 contains three domains: the N-terminal and middle domains contribute directly to ATP binding and hydrolysis and the C domain mediates dimerization. In order to study the function of Hsp90 monomers, we used a single-chain strategy that duplicated the C-terminal dimerization domain. This novel monomerization strategy had the dual effect of stabilizing the C domain to denaturation and hindering intermolecular association of the ATPase domain. The resulting construct was predominantly monomeric at physiological concentration and did not function to support yeast viability as the sole Hsp90. The monomeric construct was also defective at ATP hydrolysis and the activation of a kinase and steroid receptor substrate in yeast cells. The ability to support yeast growth was rescued by the addition of a coiled-coil dimerization domain, indicating that the parental single-chain construct is functionally defective because it is monomeric.

## Introduction

Among heat shock proteins, Hsp90 is unusual because it is not required for the proper folding of most cellular proteins (84), and instead is disproportionately linked to a select group of proteins required for receiving, transducing, and responding to environmental signals. The list of Hsp90 substrates continues to grow and includes over 40 kinases (8) and many steroid hormone receptors (91). The molecular mechanism of Hsp90 activation of both hormone receptors and kinases remains to be determined.

How does Hsp90 dimerization contribute to its function in cells? Structurally, Hsp90 contains an N-terminal domain that binds nucleotide, a middle domain, and a C-terminal dimerization domain (Figure 3.1). Truncations of Hsp90 that lack the C-domain are largely monomeric (93) and do not support yeast viability (94). These results do not demonstrate that dimerization of Hsp90 is essential because the C-domain may contribute other functional properties in addition to dimerization. The deletion of a loop from the C-domain (582-601) that is largely solvent exposed (10) prevents yeast viability (94), suggesting that dimerization is not the only essential role of the C-domain. In addition, a point mutation (A587T) in this same loop impairs the chaperoning of GR in yeast (107). Because Hsp90 activity requires co-chaperones and Hsp90 binds promiscuously to about 10 % of the yeast proteome (8), it is important to study Hsp90 function in cells where all endogenous binding partners are present. To rigorously test how dimerization affects Hsp90 function in cells requires a full-length Hsp90 monomer.

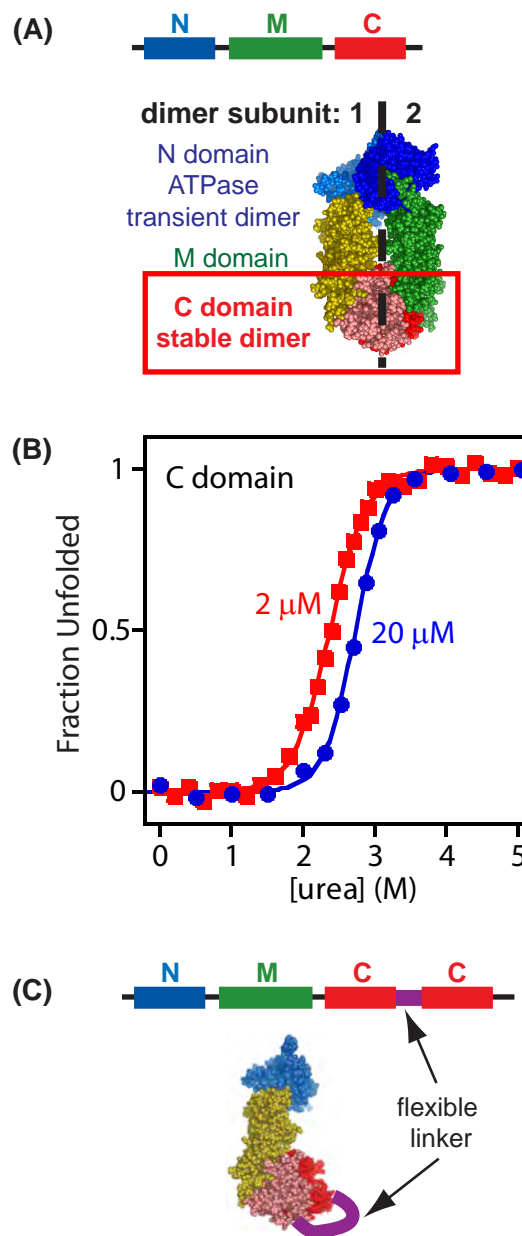


The ATPase activity of Hsp90 is required for cellular function, though the molecular mechanism that couples ATP hydrolysis to substrate activation is poorly understood. Dimerization of Hsp90 has been implicated in ATP hydrolysis. NM constructs of yeast Hsp90 lacking the C-terminal dimerization domain have concentration-dependent specific ATPase activity (93). These results indicate that the N and/or M domains can mediate weak dimerization that leads to increased ATPase activity. Consistent with this analysis, the disulfide cross-linking of truncated Hsp90 constructs increases their ATPase activity (95). These studies raise the possibility that full-length Hsp90 monomers may be inactive for ATP hydrolysis. Studies with heterodimers made up of one full-length Hsp90 subunit and one C-domain, indicate that full-length/C-domain Hsp90 heteromers have about 30 % the ATPase activity of wild-type (93), well within the 2 to 400 % range previously observed to support yeast viability (16). These observations have stimulated the current work to determine if Hsp90 monomers are functional in cells.

We have used a single-chain strategy to design a full-length NMCC Hsp90 monomer (Figure 3.1) and analyzed its function in yeast cells. To our knowledge, this is a novel approach to making full-length monomers and relative to traditional strategies that mutagenize the dimer interface, has the advantage of stabilizing the dimerization domain

**Figure 3.1. Design strategy.**

(A) Architecture of the Hsp90 gene and the dimeric protein structure. Hsp90 contains three domains referred to as N (N-terminal), M (Middle), and C (C-terminal). In the structural representation, these domains are colored blue-N, green-M, and red-C with lighter colors distinguishing the dimer subunit pictured on the left. (B) The stability to urea denaturation of the C domain is concentration dependent. At the low protein concentrations required to populate monomers, the stability of the C domain would be marginal. (C) NMCC strategy to design a full-length Hsp90 monomer with increased C domain stability.

**Figure 3.1**

to denaturation. NMCC Hsp90 will provide a tool to further explore the biochemical properties of Hsp90 monomers and their role in the chaperone cycle.

## Results

### *C domain has marginal stability to urea denaturation.*

The goal of our engineering efforts is to generate a natively folded full-length Hsp90 monomer that has one ATPase site. We considered traditional dimer disruption strategies, but were concerned that mutations at the dimer interface might destabilize the C domain causing it to mis-fold. To address this concern, we monitored the stability of the C domain. The stability of a protein is a measure of its capacity to tolerate destabilizing mutations and still fold (*III*). We analyzed the stability of the isolated C domain to urea-induced unfolding. In the absence of urea, the circular dichroism spectrum of the C domain has minima at 208 and 222 nm indicating that it forms a folded structure with significant helical content (Figure 3.3). We used CD to monitor the transition of the isolated C domain from folded to unfolded as a function of urea concentration (Figure 3.1B). The urea concentration midpoint ( $C_m$ ) of denaturation increases with higher C domain concentration (2.38 M urea at 2  $\mu$ M and 2.74 M urea at 20  $\mu$ M). The dependence of  $C_m$  on protein concentration indicates that dimerization and protein folding are coupled. At concentrations of Hsp90 (93) where monomers become populated (the midpoint of association is 60 nM), our results indicate that the C domain would be marginally stable to denaturation. Taking these observations into account, we

**Figure 3.2. Single-chain C-domains are increased in stability and monomeric.**

(A) Design of single-chain C-domain constructs with glycine-rich linkers to span the domains. In the ribbon diagram, spheres indicate the N terminus and C terminus of this domain. 27 Å is the distance that the linker needs to span in order to link the C terminus of one domain to the N terminus of the next domain. (B) All three single-chain constructs are increased in stability to urea denaturation compared to the wild-type C-domain. (C) Equilibrium analytical ultracentrifugation at 30 µM protein concentration demonstrates that C15C is monomeric. The theoretical distribution expected for a dimer is shown for comparison.

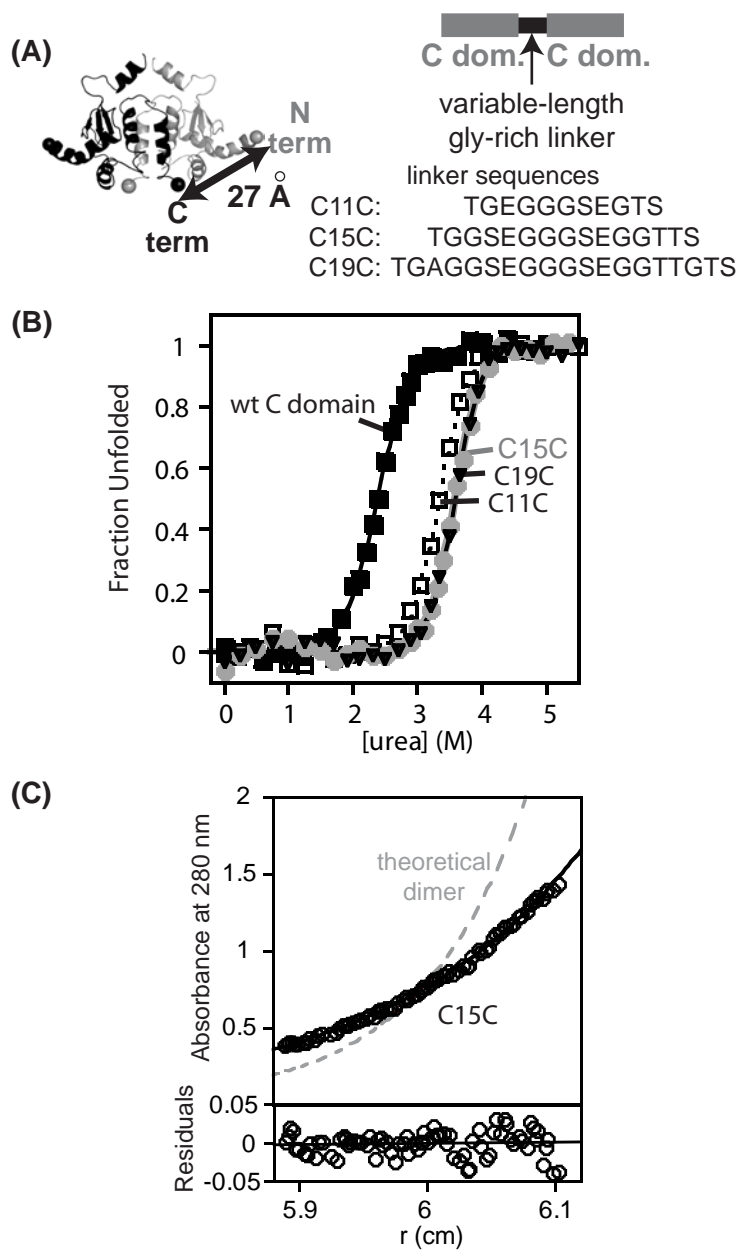


Figure 3.2

decided upon a monomerization strategy that would enhance the stability of the C domain (Figure 3.1C). Duplication of the C domain in NMCC should both increase the stability of the C domain to denaturation and disfavor intermolecular association. Thus NMCC should have one ATPase site per molecule.

***Isolated single-chain C domain is stable and monomeric.***

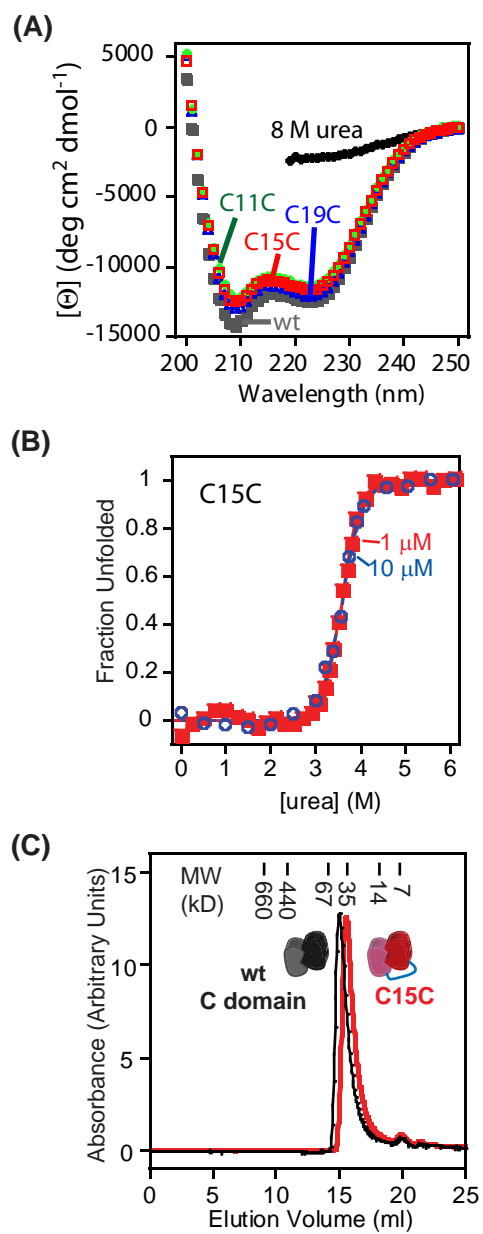
With the aim of generating a single-chain C domain that is both monomeric and stable, we generated CC constructs separated by variable length glycine-rich linkers (Figure 3.2A). Based on the crystal structure of Hsp90, the flexible linkers need to span a distance of 27 Å. While eight amino acids in a fully extended conformation can span this distance, previous single-chain studies have found that a greater number of amino acids is required to avoid strain and maximize stability (112). We made glycine-rich linkers of 11, 15, and 19 amino acids based on a proteolytically stable loop in bacteriophage gene-3-protein that had been used in a previous single-chain study (113). All three single-chain constructs (C11C, C15C, and C19C) expressed to high levels in *E. coli*, were readily purified, highly soluble and had CD spectra similar to the wild-type C domain (Figure 3.3). At a subunit concentration of 2 μM, we observe that C11C, C15C, and C19C all have increased stability to urea denaturation relative to wild type (Figure 3.2B). These results indicate that the effective concentration caused by the covalent single-chain linkages is greater than the concentration of wild-type protein (2 μM).

The 15 amino acid linker (C15C) was the smallest link eliciting the greatest stability and was chosen for further analysis. The increased stability of C15C could be caused by either a high effective concentration of covalently linked subunits as designed, or from unanticipated oligomerization. To differentiate between these possibilities, we analyzed the solution oligomeric state of C15C using equilibrium analytical ultracentrifugation (Figure 3.2C). The distribution of C15C fit very well to a single species model with a molecular weight (40.1 kD) similar to the theoretical molecular weight of the C15C construct (37.4 kD). The residuals from the single species fit are randomly distributed indicating that higher order oligomeric species are not populated enough to be detected. The results of equilibrium analytical ultracentrifugation (AUC) demonstrate that C15C is monomeric in solution. This observation is further supported by the size exclusion chromatography profile of C15C that elutes as a monomer with a similar radius of gyration to the wt C domain dimer (Figure 3.3). The CD spectra (Figure 3.3) and size exclusion profile of C15C is similar but not identical to the wild-type C domain most likely because of the truncation of an unstructured region (amino acids 681-709) from the first domain in C15C. We find that the stability of C15C to urea denaturation is independent of protein concentration (Figure 3.3) indicating that protein folding is no longer coupled to oligomerization (unfolded single-chain monomers go to folded single-chain monomers with no change in oligomeric state).



**Figure 3.3. Biophysical properties of C domain constructs.**

(A) Circular dichroism spectra of wild-type and single chain constructs all have minima near 208 and 222 nm indicating significant helical secondary structure content. In the presence of high concentrations of urea most of this secondary structure content is lost as the proteins denature. (B) Stability of C15C is concentration independent, consistent with a transition from a folded monomer to an unfolded monomer with no change in oligomeric state. (C) Size exclusion chromatography of wild-type and C15C constructs. Wild-type has a radius of gyration consistent with a spherical dimer and C15C with a spherical monomer.

**Figure 3.3**

Based on its design, the C15C domain should be monomeric when intramolecular C domain interactions outcompete intermolecular association. At very high concentrations it should be possible for intermolecular C15C association to occur. We can use the concentration dependent stability of the wild-type C domain to estimate the protein concentration that would be required for intermolecular association to energetically equal intramolecular interactions. Based on the concentration dependent stability of wild type C domain (Figure 3.1), we estimate that a concentration of 2 mM would be required to achieve the same  $C_m$  to urea denaturation as C15C. Thus, 2 mM represents the effective concentration brought about by the covalent linkage of C domains. Effective concentrations in the mM range have been reported for single-chain constructs of similar length (112). From this analysis, we predict that at a concentration of 2 mM the C15C construct will equally partition between monomers and dimers, but that at physiological Hsp90 concentration (approximately 10  $\mu$ M) C15C will be almost entirely monomeric. This analysis is supported by our observation that at 30  $\mu$ M, C15C is monomeric as determined by AUC (Figure 3.2C).

***Full-length NMCC monomer design is deficient for ATP hydrolysis.***

In order to explore the function of full-length Hsp90 monomers, we generated an NMCC construct (Figure 3.1C) with the 15 amino acid linker between the two C domains. The single-chain C domain in NMCC should hinder dimerization, resulting in a molecule with single N and M domains - the location of ATP hydrolysis as well as

numerous interactions with co-chaperones and substrates (9, 10, 14, 21, 114).

Equilibrium analytical ultracentrifugation was used to assess the oligomeric state of NMCC (Figure 3.4A). The radial distribution of NMCC at 12  $\mu$ M during centrifugation fits well to a single molecular weight species with a mass of 103 kD, similar to the mass of a monomer (99 kD). The residuals from the single species fit are randomly distributed indicating that higher order oligomers are not detected. We find that under identical centrifugation and concentration (12  $\mu$ M) conditions, wild type Hsp90 is dimeric (Figure 3.5). These results demonstrate that the single-chain C domain effectively blocks dimerization in the full-length NMCC construct.

How does blocking Hsp90 dimerization effect ATPase activity *in vitro*? Using an enzymatically coupled ATPase assay, we observed that NMCC was severely impaired for ATPase activity relative to wild-type Hsp90 (Figure 3.4B). The ATPase activity of NMCC was inhibited by GA, a small-molecule inhibitor with high specificity for Hsp90. These results indicate that the ATPase domain in NMCC can bind to both ATP and GA. To determine the fraction of NMCC molecules capable of binding to GA, we performed a stoichiometric binding experiment (Figure 3.4C). A concentration of fluorescently labeled BODIPY-GA of 1  $\mu$ M was used and Hsp90 concentrations of wild-type and NMCC were increased to determine the ratio of Hsp90 to GA where binding saturated. For both wild type and NMCC Hsp90, binding saturates at about 1.4 Hsp90 subunits to 1 GA. Taking into account uncertainty in concentration determinations and possible non-

**Figure 3.4. Full-length NMCC construct is predominantly monomeric and is defective for ATP hydrolysis.**

(A) The distribution of 12  $\mu\text{M}$  NMCC in equilibrium analytical ultracentrifugation fits well to a single species with the molecular weight of a monomer. The theoretical distribution expected for a dimer is shown for comparison. (B) At 6  $\mu\text{M}$  protein concentration, NMCC is more than 10-fold slower at ATP hydrolysis than wild type Hsp90 and can be inhibited with geldanamycin (GA) a specific inhibitor for the ATP binding site of Hsp90. (C) Stoichiometry binding experiment indicates that binding of Hsp90 to BODIPY-GA saturates at a ratio of approximately 1 GA molecule per 1 Hsp90 subunit for both wild type and NMCC Hsp90. (D) The specific ATPase activity of NMCC Hsp90 is concentration dependent.

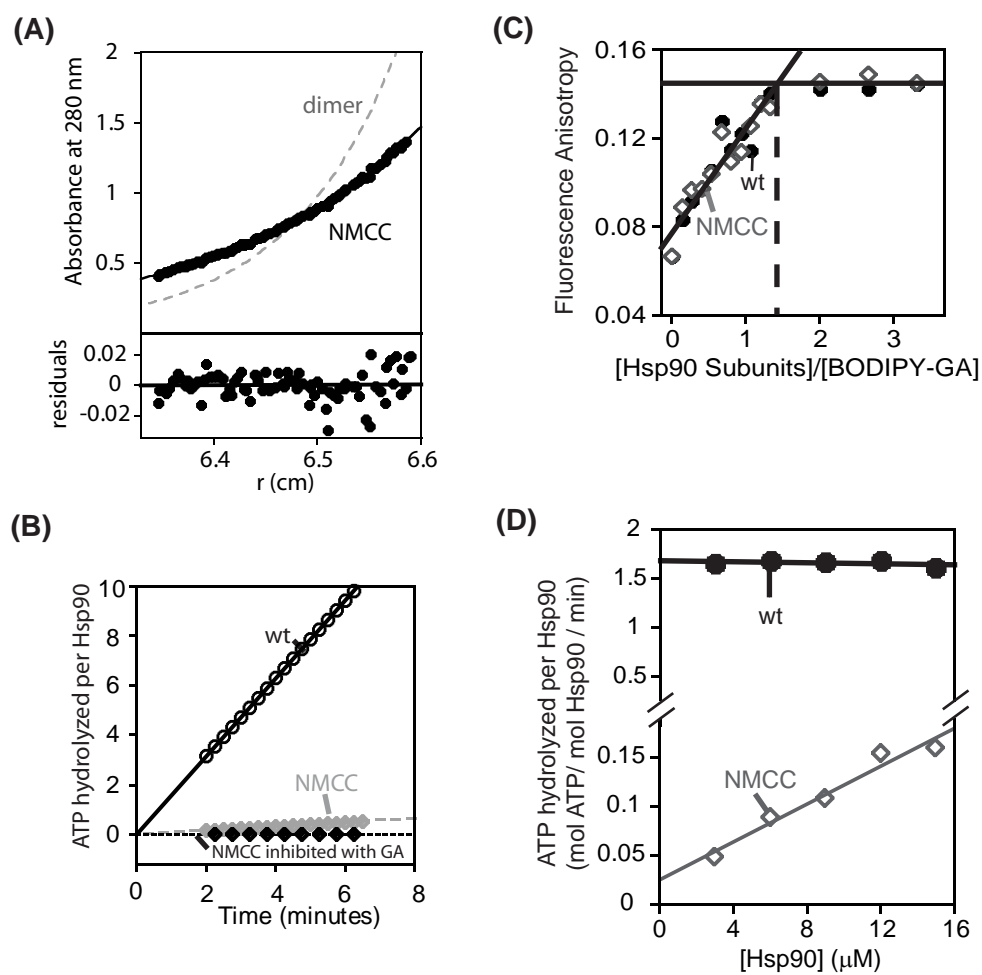
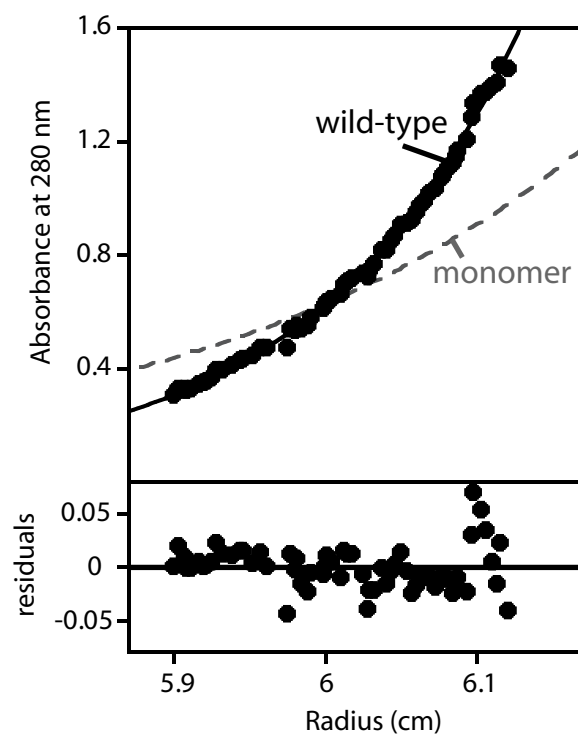


Figure 3.4

**Figure 3.5. Equilibrium analytical ultracentrifugation of wild-type Hsp90.**

The radial distribution of protein at 12  $\mu$ M fits well to a single species model with the molecular weight of a dimer.

**Figure 3.5**



fluorescent contaminants in the BODIPY-GA preparation, these experiments indicate that both wild-type and NMCC are capable of high-affinity binding of 1 molecule of GA per Hsp90 subunit. These results indicate that the ATP binding site of NMCC is structured similarly to wild type Hsp90. Consistent with the engineering strategy of NMCC, the single-chain C domain does not destroy the ATP or GA binding function of the N domain.

Is the observed ATPase activity of NMCC from monomer species or a low proportion of dimer species? To differentiate between these possibilities, we monitored specific ATPase activity as a function of protein concentration (Figure 3.4D). The ratio of dimer:monomer species varies with concentration enabling the activity from monomer and dimer species to be assessed. For wild-type Hsp90, specific ATPase activity is independent of protein concentration indicating that dimers are the dominant molecular form over the concentration range tested (3-15  $\mu$ M). This result is consistent with the protein concentration being well over the dimer dissociation constant, previously measured as 60 nM for wild-type Hsp90 (93). In contrast, the specific ATPase rate of NMCC increases over the same protein concentration range. This result is consistent with NMCC monomers and dimers having different ATPase rates, and the ratio of NMCC dimers:monomers changing over the concentration range tested.

The linear increase in specific activity of NMCC indicates that these experiments do not saturate the dimer species over this concentration range, preventing the direct determination of the dimer dissociation constant. Assuming that the NMCC dimers have the ATPase activity of wild-type dimers, we estimate that NMCC has a dimer dissociation constant of 200  $\mu\text{M}$  under the conditions of the ATPase assay. This result is consistent with interactions between the N and M domains driving weak association of NMCC. Consistent with this interpretation, NM constructs show concentration dependent ATPase activity with similar apparent dimer dissociation constants (93). In addition, this dissociation constant for NMCC is about 10-fold tighter than the dissociation constant we estimate for the single-chain C domain alone which corresponds to a free energy of NM association of about 5 kJ/mol. Based on the ATPase activity at low NMCC concentration, we estimate the upper limit for monomer activity as  $0.05 \text{ min}^{-1}$ , or 3% the rate of wild-type Hsp90.

### ***Function of NMCC in vivo.***

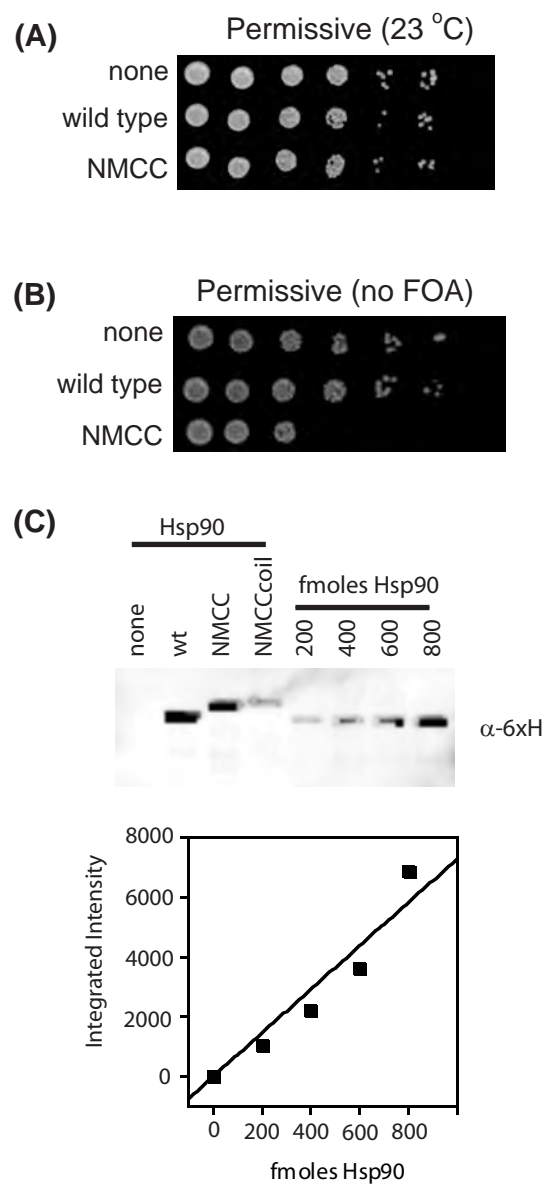
Hsp90 is an essential gene in eukaryotes (4, 115, 116). Interestingly, Hsp90 point mutants with *in vitro* ATPase levels less than 2 % of wild-type can function to support yeast viability (16, 107). Therefore, we tested the ability of NMCC to support viability as the sole Hsp90 in yeast. Both NMCC and wild-type Hsp90 with N-terminal His<sub>6</sub> epitope tags were constitutively expressed from a plasmid system previously shown to accumulate Hsp90 to near wild-type levels (117). These plasmids were introduced into

two yeast strains: one whose other source of Hsp90 was a temperature sensitive allele, and one whose other source of Hsp90 was encoded on a *URA3* plasmid that can be swapped out using 5-FOA which is converted to the toxic fluoroorotidine monophosphate when the *URA3* gene is expressed. Under conditions where active dimeric wild-type Hsp90 is present, expression of NMCC did not compromise cell growth in either strain (Figure 3.6). Under conditions that select for NMCC as the sole active Hsp90, both strains failed to grow (Figure 3.7).

The failure to support growth could be due to low expression level of NMCC. To test this possibility, we analyzed expression level by Western blotting cell lysates for the quantity of His<sub>6</sub> epitope tag (Figure 3.7C). Expression levels of His<sub>6</sub> tagged wild type and NMCC Hsp90 is similar. In addition, the SDS mobility of NMCC indicates that it is full length and that degradation products do not accumulate. Thus the glycine rich linker between the C domains is proteolytically stable in yeast. By comparing the Western signal to a standard curve of purified His<sub>6</sub> Hsp90 in cell lysate (Figure 3.6), we estimate that His<sub>6</sub> wild-type Hsp90 accumulates to 130,000 copies per cell and NMCC accumulates to 110,000 copies per cell. Assuming an average cell volume of 40 fL (*118*), and excluding nuclear volume (*119*), we estimate the cytoplasmic concentrations as approximately 7  $\mu$ M for NMCC and 8  $\mu$ M for wild-type. Wild-type Hsp90 is predominantly dimeric at these concentrations and NMCC is predominantly monomeric.

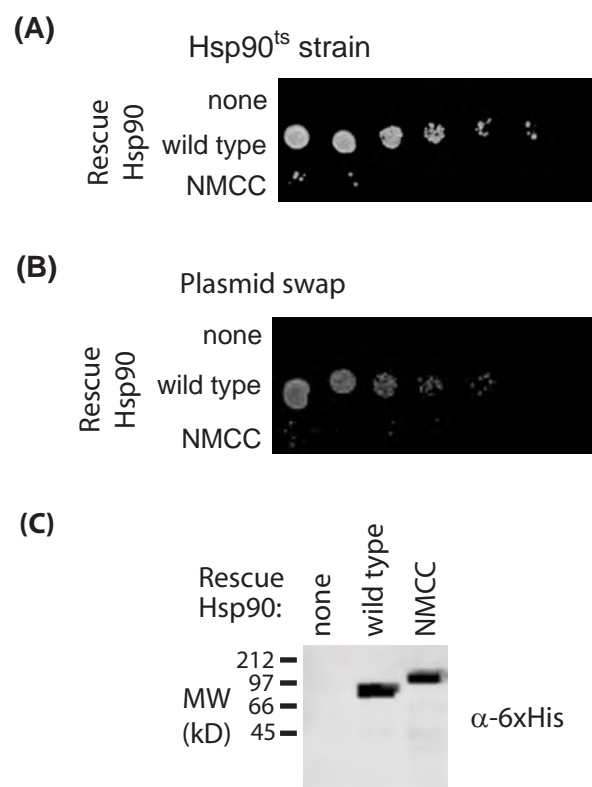
**Figure 3.6. NMCC protein accumulates to similar levels as wild-type Hsp90 and does not prevent growth when wild-type Hsp90 is present.**

(A) Growth of Hsp90<sup>ts</sup> yeast at permissive temperature is not impeded by the expression of NMCC Hsp90. (B) Expression of NMCC in yeast with wild-type Hsp90 does not prevent growth. (C) Expression level of NMCC, wild-type, and NMCCcoil in yeast determined by quantitative Western blotting.

**Figure 3.6**

**Figure 3.7. NMCC as the sole Hsp90 does not support yeast viability.**

(A) NMCC does not rescue growth of a Hsp90<sup>ts</sup> strain at 37 °C. (B) NMCC does not rescue growth at 23 °C in the absence of other Hsp90 sources. (C) Western blot analysis of cell lysates demonstrates that NMCC protein accumulates to similar levels as wild-type Hsp90.

**Figure 3.7**

Together, these results indicate that monomeric NMCC cannot function as the sole Hsp90 *in vivo*.

***Activation of v-src and GR in vivo.***

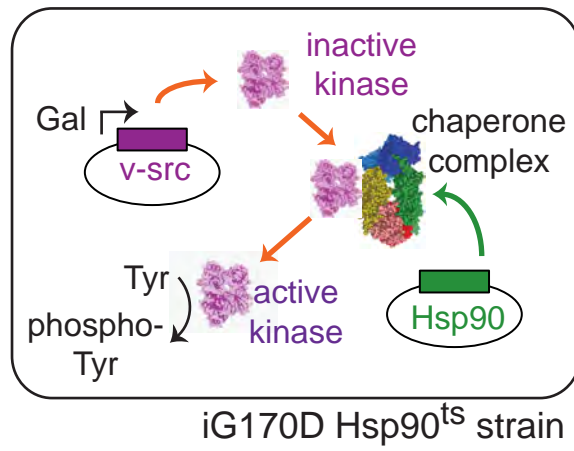
The molecular mechanism by which Hsp90 activates substrates is poorly understood. The variable co-chaperone requirements for kinase and hormone receptor substrates (46, 60) suggests different mechanisms for each class of substrate. Using NMCC, we analyzed the requirement of Hsp90 dimerization for the activation of both a kinase (v-src) and a hormone receptor (GR). Both of these substrates can be readily analyzed *in vivo* where the full complement of co-chaperones is present. These experiments were done in yeast with a Hsp90<sup>ts</sup> background such that cells with NMCC could be grown to sufficient number, then transferred to non-permissive temperature in order to monitor NMCC-dependent substrate activity (Experimental setup illustrated in Figure 3.8).

V-src is a promiscuous tyrosine kinase. Yeast have very low background levels of phosphotyrosine and expression of v-src causes a dramatic and Hsp90-dependent increase in phosphotyrosine (71). When v-src is induced from a galactose inducible promoter in the presence of wild-type Hsp90, Western blotting with an anti-phosphotyrosine antibody shows that many yeast proteins are phosphorylated by v-src (Figure 3.9A). In contrast, when v-src is induced with NMCC Hsp90, the v-src kinase accumulates, but proteins

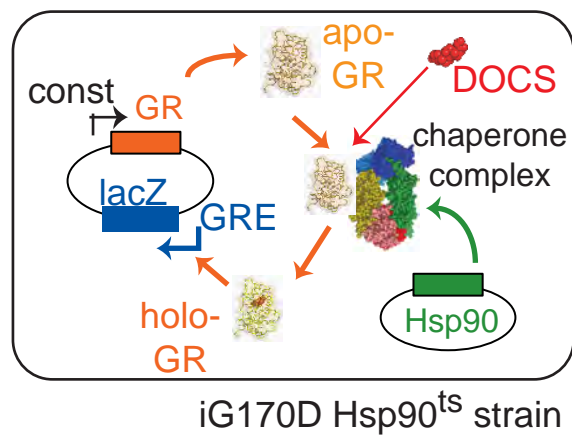


**Figure 3.8. Experimental setup to analyze client protein activity in Hsp90<sup>ts</sup> yeast.**  
Experimental setup to analyze (A) v-src and (B) GR activity in Hsp90<sup>ts</sup> yeast.

**(A)**

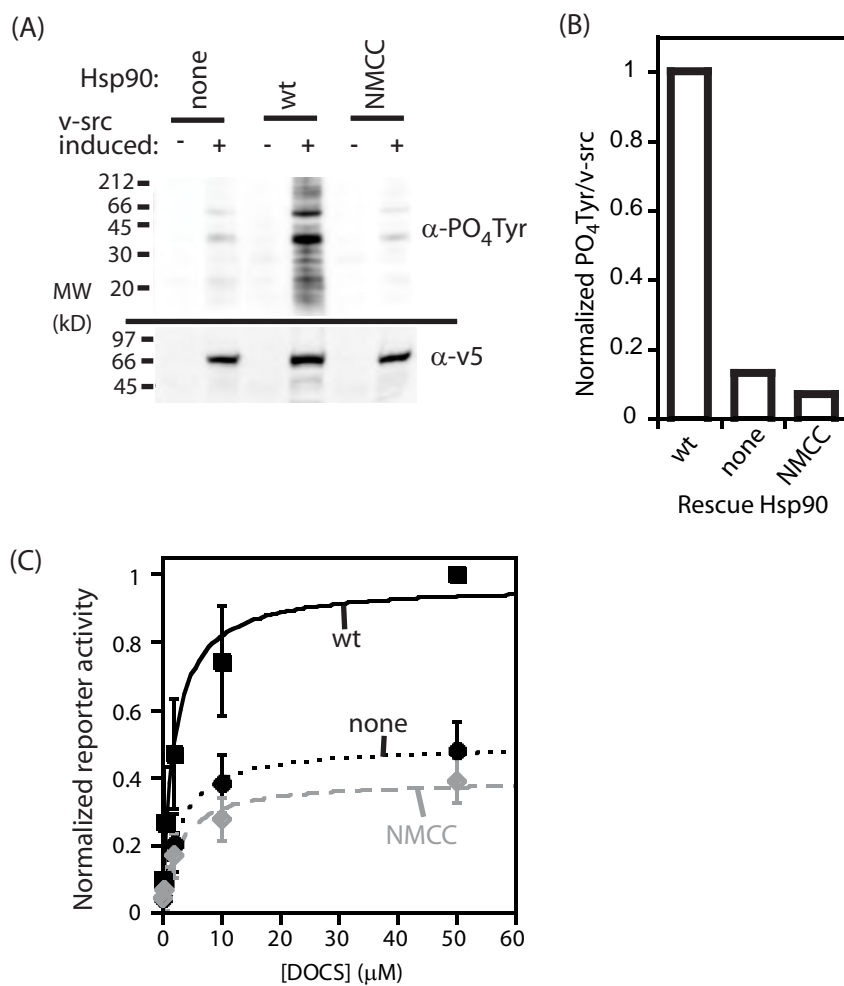


**(B)**



**Figure 3.8**

**Figure 3.9. In yeast cells, NMCC does not aid in the activation of v-src or GR.**  
(A) Western blots to detect v-src levels and phosphotyrosine levels in yeast with no active Hsp90, wt Hsp90, or NMCC Hsp90. In yeast with NMCC and all other Hsp90 inactive, v-src activity is compromised relative to cells with wild-type Hsp90. (B) Quantification of phosphotyrosine and v-src levels. (C) Reporter activity from a GRE driven promoter is defective with NMCC compared to wild-type Hsp90.

**Figure 3.9**

with phosphotyrosine do not accumulate indicating that v-src is inactive (Figure 3.9 A&B). NMCC Hsp90 does not activate v-src *in vivo*.

In yeast, GR responds to steroid agonists including deoxycorticosterone (DOCS) to enhance expression from promoters with glucocorticoid response elements (GRE's) (7). When yeast expressing GR are stimulated with DOCS, wild-type Hsp90 aids in the hormone induced expression of  $\beta$ -Gal from a GRE containing promoter (Figure 3.9B). In contrast, NMCC does not increase reporter expression relative to cells with no active Hsp90. NMCC Hsp90 does not activate GR *in vivo*.

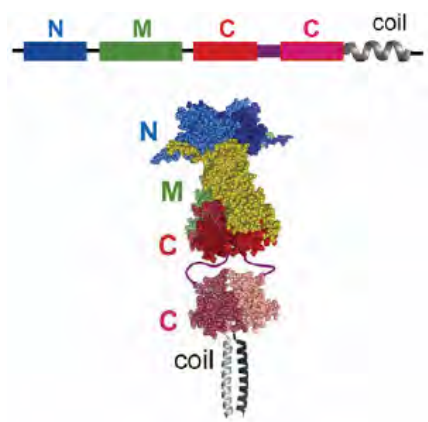
***NMCC function is rescued by addition of a coiled-coil dimerization motif.***

The lack of function observed for NMCC Hsp90 could be due to lack of dimerization or some other unintended consequence of the engineering strategy. For example, function of Hsp90 may require transient dissociation of the C domain and NMCC may be non-functional because it slows C domain dissociation. To address these concerns, we appended a coiled-coil dimerization domain to generate NMCCcoil (Figure 3.10A). The coiled-coil should induce this construct to form dimers. If NMCC is functionally defective because it is monomeric, then NMCCcoil should rescue both dimerization and function. In size exclusion chromatography NMCCcoil has a radius of gyration consistent with the dominant solution form being dimeric, with a small amount of tetramer also observed (Figure 3.10B).

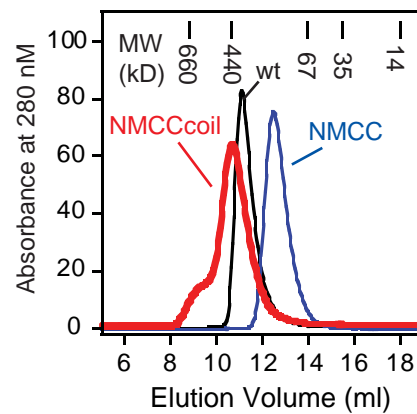
**Figure 3.10. Dimerization of NMCCcoil rescues *in vitro* and *in vivo* function.**

(A) Architecture and putative structural model of NMCCcoil dimer. (B) Size exclusion chromatography indicates that appending the coiled-coil domain transforms the parental NMCC monomer into a predominantly dimeric NMCCcoil. (C) ATPase activity of NMCCcoil is rescued compared to NMCC. (D) As the sole Hsp90 source, NMCCcoil supports yeast viability.

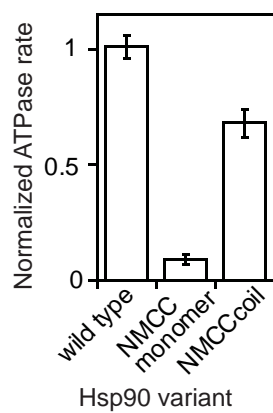
(A)



(B)



(C)



(D)

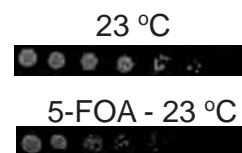


Figure 3.10

Is NMCCcoil functionally active? It is about 70% as active as wild-type Hsp90 for ATPase activity *in vitro* (Figure 3.10C). In addition, NMCCcoil enables yeast growth as the sole source of Hsp90 (Figure 3.10D). NMCCcoil expresses to about one third the level of wild-type Hsp90 (Figure 3.6). Consistent with previous findings that decreased Hsp90 levels result in reduced growth at elevated temperatures (4), yeast with NMCCcoil are temperature sensitive (data not shown). Our analysis of NMCCcoil demonstrates that the coiled-coil domain rescues dimerization, *in vitro* ATPase activity, and the ability to serve as the sole Hsp90 in yeast. Because coiled-coil induced dimerization rescues function in NMCCcoil, we conclude that the parental NMCC construct is defective because it is monomeric.

## Discussion

Our results indicate that dimerization of NMCC Hsp90 is required to position the catalytic machinery for efficient ATP hydrolysis. The recently determined crystal structure of yeast Hsp90 with AMPPNP and Sba1p (10) indicates that ATP binding induces a conformational change in the N domain that contributes to NM dimerization (10). Specifically, amino acids 94-125 change conformation relative to both the apo and ADP structures of the N domain (9) forming a lid over the bound nucleotide. When this lid is closed over ATP, hydrophobic interactions (primarily by I96 and F120) are made across the interface that favors dimerization. Our results indicate that these cross-subunit interactions are required to position the catalytic machinery for efficient ATP hydrolysis.



We find that NMCC monomers have an *in vitro* ATPase activity that is at most 3 % the level of wild-type Hsp90. This level of ATPase activity is at the extreme low end of the spectrum of ATPase activities that have been observed in Hsp90 point mutants that support yeast growth (16). Of note, studies on mixtures of full-length and C domain constructs show that full-length/C-domain heterodimers have an ATPase activity approximately 30 % that of wild-type homodimers (93), well within the range of ATPase activity required for *in vivo* activity. Why does the NMCC monomer have lower *in vitro* ATPase activity compared to full-length/C-domain heterodimers? The ATPase activity measured for NMCC monomers was determined at low NMCC concentration where monomers dominate. The ATPase activity for full-length/C-domain heterodimers was determined by titrating increasing concentration of C-domain and assuming equal dimerization probability for all species. This last assumption was based on the observation that both full-length and C-domain constructs have similar dimerization constants in the absence of nucleotide. Under the conditions of the ATPase assay nucleotide promoted dimerization of the NM domains may favor full-length homodimers over full-length/C-domain heterodimers. In this case the activity of full-length/C-domain heterodimers would be an overestimate.

Human Hsp90 has high sequence conservation with yeast Hsp90 (58 % sequence identity), but different ATPase properties (22, 29). The *in vitro* ATPase activity of human

Hsp90 is about 10 % that of yeast. A monomeric NM construct of human Hsp90 is reduced in activity by 10-fold relative to the full-length, suggesting that dimerization is important for efficient ATP hydrolysis in human Hsp90 as well as in yeast. However, human NM constructs do not exhibit concentration dependent ATPase activity at protein concentrations up to 100  $\mu$ M. Thus the activity of human NM Hsp90 monomers appears to be about 1 % the rate of full-length yeast Hsp90. With the data in this paper we cannot accurately determine the level of ATPase activity of yeast NMCC monomers, but find that it is less than 3 % of full-length yeast Hsp90 and it may be similar to monomers of human Hsp90.

Two possible explanations for the human NM results are that either human Hsp90 does not require NM dimerization for efficient ATPase hydrolysis, or the dimerization constant of NM is weaker in human Hsp90 than in yeast. We note that there are two amino acid changes at the NM dimer interface (V23F and L378I – yeast to human) that may reduce the affinity of this interface in human Hsp90. Also, human NM constructs have greatly reduced ATPase activity compared to full-length, indicating that dimerization contributes to efficient ATPase activity. Alternatively, it is possible that human NM constructs have reduced activity because of removal of the C domain. The monomer design strategy used in this paper could be used to differentiate these possibilities by generating human monomers with intact C domains. Lastly, human Hsp90 rescues yeast with endogenous Hsp90 knocked out (7), indicating that human

Hsp90 functions with yeast co-chaperones and substrates, some of which bind in a nucleotide-dependent manner to Hsp90 (22, 91). These lines of reasoning suggest that human Hsp90 functions by the same basic mechanism as yeast Hsp90, but that the affinity between the NM domains is stronger in yeast.

Changes in Hsp90's *in vitro* ATPase activity correlate loosely with *in vivo* function. Point mutations that destroy *in vitro* ATPase activity are non-functional in yeast (11, 96), but mutations that alter ATPase activity from 2 % to 400 % of wild-type levels are tolerable under non-stressful conditions (16). The *in vivo* ATPase activity of Hsp90 mutants may be buffered through binding to co-chaperones. Hundreds of yeast proteins interact with Hsp90 (8), and at least three have been shown to impact the ATPase rate of Hsp90 (23, 30, 34). Modulating the level of one of these co-chaperones in human cells has been shown to dramatically alter the activity level of an Hsp90 substrate (48). One of the unmet challenges in the study of Hsp90 is to understand how ATPase hydrolysis contributes to substrate activation.

NMCC will be a useful model for analyzing the binding properties of monomers to co-chaperones and substrates and the potential role of monomers in the Hsp90 conformational cycle. At cytoplasmic concentrations, Hsp90 is predominantly dimeric, However, Hsp90 subunits exchange rapidly, on the same time scale as ATP hydrolysis, suggesting that monomers of Hsp90 form transiently during the activation of substrates

(93). In addition to transient formation of Hsp90 monomers, the equilibrium population of monomeric Hsp90 in the cytosol is approximately 1000 copies/cell (based on expression level and the observed dimer dissociation constant) compared to 130,000 copies of Hsp90 dimers. Some substrates or co-chaperones may preferentially interact with Hsp90 monomers during part of the Hsp90 chaperone cycle. In addition, the binding of Hsp90 to transcription factors and other proteins with nuclear localization signals causes Hsp90 to traffic to the nucleus where it can accumulate at low abundance (120). The low concentration of Hsp90 in the nucleus should favor dimer dissociation, and perhaps Hsp90 monomers have a function in the nucleus. NMCC Hsp90 provides a tool to study full-length Hsp90 monomers both *in vitro* and inside cells.

## Conclusions

We find that the *in vitro* ATPase activity of NMCC is at best at the extreme low end of the range observed to support yeast viability and that NMCC does not support yeast viability. These observations indicate that the cellular environment is not sufficient to rescue the chaperone function of monomeric Hsp90. In addition, NMCC does not increase the activation of v-src nor GR in cells, indicating that Hsp90 dimerization is required to chaperone these specific substrates in yeast.

## CHAPTER IV

### **Hsp90 ATPase activity is required for *in vivo* function**

This work was previously published as:

Natalie Wayne, YuShuan Lai, Les Pullen, and Daniel N. Bolon. (2010) Modular Control of Cross-oligomerization: Analysis of Superstabilized Hsp90 Homodimers *In Vivo*. *The Journal of Biological Chemistry*. **285**(1), 234-241.

Experiments designed to analyze dimer assembly (Figure 4.4A&B) were performed by YuShuan Lai. NMCcoil protein for AUC experiments (Figure 4.2B) was provided by Les Pullen.

## Abstract

Homo-oligomeric proteins fulfill numerous functions in all cells. The ability to co-express subunits of these proteins that preferentially self-assemble without cross-oligomerizing provides for controlled experiments to analyze the function of mutant homo-oligomers *in vivo*. Hsp90 is a dimeric chaperone involved in the maturation of many kinases and steroid hormone receptors. We observed that co-expression of different Hsp90 subunits in *Saccharomyces cerevisiae* caused unpredictable synthetic growth defects due to cross-dimerization. We engineered super-stabilized Hsp90 dimers that resisted cross-dimerization with endogenous Hsp90 and alleviated the synthetic growth defect. Super-stabilized Hsp90 dimers supported robust growth of *S. cerevisiae* indicating that dissociation of Hsp90 dimers could be hindered without compromising essential function. We utilized super-stabilized dimers to analyze the activity of ATPase mutant homodimers in a temperature sensitive yeast background where elevated temperature inactivated all other Hsp90 species. We found that ATP binding and hydrolysis by Hsp90 are both required for the efficient maturation of GR and v-src confirming the critical role of ATP hydrolysis in the maturation of steroid hormone receptors and kinases *in vivo*.

## Introduction

The advent of modern genetic technology, including synthetic biology, enables many powerful approaches for both medical intervention and scientific exploration. Unfortunately, genetic manipulations frequently have unanticipated and hard-to-predict biochemical and physiological consequences. The analysis and manipulation of homo-oligomeric systems is particularly challenging because co-expression often leads to cross-oligomers with unanticipated activity (121). The ability to control cross-oligomerization is important for the investigation of numerous essential oligomeric proteins *in vivo*. Here, we present a general and modular approach to restrict cross-oligomerization and apply it to examine the role of ATP hydrolysis in the essential Hsp90 chaperone *in vivo*.

Hsp90 forms a thermodynamically stable dimer (122) that has a dissociation constant of about 60 nM (93) well below the estimated concentration of Hsp90 (about 15  $\mu$ M) in *S. cerevisiae* cells (5). Of note, Hsp90 subunits undergo subunit exchange with a half-life of less than a minute (93), while Hsp90 hydrolyzes ATP with a turnover rate of about 1 min<sup>-1</sup> (93). Because subunit exchange requires dimer dissociation, these results indicate that Hsp90 monomers can form during the Hsp90 ATPase cycle.

*In vitro* studies have identified point mutations in Hsp90 that disrupt ATP binding and/or hydrolysis. In the N-domain, the D79N point mutation disrupts hydrogen bonding

with the adenine base and prevents nucleotide binding (11). While Hsp90 does not contain signature Walker motifs, it does contain catalytic groups common to many ATPases including glutamate 33 that is positioned to activate a water molecule for nucleophilic attack on the scissile phosphodiester bond (11). The E33A point-mutation results in Hsp90 competent to bind but not hydrolyze ATP. Both the E33A ATP hydrolysis mutant and the D79N ATP binding mutant fail to support yeast viability demonstrating the critical role of ATP hydrolysis by Hsp90 *in vivo* (11, 96).

The function of Hsp90 is tied into many different biochemical pathways. Roughly ten percent of the yeast proteome binds to Hsp90 (8) emphasizing the importance of studying Hsp90 in its cellular environment where all binding partners are present. Many of these Hsp90 binding partners are co-chaperones required for the maturation of clients (8, 45, 123, 124).

Investigating ATPase deficient Hsp90 mutants *in vivo* has been challenging for two reasons: (1) ATPase mutants are inviable and (2) co-expression of different Hsp90 variants leads to cross-dimerization. Temperature sensitive (ts) Hsp90 mutants (107) provide a potential means to grow cells co-expressing ATPase mutants that can then be studied at elevated temperatures where Hsp90<sup>ts</sup> is inactivated. However, co-expression of different Hsp90 subunits leads to the formation of cross-dimers whose biochemical



activity is unpredictable. To overcome this challenge, we developed a strategy to thwart cross-dimerization. Using this system combined with inducible client expression systems, we investigated the maturation of clients in yeast where the only potential Hsp90 activity was from ATPase-deficient homodimers.

## Results

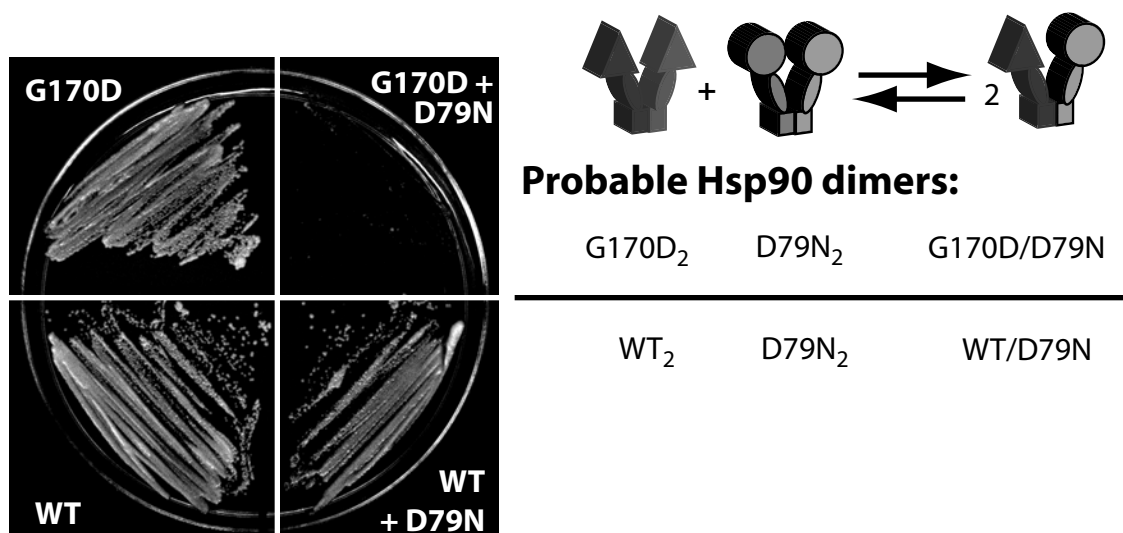
### *Cross-dimers of Hsp90 have unpredictable functions.*

Co-expression of ts NMC<sup>G170D</sup> (NMC refers to full-length Hsp90 containing the N, M, and C domains) in iG170D cells with the ATP-binding deficient NMC<sup>D79N</sup> caused a synthetic growth defect in yeast (Figure 4.1A). In contrast, healthy growth was observed when the same NMC<sup>D79N</sup> construct was introduced into W303 yeast with wild-type NMC. The G170D and D79N mutations are unlikely to affect dimer association as they are both located in the N-domain that is physically distant from the constitutive dimer interface in the C-domain (10). In the co-expression strains, dimers should equilibrate to form a distribution of three possible dimer species (Figure 4.1A). The synthetic growth defect from co-expression of G170D and D79N point mutants could be caused by G170D/D79N cross-dimers.

**Figure 4.1. Co-expression of different NMC Hsp90 variants *in vivo* leads to the formation of cross-dimers with unpredictable function.**

(A) Growth of yeast expressing different NMC variants: temperature sensitive G170D alone (top left), G170D with the ATP-binding deficient D79N point mutant (top right), wild-type Hsp90 alone (bottom left), wild-type with D79N (bottom right). Expression of NMC<sup>D79N</sup> caused an unanticipated growth defect when expressed with NMC<sup>G170D</sup>. Dimer exchange model illustrated on the right shows the probable NMC dimers species present in the co-expression cells. (B) Strategy to hinder cross-dimerization. Appending a coiled-coil dimerization domain super-stabilizes NMCcoil homodimer species and shifts the dimer exchange equilibrium to disfavor NMCcoil/NMC cross-dimers.

(A)



(B)

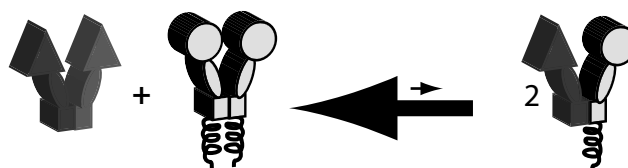


Figure 4.1

***Super-stabilization strategy to hinder cross-dimerization.***

Cross-dimerization is governed by a subunit exchange reaction where the free energy of association for each dimer species dictates the equilibrium distribution (125). The difference in free energy of dimerization between the heterodimer and the average of both homodimers controls the equilibrium population of all species. To disfavor cross-dimerization, we fused NMC to an additional dimerization domain consisting of a 33 amino-acid coiled-coil peptide (see methods in Chapter II for sequence) to create super-stabilized Hsp90 dimers that we refer to as NMCcoil (Figure 4.1B). In theory, the super-stabilization of one homodimer is sufficient to shift the equilibrium away from cross-dimers.

***The coiled-coil super-stabilizes Hsp90 dimers.***

Because dimerization and folding of the C-domain are coupled (126), dimer strength can be determined from unfolding studies of this domain. We compared the thermodynamic unfolding stability of the isolated C-domain to a construct with the coiled-coil that we refer to as Ccoil (C-domain plus coiled-coil). Addition of the coiled-coil enables it to remain folded at concentrations of urea where the isolated C-domain itself unfolds (Figure 4.2A). Fits of the denaturation curves indicate that the coiled-coil increases stability by 12 kJ/mol/M subunit. In a dimer exchange model, this energetic

**Figure 4.2. Superstabilization strategy is compatible with Hsp90 function.**

(A) Appending a coiled-coil super-stabilizes the C-domain of Hsp90 as determined by urea denaturation monitored by circular dichroism. (B) Full-length NMCcoil behaves as a dimer during analytical ultracentrifugation. Single species fit indicates that the molecular weight is 181 kD (similar to the theoretical MW of a dimer: 172 kD). (C) NMCcoil is compatible with efficient ATP hydrolysis. ATP hydrolysis can be blocked with the Hsp90-specific inhibitor geldanamycin (GA). (D) NMCcoil supports yeast viability as the sole Hsp90 and expressed to similar levels as NMC based on Western blotting of yeast lysates. Both NMC and NMCcoil samples were analyzed on the same SDS PAGE gel and blot and intervening lanes were removed for presentation clarity.

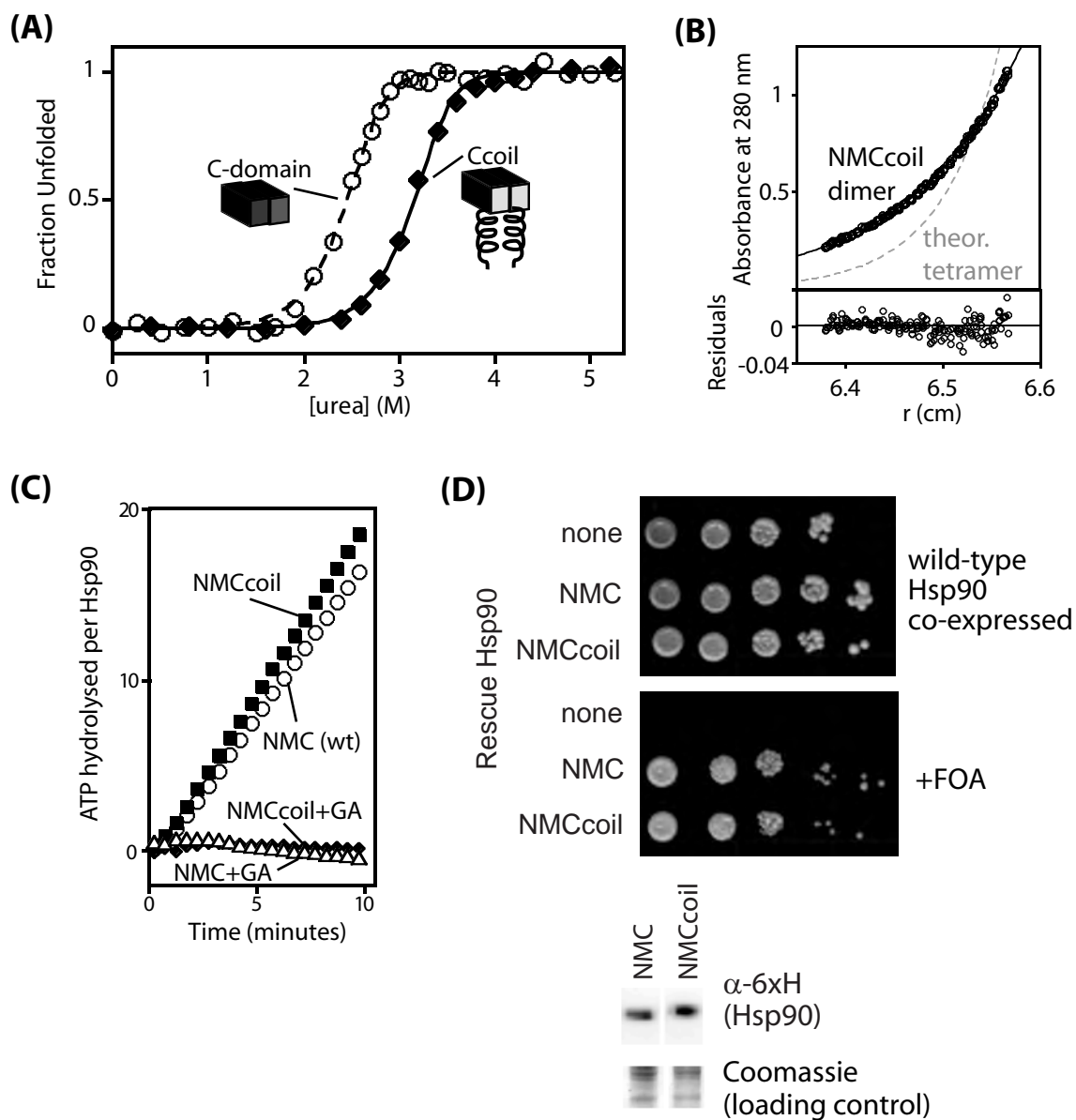


Figure 4.2

difference reduces cross-dimer accumulation to less than 1 % of the total population when each subunit is at equal abundance.

***The coiled-coil is compatible with Hsp90 function.***

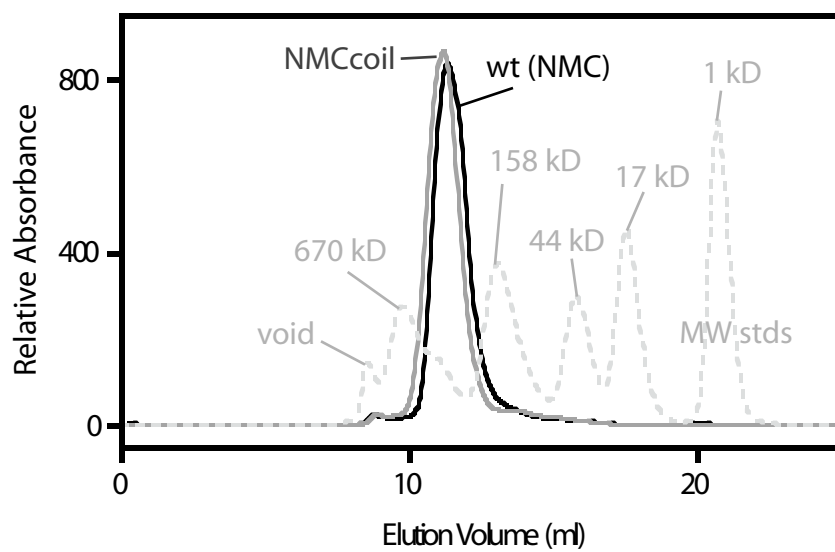
To avoid perturbing Hsp90 function, we chose a small coiled-coil dimerization domain and inserted it into the disordered C-terminal tail of Hsp90. Having multiple dimerization domains in one polypeptide raises the possibility for higher order aggregation. However, analytical ultracentrifugation (Figure 4.2B) confirms that NMCcoil is dimeric at physiological concentration. In addition, higher order oligomers are not observed even at 20-fold higher concentration in size exclusion chromatography (Figure 4.3).

The slow rate of ATP hydrolysis by NMC (about  $1 \text{ min}^{-1}$ ) occurs on the same time scale as subunit exchange (93), raising the possibility that strengthened dimerization may impair ATPase activity. However, we find that NMCcoil hydrolyzes ATP at a rate similar to wild-type NMC lacking the coiled-coil (Figure 4.2C). We confirm that the observed ATPase activity is from Hsp90 by using the Hsp90-specific inhibitor GA. Because Hsp90 interacts with multiple co-chaperones and clients that may be impacted by the coiled-coil inside cells, we next tested the function of super-stabilized NMCcoil dimers to support yeast viability. NMCcoil was introduced into yeast whose only other

**Figure 4.3. Superstabilized NMCcoil is dimeric.**

Superstabilized NMCcoil has a similar elution profile to wild-type Hsp90 on a Sephadex 200 size exclusion column indicating that both molecules assume extended dimeric conformations. Protein samples were injected at about 250  $\mu$ M. The theoretical molecular weight of dimers are 164 kD (wt) and 172 kD (NMCcoil).



**Figure 4.3**

copy of Hsp90 was encoded on a *URA3* marked plasmid subject to negative selection using 5-FOA. We find that NMCcoil supports healthy yeast growth as the sole Hsp90 when 5-FOA was utilized to select for loss of the *URA3* marked plasmid (Figure 4.2D). In addition, NMCcoil expresses to similar steady state levels as NMC (Figure 4.2D). From these results we conclude that the coiled-coil is compatible with Hsp90 function.

***Super-stabilization leads to preferential homodimer assembly.***

To experimentally analyze dimer assembly, we took advantage of the observation that NMC and truncated C-domain form cross-dimers with distinct ATPase activity (93, 126). Increasing C-domain concentration caused a marked decrease in ATPase activity from NMC (Figure 4.4A). In contrast, the strengthened self-association of NMCcoil prevented cross-dimerization with C-domain and resulted in NMCcoil ATPase activity that was refractory to inhibition by C-domain. In principle, the observed lack of ATPase inhibition of NMCcoil by the C-domain could also be caused by either slow kinetics of subunit exchange (and failure to reach equilibrium dimer distributions), or NMCcoil/C-domain heterodimers having robust ATPase activity. In either of these cases, mixtures of NMCcoil and Ccoil would exhibit uninhibited ATPase levels. We find that mixtures of NMCcoil and Ccoil display essentially the same equilibrium ATPase inhibition response as NMC and C mixtures (Figure 4.4B). Thus, NMCcoil dimer exchange equilibrates in the experiment and NMCcoil ATPase activity can be reduced through cross-dimerizing

**Figure 4.4. Superstabilization disfavors cross-dimerization.**

(A) NMCcoil Hsp90 is refractory to cross-dimerization with C-domain subunits lacking the coiled-coil domain. (B) Similarly, superstabilized Ccoil prevents cross-dimerization with NMC subunits lacking the coiled-coil. (C) Hindering cross-dimerization enabled the co-expression of NMCcoil<sup>D79N</sup> with NMC<sup>G170D</sup> without severe growth defects. Growth of yeast expressing the temperature sensitive Hsp90<sup>G170D</sup> alone (left), or in combination with NMCcoil<sup>D79N</sup> (right).

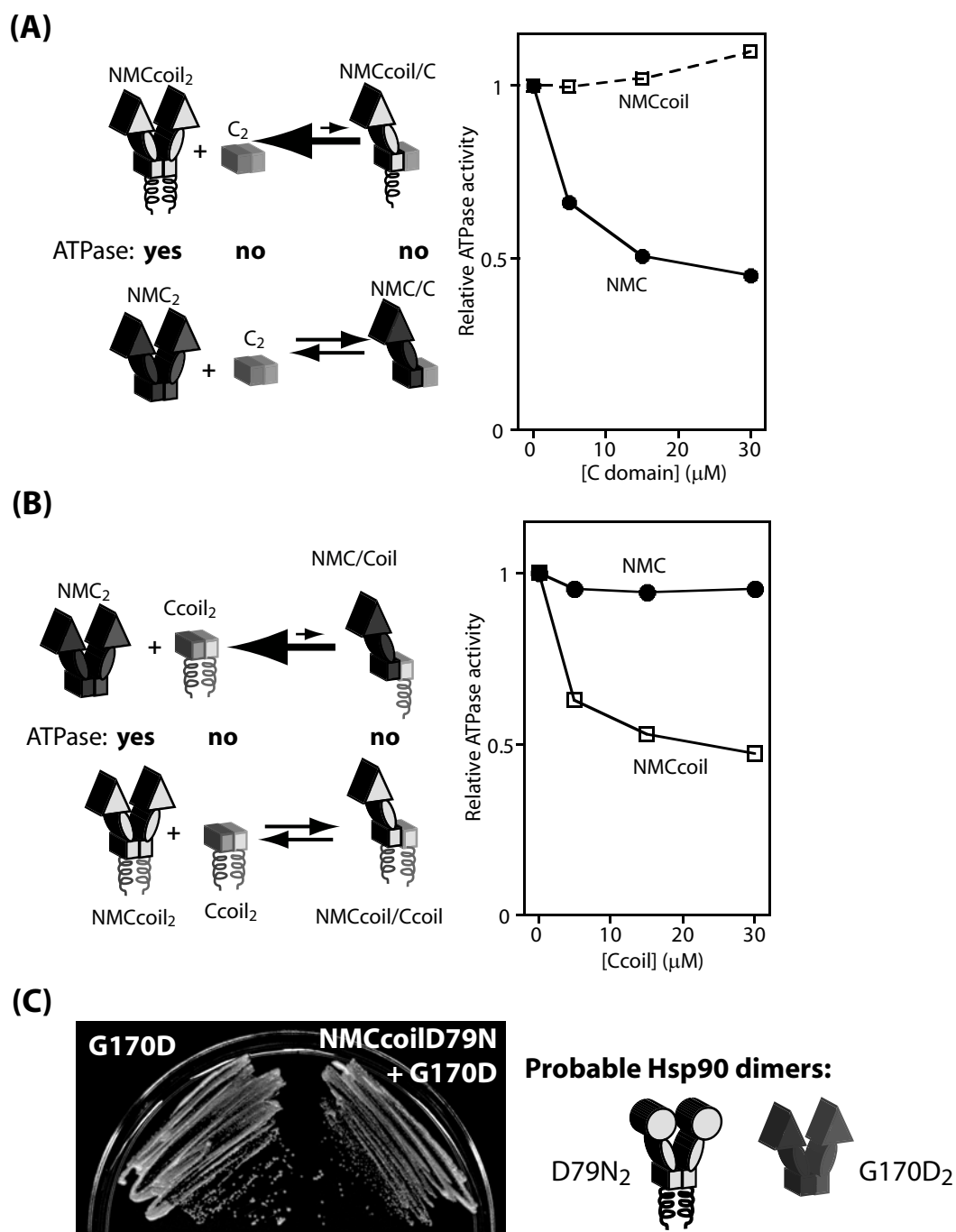


Figure 4.4

with a truncated Ccoil. We conclude that NMCcoil dimers are refractory to cross-dimerization with Hsp90 subunits lacking the coiled-coil.

As observed previously, full-length/C-domain heterodimers have residual ATPase activity (93) which contradicts our finding in Chapter III that Hsp90 monomers have at most 3 % of wild-type ATPase activity (Figure 3.4). When titrating increasing concentrations of C-domain, we are assuming equal dimerization probability for all species based on the observation that full-length and C-domain constructs have similar dimerization constants in the absence of nucleotide. In the ATPase assay, nucleotide promoted dimerization of the NM domains may favor full-length homodimers making the ATPase activity of full-length/C-domain heterodimers an overestimate.

***NMCcoil<sup>D79N</sup> rescues growth when co-expressed with ts NMC<sup>G170D</sup>.***

If the synthetic growth defect of cells co-expressing G170D and D79N point-mutants was caused by cross-dimerization, then preventing cross-dimerization should enable healthy growth of cells expressing both Hsp90 variants. Indeed, we observed that co-expressing NMC<sup>G170D</sup> and NMCcoil<sup>D79N</sup> resulted in healthy growth (Figure 4.4C). This yeast strain is virtually identical to the strain in Figure 4.1A (top), with the exception that cross-dimers are suppressed. The phenotypic effect of this small change

demonstrates the sensitive nature of the complex Hsp90 interactome *in vivo* and underscores the importance of robust regulation of cross-dimers.

***ATPase-deficient Hsp90 mutants function at elevated temperature.***

The yeast system that we developed to study ATPase deficient Hsp90 mutants *in vivo* requires the inactivation of ts NMC<sup>G170D</sup> at elevated temperature; therefore, we first sought to ensure that the ATPase mutants are refractory to heat inactivation at the required temperature of these experiments (37 °C). Temperature scans of both E33A and D79N ATPase-deficient mutants and wild-type NMC, monitored by circular dichroism reproducibly show a small-amplitude transition at about 55 °C (Figure 4.5A). However, because of the small amplitude of this change, we sought a more robust metric of temperature induced Hsp90 mis-folding. Higher order aggregation was the most pronounced physical affect that we observed for mis-folded Hsp90. Using native PAGE, we observed temperature-dependent formation of higher order aggregates for wild-type Hsp90 (Figure 4.5B) that occurred at the same transition temperature observed by CD. Using the native gel approach, we find that both of the ATPase mutants are natively structured at 37 °C (Figure 4.5C). Next, we analyzed the ability of the ATPase mutants to serve as anti-aggregation chaperones, an ATP-independent function of wild-type Hsp90 (88, 90). We performed light-scattering experiments to analyze aggregation of the hard-to-fold CFTR-NBD1. As previously observed (88), NBD1 aggregation at elevated temperatures can be reduced *in vitro* by Hsp90 in the absence of ATP (Figure 4.5D).

**Figure 4.5. Hsp90 ATPase mutants are stable at 37 °C.**

(A) The E33A ATP hydrolysis and D79N ATP binding point mutants as well as wild-type NMC all maintain native secondary structure content as judged by circular dichroism at temperatures up to 50 °C. Data plotted as a change in ellipticity with a +1 offset between samples. (B) Higher order aggregates of wild-type NMC are detectable at temperatures above 55 °C by Coomassie-stained Native PAGE. (C) At 37 °C both point mutants are natively folded as judged by Native PAGE. (D) The ATPase mutants function at 37 °C to rescue aggregation of the hard-to-fold CFTR NBD1 domain *in vitro* (an ATP independent function of Hsp90) as assessed by light scattering of aggregated particles.

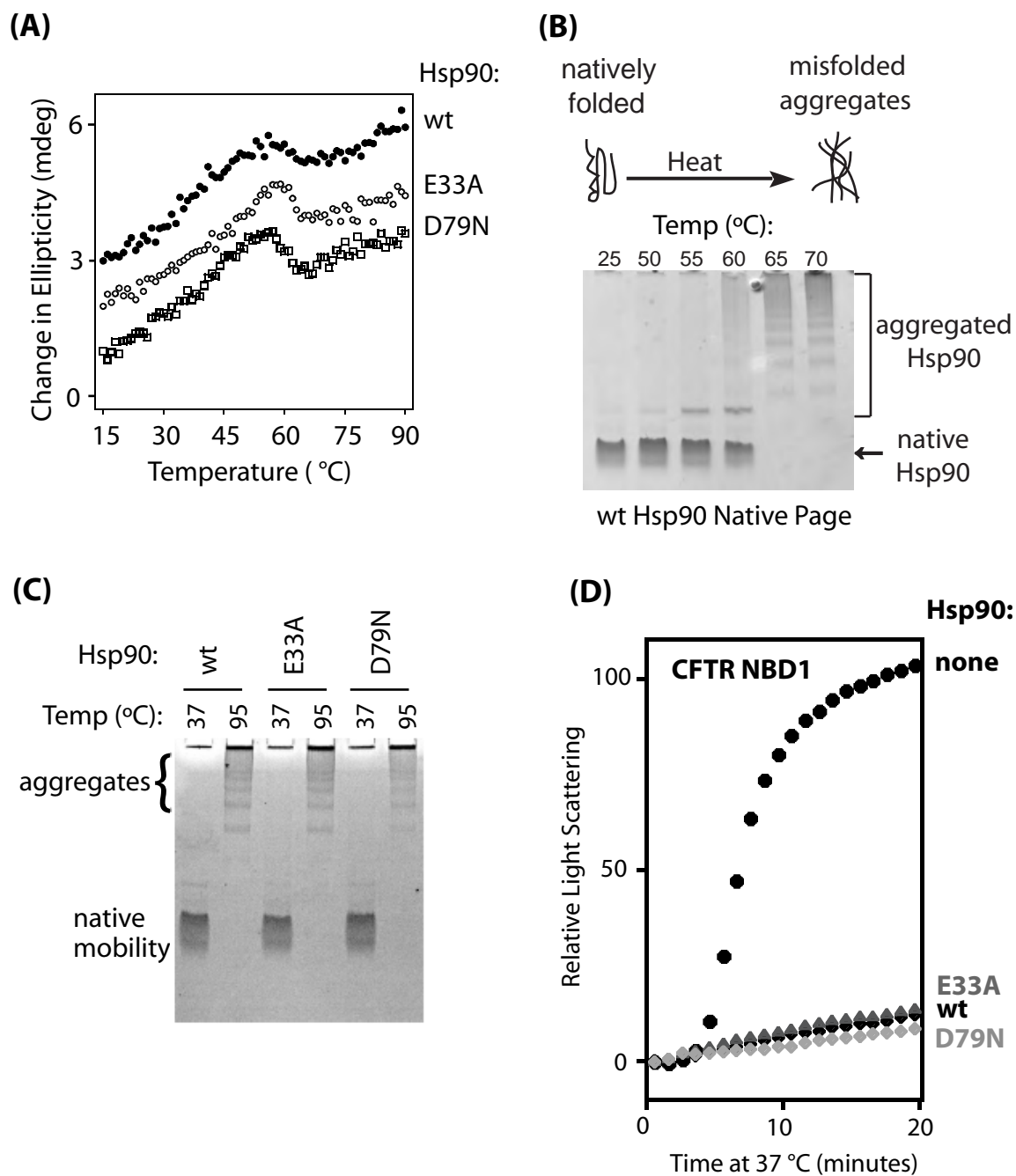


Figure 4.5



Both E33A and D79N NMC are capable of suppressing NBD1 aggregation at 37 °C (Figure 4.5D). From these results, we conclude that the ATPase mutants of Hsp90 are stable at 37 °C.

### ***Maturation of v-src.***

Co-expression of ts NMC<sup>G170D</sup> with ATPase-deficient NMCcoil mutants enabled healthy growth at permissive temperature providing a large reservoir of cells that could be heat inactivated prior to inducing the expression of a client (Figure 4.6 A). When v-src expression was induced at elevated temperature in ts NMC<sup>G170D</sup> yeast, v-src accumulated at relatively low levels and failed to phosphorylate the tyrosines of endogenous yeast proteins (Figure 4.6B). Because yeast have extremely low amounts of endogenous tyrosine kinases, background phosphotyrosine levels were minute. Importantly, both v-src accumulation and kinase function could be rescued by co-expression with wild-type NMC or NMCcoil indicating that the super-stabilizing coiled-coil is compatible with efficient v-src maturation. The E33A and D79N ATPase-deficient NMCcoil mutants both resulted in decreased v-src accumulation and background levels of phosphotyrosine. Accumulation of SspB, a non-Hsp90 dependent protein, is not dramatically impacted by the ATPase mutants indicating that general aspects of transcriptional activation (127) are functional in these cells (Figure 4.6C).

**Figure 4.6. ATPase deficient NMCcoil variants are unable to mature v-src kinase in yeast.**

(A) Experimental setup to analyze ATPase deficient Hsp90 mutants in yeast. (B) In yeast, NMCcoil mutations that disrupt ATP binding (D79N) or hydrolysis (E33A) both lead to reduced v-src accumulation and background levels of tyrosine kinase activity. (C) Induction of general protein expression is only modestly impacted by the NMCcoil ATPase mutants as evidenced by the accumulation of a non-Hsp90 client, the SspB protein from *E. coli*.

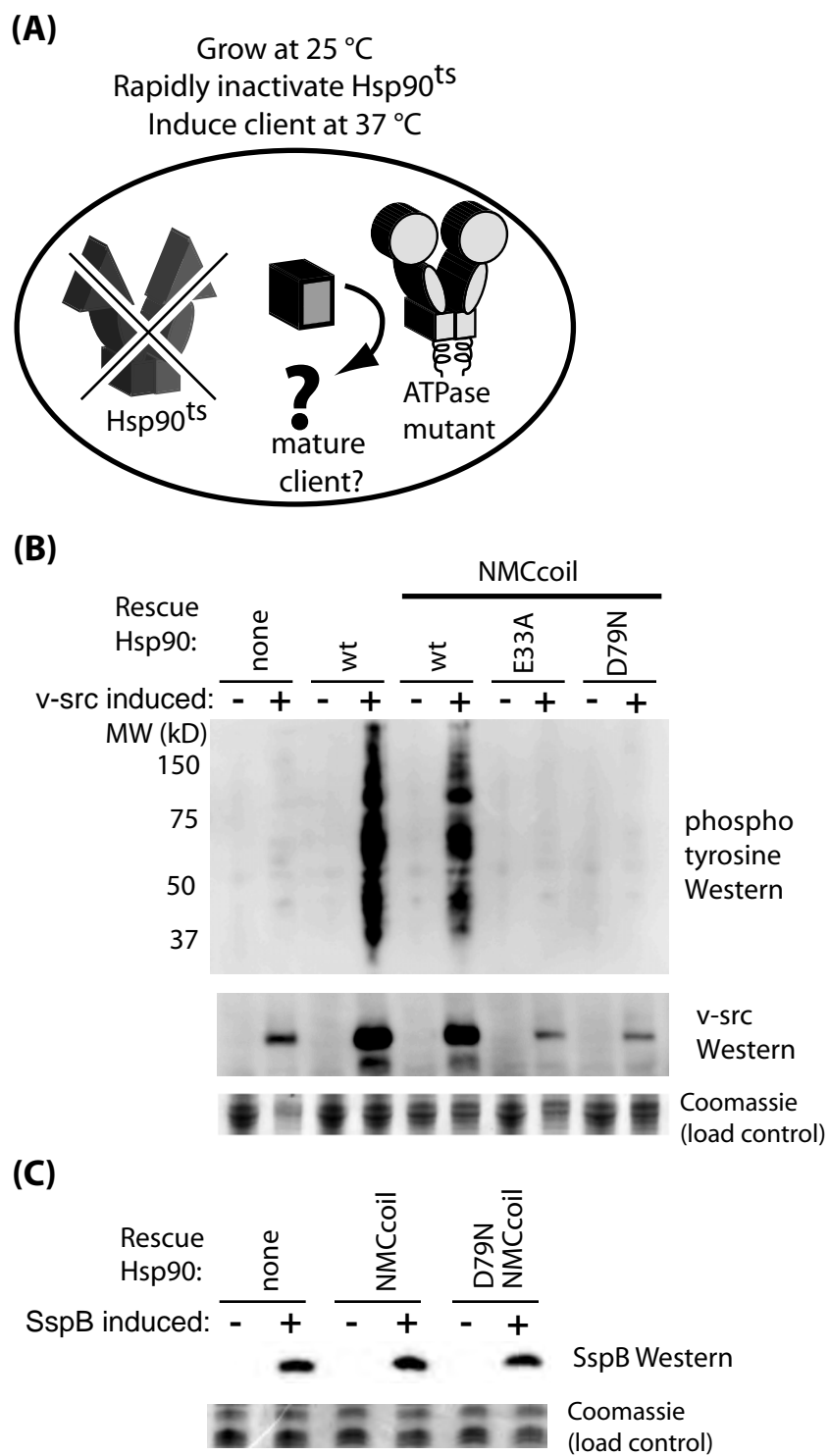


Figure 4.6

***Glucocorticoid receptor (GR) activation.***

GR transcriptional activation in response to the hormone activator deoxycorticosterone (DOCS) was monitored using a  $\beta$ -galactosidase reporter (7). Yeast harboring wild-type NMC showed a robust increase in hormone-stimulated reporter activity compared to yeast whose sole source of Hsp90 was heat inactivated (Figure 4.7A). We observed similar hormone stimulated GR activity with both wild-type NMC and NMCcoil indicating that the coiled-coil fusion is compatible with efficient hormone receptor activation. Both the ATP binding mutant (D79N) and the ATP hydrolysis mutant (E33A) NMCcoil variants showed markedly reduced GR activity indicating that both ATP binding and hydrolysis by Hsp90 are important for efficient hormone receptor activation. The accumulation of GR was impacted by the ATPase mutants with E33A and D79N resulting in increased accumulation of GR (Figure 4.7B).

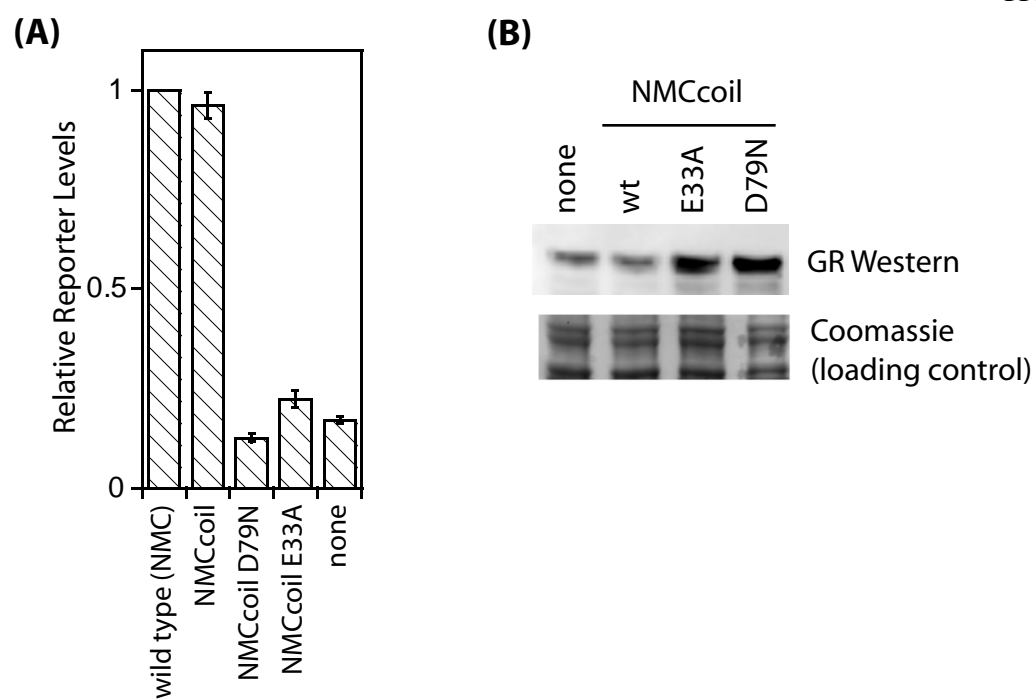
***Hsp90 dimers constitute the essential biological oligomer.***

Hsp90 dimers transiently dissociate to monomers on the same time scale as ATP hydrolysis (93) leading to the possibility that both monomers and dimers are part of the chaperone cycle. In contrast to the rapid dimer exchange of wild-type subunits, we observed that super-stabilized NMCcoil dimers have a half-life of eight hours to equilibrate (Figure 4.8A). NMC dimers equilibrate with a half-life of about 30 seconds (Figure 4.9). These results indicate that dimer dissociation is the rate limiting step in the

**Figure 4.7. Hsp90 ATPase mutants do not mature GR in yeast.**

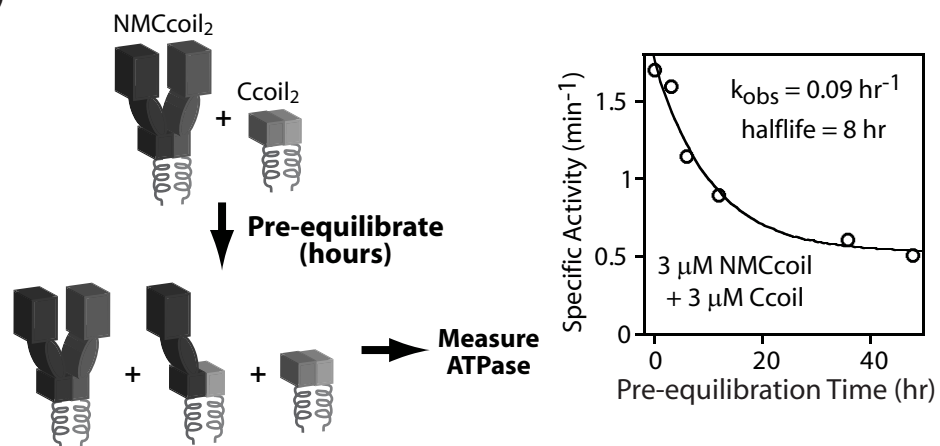
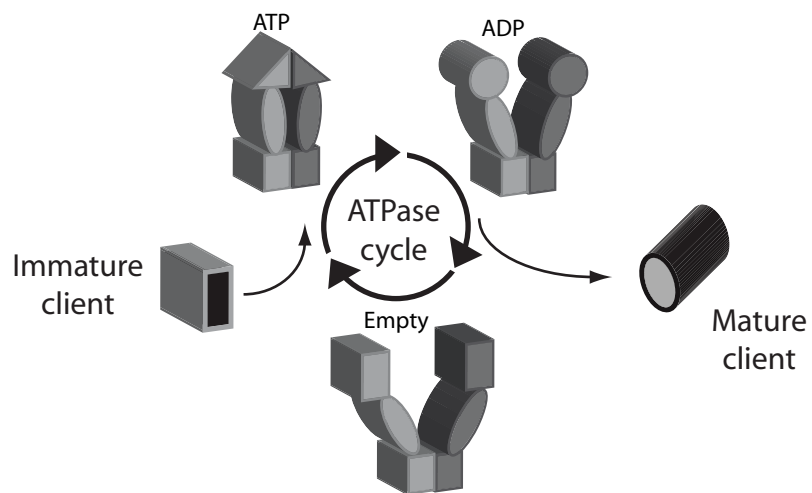
(A) Glucocorticoid receptor activation monitored in yeast. Yeast with the temperature sensitive NMC<sup>G170D</sup> as well as ATPase deficient NMCcoil variants were heated to inactivate NMC<sup>G170D</sup> prior to stimulation with saturating levels of DOCS (10  $\mu$ M). Neither D79N nor E33A NMCcoil resulted in reporter activity levels significantly greater than background using a single-tailed student T-test. Error bars represent SEM.

(B) Expression level of GR analyzed by Western blots of yeast lysates.

**Figure 4.7**

**Figure 4.8. Dimers of Hsp90 constitute the essential biological oligomer whose ATPase function is required for maturation of clients.**

(A) NMCcoil reduces the rate of subunit exchange to time-scales that are irrelevant to the biochemical function of Hsp90 *in vivo*. Truncated and full-length protein were mixed and allowed to exchange subunits prior to assessing the amount of full-length/full-length dimers by monitoring specific ATPase activity. (B) Model of the ATPase dependent function of Hsp90 dimers *in vivo*. ATP hydrolysis by Hsp90 dimers leads to the maturation of clients.

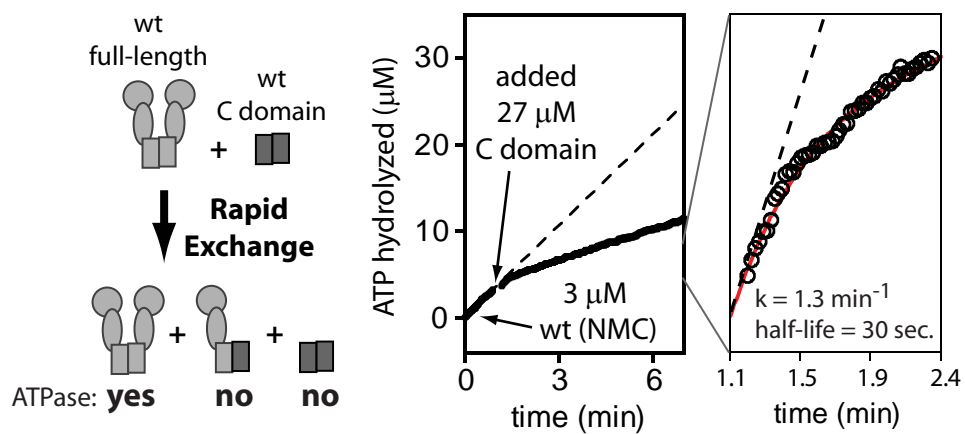
**(A)****(B)****Figure 4.8**



**Figure 4.9. Subunit exchange of Hsp90 dimers.**

(A) Wild-type Hsp90 exchanges dimer subunits rapidly. Addition of excess truncated C-domain leads to the rapid formation of full-length/C-domain heterodimers. (B) Addition of a coiled-coil dimerization domain to the C terminus of Hsp90 stabilizes the dimer state and slows dimer exchange.

(A)



(B)

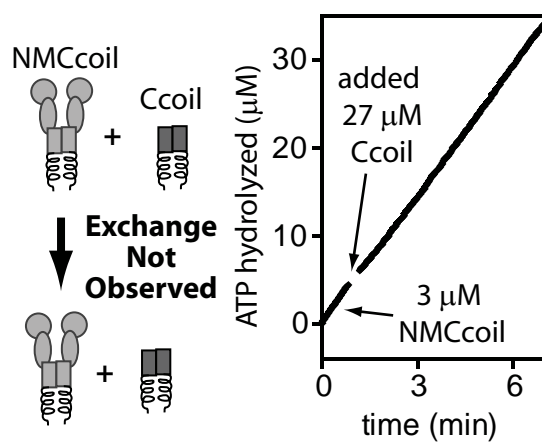


Figure 4.9

dimer exchange reaction and that NMCcoil Hsp90 dimers dissociate on a time scale that is too slow to be relevant for cellular processes such as signal transduction. Our observation that NMCcoil hydrolyzes ATP at a similar rate to NMC indicates that dissociation of yeast Hsp90 subunits is not required for ATP hydrolysis *in vitro*. In addition, our observations that NMCcoil Hsp90 function is indistinguishable from wild-type Hsp90 *in vivo* indicate that Hsp90 dimers are capable of providing all essential functions (Figure 4.8B).

## Discussion

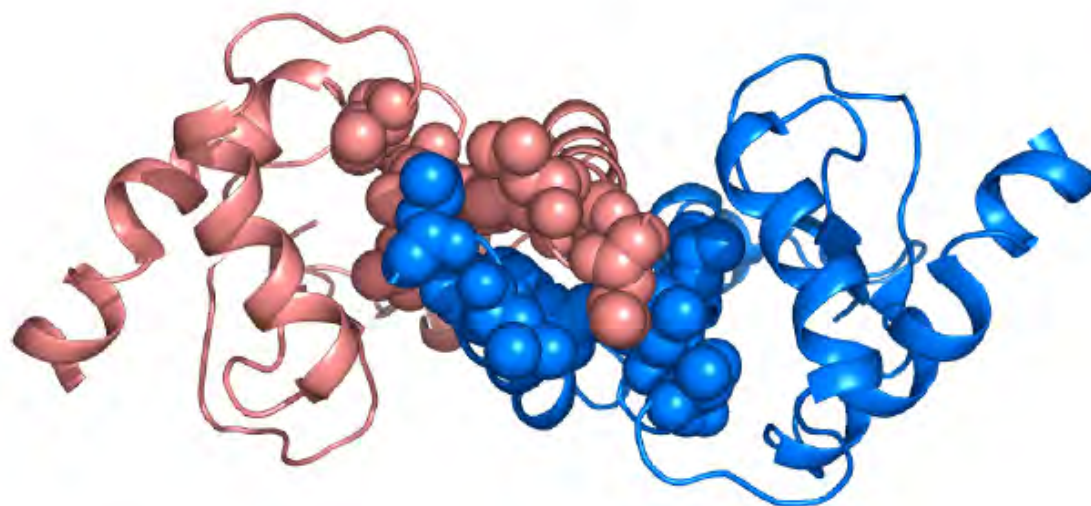
The ability of NMCcoil to efficiently chaperone clients and support viability shows that super-stabilized Hsp90 dimers are functional *in vivo*. The strength of NMCcoil subunit association *in vivo* may be influenced by interactions with co-chaperones. However, the 1000-fold reduced rate of subunit exchange observed *in vitro* for NMCcoil (Figure 4.8A) makes it probable that subunit association is also strengthened *in vivo*. In addition, appending the coiled-coil to D79N rescues robust growth of yeast with the temperature sensitive G170D (Figure 4.4C) consistent with the coiled-coil strengthening dimerization and preventing subunit mixing *in vivo*. Together these results indicate that strengthened subunit association is compatible with Hsp90 function.

C-domain dimerization is critical for Hsp90 function. We have observed that strengthened Hsp90 dimerization is compatible with function and previously reported that preventing association of Hsp90 subunits abrogates chaperone function (126). Of note, the C-domain dimer interface is composed of a large patch of hydrophobic amino acids rich in Ile, Val, and Leu (Figure 4.10). Protein folding studies indicate that clusters of these three aliphatic amino acids form strong associations capable of directing folding pathways (128, 129). The aliphatic patch at the C-domain dimer interface is consistent with the critical role of subunit association in the function of the Hsp90 and our observations that subunit dissociation does not appear to be required for essential Hsp90 function.

The value of preventing cross-dimerization in co-expression studies is dramatically illustrated by the growth defect caused by co-expression of NMC<sup>D79N</sup> and NMC<sup>G170D</sup>. This growth defect is clearly mediated by the formation of NMC<sup>D79N/G170D</sup> heterodimers as healthy growth is restored when cross-dimerization is abrogated using NMCcoil<sup>D79N</sup> homodimers. The growth defect caused by NMC<sup>D79N/G170D</sup> heterodimers could formally be due to either depletion of NMC<sup>G170D</sup> homodimers or by toxicity of the NMC<sup>D79N/G170D</sup> heterodimers. In either case, using NMCcoil ATPase mutant homodimers to prevent cross-dimerization enabled direct analysis of the activity of both E33A and D79N ATPase mutants without contributions from cross-dimer species.

**Figure 4.10. Molecular image of the C-domain dimer interface of Hsp90.**

Molecular image highlighting the cluster of ILV (Ile, Val and Leu) positions. The C-domain is shown in cartoon form from position 540-680 of the PDB file 2CG9 and the ILV amino acids are shown as spheres (amino acids V639, L642, L645, L646, I668, L671, I672, L674, and L676) .



**Figure 4.10**

Our experiments clearly demonstrate that ATP binding and hydrolysis by Hsp90 are required for the maturation of both v-src and GR in *S. cerevisiae*. Mutations that abrogate the hydrolytic-activating glutamate (E33A) or binding to the adenine ring (D79N) both resulted in null levels of v-src and GR activity *in vivo*. These findings provide important confirmation that the ATPase based models proposed for Hsp90 activity *in vitro* (9, 17, 18, 130) extend to Hsp90 function *in vivo*. The mechanistic details of Hsp90 ATPase activity have been well-examined in its purified form (22, 93, 124); however, until now it has not been possible to extend these analyses monitoring client activation *in vivo*. Our findings that E33A and D79N NMCcoil fail to mature GR *in vivo* are consistent with previous observations that analogous mutations prevent Hsp90 from stimulating the binding of progesterone receptor to its hormone ligand *in vitro* (66). Many studies demonstrate that Hsp90's primary role in stimulating hormone receptors is opening of the receptor to enable access of hormone to the otherwise sequestered binding site (131). Our results indicate that *in vivo* this process requires both ATP binding and hydrolysis.

We have presented a modular strategy to control cross-oligomerization and utilized it to analyze ATPase mutants of Hsp90 in a temperature sensitive yeast background. These studies confirm the critical role of ATP binding and hydrolysis by Hsp90 in the maturation of kinases and steroid hormone receptors *in vivo*. The super-stabilized Hsp90 tools that we developed provide a foundation to explore other non-

viable Hsp90 mutants *in vivo* and to extend our analysis to other clients. Because our super-stabilization strategy is based on coiled-coil peptides whose characteristics are extremely modular, it is directly applicable to many homodimeric systems. In addition, the existence of  $\alpha$ -helical peptides that specifically self-assemble with different orders including dimers, trimers, tetramers, and pentamers (132, 133) make the approach described here widely applicable to the investigation of homo-oligomeric systems.

From the engineering of a monomeric Hsp90 variant, it is clear that dimerization of Hsp90 is critical for efficient ATP hydrolysis as well as the activation of a kinase and a steroid hormone receptor client (126). How each subunit in the Hsp90 dimer binds to and hydrolyzes ATP during the maturation of a client remains unclear.



## CHAPTER V

### **Charge-rich regions modulate the anti-aggregation activity of Hsp90**

This work was previously published as:

Natalie Wayne and Daniel N. Bolon. (2010) Charge-Rich Regions Modulate the Anti-Aggregation Activity of Hsp90. *Journal of Molecular Biology*. **401**(5):931-9.

## **Abstract**

Protein aggregation can have dramatic effects on cellular function and plays a causative role in many human diseases. In all cells, molecular chaperones bind to aggregation-prone proteins and hinder aggregation. The ability of a protein to resist aggregation and remain soluble in aqueous solution is linked to the physical properties of the protein. Numerous physical studies demonstrate that charged atoms favor solubility. We note that many molecular chaperones possess a substantial negative charge that may allow them to impart solubility on aggregation-prone proteins. Hsp90 is one such negatively charged molecular chaperone. The charge on Hsp90 is largely concentrated in two highly acidic regions. To investigate the relationship between chaperone charge and protein solubility, these charge-rich regions were deleted and the resulting Hsp90 constructs analyzed for anti-aggregation activity. We found that deletion of both charge-rich regions dramatically impaired Hsp90 anti-aggregation activity. The anti-aggregation role of the deleted charge-rich regions could be due to net charge or sequence-specific features. To distinguish these possibilities, we attached an acid-rich region with a distinct amino acid sequence to our double-deleted Hsp90 construct. This charge-rescue construct displayed effective anti-aggregation activity indicating that the net charge of Hsp90 contributes to its anti-aggregation activity.

## Introduction

The propensity of a protein to aggregate is linked to the physical properties of the protein. Understanding these physical properties has important implications for many biological processes that involve protein aggregation including numerous human diseases (*134-139*). The propensity of a protein to aggregate is governed by the energetic and kinetic balance between interactions of the protein with solvent versus self-association. Both of these interactions must be considered in order to understand the process of protein aggregation.

The strength of protein self-association is dramatically influenced by hydrophobic contacts (*140*). By chemical definition, hydrophobic groups prefer to associate with other hydrophobic groups relative to aqueous solvent. In order to remain soluble, most natively-folded cytoplasmic proteins sequester hydrophobic side-chains from solvent in the core of the protein. These hydrophobic side-chains become increasingly exposed to solvent when proteins transiently sample mis-folded conformations. For this reason, mis-folded conformations frequently aggregate in an energetic effort to bury exposed hydrophobic surfaces (*141*).

In contrast to hydrophobic effects, charged amino acids have been shown to increase protein solubility. It is well appreciated in biochemistry that proteins are usually least soluble at a pH where their net charge is zero (*142*). From a chemical perspective,

charged groups interact favorably with aqueous solvent and are unlikely to self-associate. Coulombic repulsive forces between like-charges also influence self-association. Experimentally increasing the net charge of aggregation-prone proteins, and increasing Coulombic self-repulsion, has been shown to improve protein solubility (97, 143).

Because aggregation is a concentration-dependent event, the aggregation of mis-folded proteins is enhanced by the crowded environment of the cell (136, 141, 144, 145). In cells, many aggregation-prone proteins rely on interactions with molecular chaperones (136, 137, 141, 144-146). Molecular chaperones hinder protein aggregation and facilitate folding and assembly of proteins into higher order structures (146-148). Many molecular chaperones bind to mis-folded proteins and reduce aggregation by shielding hydrophobic side-chains from bulk solvent (141). For example, the GroEL (Hsp60) chaperone forms a closed barrel around mis-folded proteins, effectively shielding the entire protein from bulk solvent (149, 150).

Other chaperones, including Hsp90 and Hsp70, have smaller hydrophobic patches capable of binding to mis-folded proteins and partially shielding exposed hydrophobic side-chains from solvent (151, 152). Because these systems do not form closed barrels, they cannot completely shield mis-folded proteins from solvent exposure. The solubility of this type of complex may benefit from additional pro-solubility mechanisms. A high net charge on the chaperone complex is one physical property that may improve

solubility. The net charge on a chaperone complex has the potential to influence solubility through direct solvent interactions and Coulombic self-repulsion.

## Results

### *Negative charge is a common feature of molecular chaperones.*

We observed that three chaperones with anti-aggregation activity (Hsp90, Hsp70, and Hsp33) are characterized by a high negative charge that is evolutionarily conserved (Tables 5.1 and 5.2). These three highly charged chaperones all have hydrophobic patches that are could partially shield mis-folded proteins from solvent (151-153). In addition, the Hsp60 chaperone completely encloses mis-folded proteins (149) and is not highly charged. For comparison, the non-chaperone protein triosphosphate isomerase is also not highly charged. These observations suggest that the conservation of negative charge we observed for Hsp90, Hsp70, and Hsp33 may be due to shared mechanisms of anti-aggregation activity.

Hsp90 was one of the most highly charged chaperones we analyzed. It is known to suppress the *in vitro* aggregation of numerous proteins including citrate synthase, amyloid beta, p53, and the nucleotide binding domain of the cystic fibrosis transmembrane conductance regulator (CFTR-NBD1) (85-88). The ability of Hsp90 to suppress protein aggregation *in vitro* often does not require ATP (88-90). Hsp90 is an abundant protein under physiological conditions and its level increases in response to cell

**Table 5.1.** Charge conservation of select cytoplasmic proteins

Molecular Chaperone	Average charge per 100 amino acids ( $\pm$ SD; n=6 <sup>a</sup> )
Hsp90	-5.0 $\pm$ 0.4
Hsp70	-2.5 $\pm$ 0.9
Hsp33	-5.6 $\pm$ 2.0
Hsp60	-1.1 $\pm$ 0.4
Triosephosphate Isomerase <sup>b</sup>	-0.7 $\pm$ 0.5

<sup>a</sup>Net charge of each chaperone was averaged for six species (Table 5.2).

<sup>b</sup>Non-chaperone cytoplasmic protein analyzed for comparison.

**Table 5.2.** Protein charge analysis of select cytoplasmic proteins

Species	GenBank accession number	net charge <sup>a</sup>	number of amino acids	charge per 100 amino acids
Hsp90				
<i>Homo sapiens</i>	NP 005339	-39.2	731	-5.4
<i>Mus musculus</i>	NP 034610	-40.2	733	-5.5
<i>Drosophila melanogaster</i>	NP 523899	-35.5	717	-5.0
<i>Caenorhabditis elegans</i>	Q18688	-31.8	702	-4.5
<i>Saccharomyces cerevisiae</i>	CAA97961	-37.3	709	-5.3
<i>Arabidopsis thaliana</i>	CAA68885	-31.8	704	-4.5
Hsp70				
<i>Homo sapiens</i>	EAX03528	-10.1	641	-1.6
<i>Mus musculus</i>	AAC84169	-10.0	641	-1.6
<i>Drosophila melanogaster</i>	NP 524798	-11.6	642	-1.8
<i>Caenorhabditis elegans</i>	P27420	-26.1	661	-4.0
<i>Saccharomyces cerevisiae</i>	AAC04952	-20.3	642	-3.2
<i>Arabidopsis thaliana</i>	CAA05547	-18.1	650	-2.8
Hsp33				
<i>Synechococcus elongatus</i>	BAD79153	-14.5	297	-4.9
<i>Gloeobacter violaceus</i>	Q7NIA2	-11.5	306	-3.8
<i>Lactobacillus plantarum</i>	AAU05733	-15.1	295	-5.1
<i>Streptococcus pneumoniae</i>	P64403	-15.6	290	-5.4
<i>Bacillus subtilis</i>	1VZY A	-12.6	291	-4.3
<i>Escherichia coli</i>	AP 004389	-29.1	292	-10.0
Hsp60				
<i>Homo sapiens</i>	AAA36022	-4.7	573	-0.8
<i>Mus musculus</i>	NP 034607	-3.5	573	-0.6
<i>Drosophila melanogaster</i>	NP 511115	-6.9	573	-1.2
<i>Caenorhabditis elegans</i>	NP 497429	-7.9	568	-1.4
<i>Saccharomyces cerevisiae</i>	CAY81488	-10.8	572	-1.9
<i>Arabidopsis thaliana</i>	CAA77646	-4.0	577	-0.7
Trisosephosphate Isomerase				
<i>Homo sapiens</i>	CAA49379	-0.7	249	-0.3
<i>Mus musculus</i>	CAA37420	0.3	249	0.1
<i>Drosophila melanogaster</i>	CAA40804	-1.8	247	-0.7
<i>Caenorhabditis elegans</i>	NP 496563	-1.5	247	-0.6
<i>Saccharomyces cerevisiae</i>	EDN60396	-2.8	248	-1.1
<i>Arabidopsis thaliana</i>	AAF70259	-4.0	254	-1.6

<sup>a</sup>Predicted net charge at pH 7, determined with the program SEDNTERP.

stress where the probability of protein mis-folding and aggregation is increased (5, 154). Hsp90 can act as a holder chaperone, protecting mis-folded proteins from unfolding further and maintaining them in a folding-competent state (90, 155).

The negative charge of Hsp90 is largely localized in two regions of the protein (Figure 5.1A). The acid-rich charged linker (CL) is located between the structured N-terminal and middle domains of Hsp90. The other acidic region is located at the C-terminus and is referred to here as the C-terminal extension (CX). Both of these regions are believed to be unstructured based on amino-acid composition and were deleted in the full-length crystal structure of Hsp90 (10).

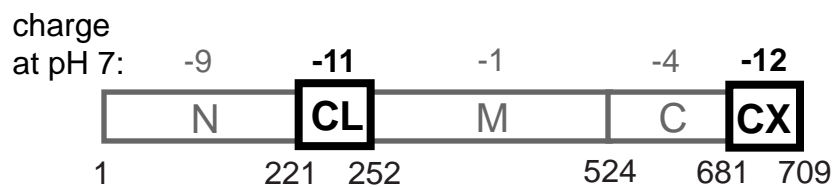
Both highly charged regions of Hsp90 can be individually deleted without compromising essential chaperone function (94). Flexible regions at the ends of the acid-rich CL are required for essential chaperone function (156) and were retained in all constructs reported here. Hsp90, like many other chaperones, (150, 152) is believed to utilize hydrophobic surfaces to bind to exposed hydrophobic regions of mis-folded proteins (151). The acid-rich CL and CX (Figure 5.1A) are among the least hydrophobic regions of Hsp90 (Figure 5.2) (157). Thus, deletion of the CL and CX is unlikely to interfere with Hsp90 binding to mis-folded proteins. These dispensable charge-rich regions provide a convenient system to investigate the role of charge in Hsp90 anti-aggregation activity.



**Figure 5.1. Hsp90 constructs to test the role of charge-rich regions in anti-aggregation activity.**

(A) Schematic representation of *Saccharomyces cerevisiae* Hsp90. Hsp90 is composed of an N-terminal domain (N), charged-linker (CL), middle domain (M), C-terminal domain (C), and C-terminal extension (CX). The charge of Hsp90 is highly concentrated in the acid-rich CL and CX regions. (B) To test the role of these charge-rich regions in Hsp90 anti-aggregation activity, we made Hsp90 deletion constructs with reduced net charge.

(A)



**CL** = **E**E**E****K****K****D**E**E****K****K****D**E**E****K****D**E**D****D****K****K****P****K****L**E**E****V****D**E**E**E**E**

**CX** = **D**E**E****T**E**T**A**P**E**A**S**T**A**A****P****V**E**E****V****P**A**D**T**E**M**E**E**V****D**

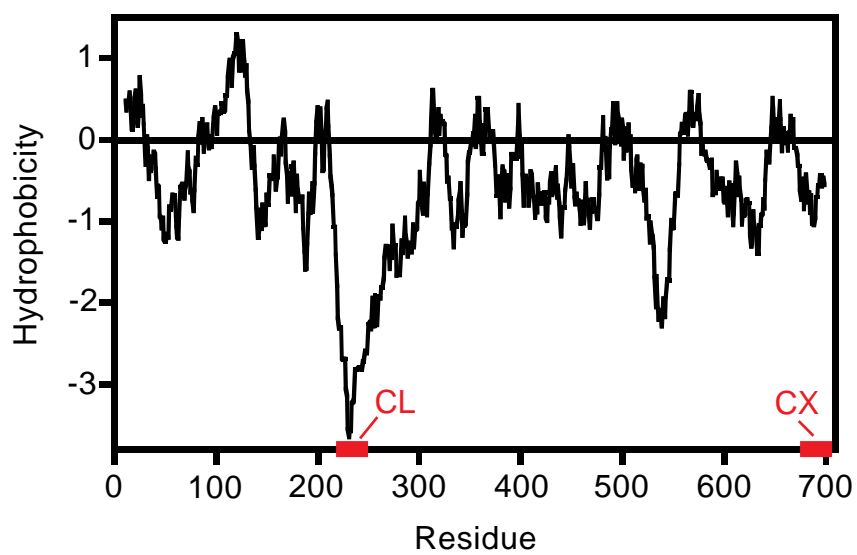
(B)

Hsp90 construct	mutations	net charge
wild-type  CL      CX	none	-37
$\Delta$ CL  CL      CX	$\Delta$ 221-252	-26
$\Delta$ CX  CL      CX	$\Delta$ 681-709	-25
$\Delta$ CL $\Delta$ CX  CL      CX	$\Delta$ 221-252 $\Delta$ 681-709	-14

Figure 5.1

**Figure 5.2. Hydrophobicity Plot for Hsp90.**

Hydrophobicity of individual Hsp90 residues determined based on the Kyte-Doolittle scale using the ExPASy proteomics server from the Swiss Institute of Bioinformatics (157).



**Figure 5.2**

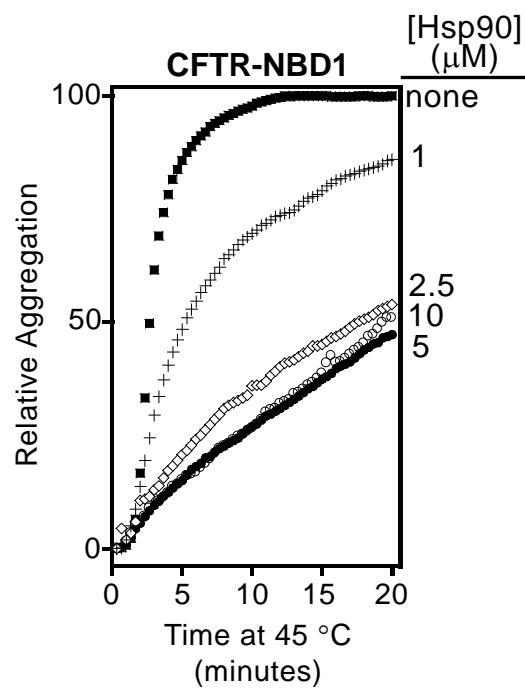
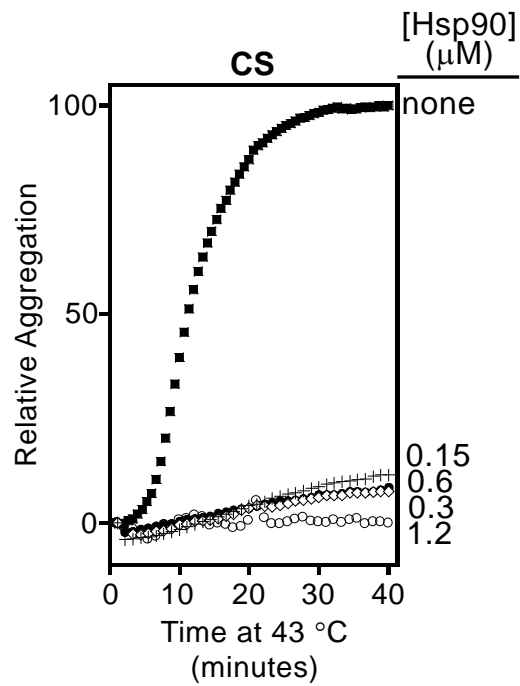
***The charge-rich regions of Hsp90 influence anti-aggregation activity.***

To test the role of charge in Hsp90 anti-aggregation activity, we generated constructs where the CL, the CX, or both were deleted. Hsp90 has previously been shown to reduce the aggregation of CFTR-NBD1, which is highly prone to aggregation at elevated temperatures (Figure 5.3) (88, 158). Hsp90 constructs lacking either the charged linker ( $\Delta$ CL) or the C-terminal extension ( $\Delta$ CX) maintained near wild-type anti-aggregation activity (Figure 5.4A), consistent with previous observations that deleting the charged linker from the N-domain resulted in only a modest impact on insulin aggregation (159). However, the Hsp90 construct lacking both the charged linker and the C-terminal extension ( $\Delta$ CL $\Delta$ CX) was inefficient at suppressing CFTR-NBD1 aggregation.

Deletion of the CL and CX reduces the net charge of Hsp90 and may therefore have unfavorable effects on the solubility of the chaperone. To test this possibility, we measured the propensity of our Hsp90 constructs to aggregate at elevated temperature in the absence of CFTR-NBD1. We found that deletion of the CL and the CX of Hsp90 does not impair the solubility of the chaperone under conditions where CFTR-NBD1 aggregates (Figure 5.4A right panel, Figure 5.5). These results indicate that the charge-rich regions of Hsp90 are important for suppressing CFTR-NBD1 aggregation, but not for the solubility of Hsp90.

**Figure 5.3. Suppression of CFTR-NBD1 and CS aggregation by Hsp90.**

The ability of Hsp90 to suppress CFTR-NBD1 (A) and CS (B) aggregation was measured with different concentrations of Hsp90. Of note, we find that different preparations of CFTR-NBD1 vary in the amount of aggregation that can be suppressed by Hsp90. However, for a given preparation, we find that aggregation suppression is very reproducible.

**(A)****(B)****Figure 5.3**

**Figure 5.4. Charge-rich regions influence the anti-aggregation activity of Hsp90.**

(A) The combined deletion of both the CL and CX impaired the ability of Hsp90 to suppress CFTR-NBD1 aggregation at elevated temperature measured by right angle light scattering (left panel). In the absence of CFTR-NBD1, all Hsp90 constructs maintained wild-type solubility at 45 °C (right panel). (B) The combined deletion of both the CL and CX also impaired the ability of Hsp90 to suppress CS aggregation at elevated temperature measured by right angle light scattering (left panel). In the absence of CS, all Hsp90 constructs maintained wild-type solubility at 43 °C (right panel).



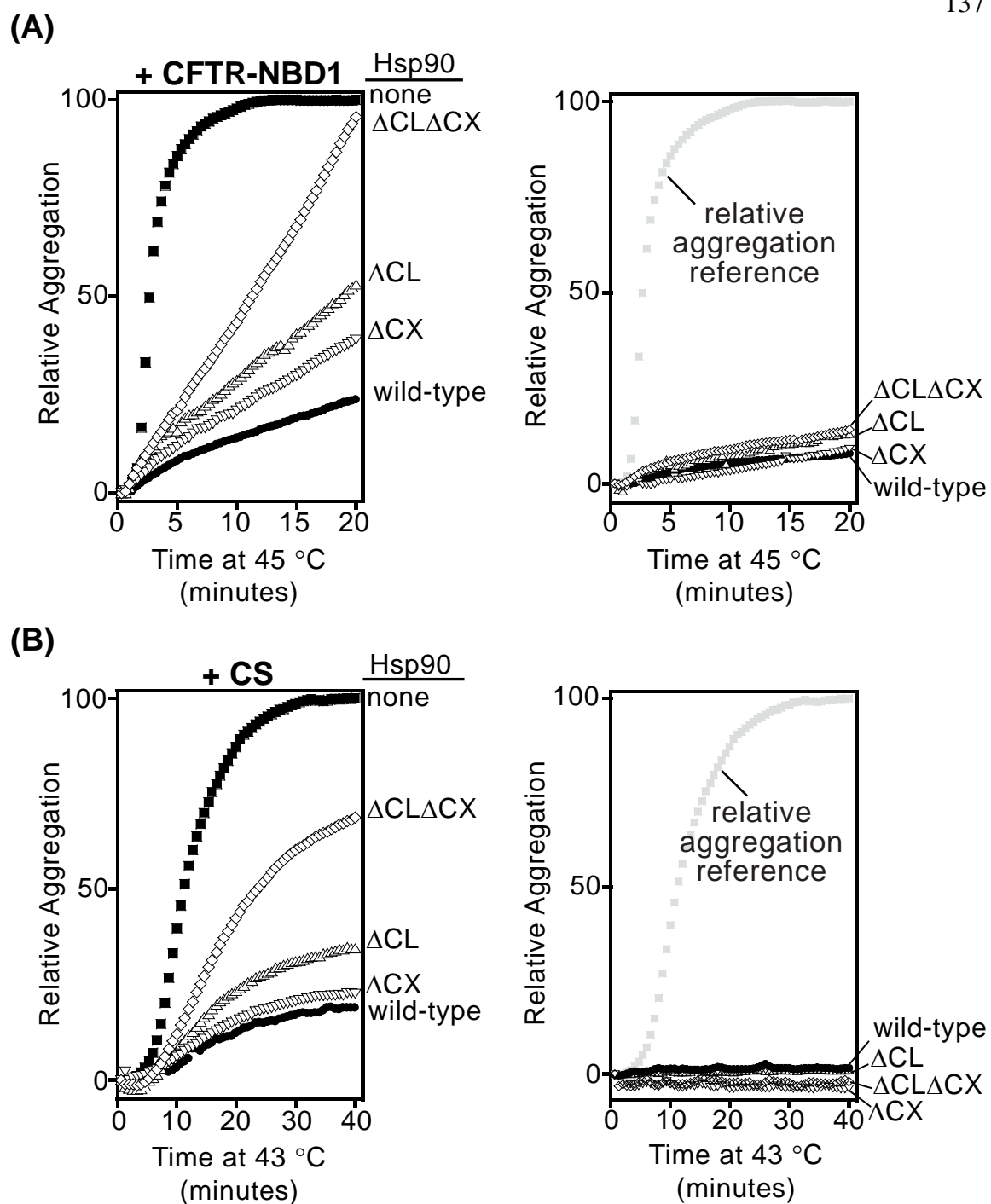
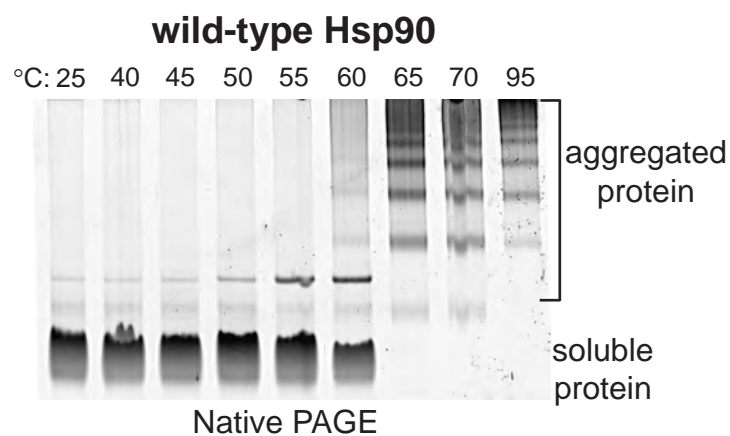
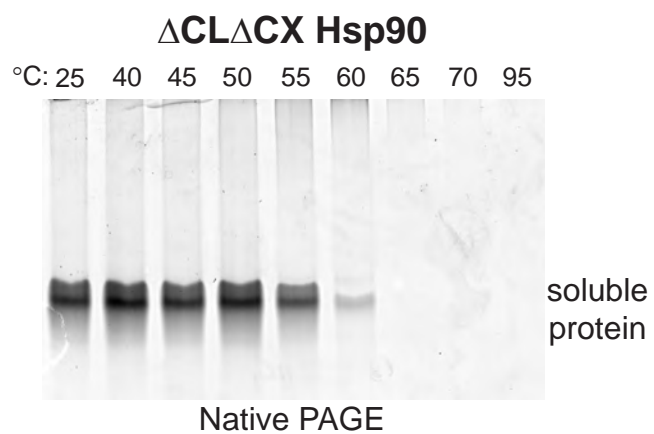


Figure 5.4

**Figure 5.5. Solubility of wild-type and  $\Delta\text{CL}\Delta\text{CX}$  Hsp90.**

The solubility of wild-type (A) and  $\Delta\text{CL}\Delta\text{CX}$  (B) Hsp90 was analyzed by heating protein samples to the indicated temperature for five minutes and separating soluble and aggregated protein by Native PAGE.

**(A)****(B)****Figure 5.5**

We next investigated how charge-rich regions of Hsp90 affect the aggregation of a different mis-folded protein, citrate synthase (CS). Previous studies demonstrate that wild-type Hsp90 is able to suppress the temperature-induced aggregation of CS (Figure 5.3) (85). As observed for CFTR-NBD1, the  $\Delta$ CL and  $\Delta$ CX Hsp90 constructs maintained near wild-type anti-aggregation activity while  $\Delta$ CL $\Delta$ CX was inefficient at suppressing CS aggregation (Figure 5.4B). Under the conditions of the CS aggregation experiments, our Hsp90 constructs do not aggregate in the absence of CS (Figure 5.4B right panel, Figure 5.5). Together, these results indicate that the charge-rich regions are important for the anti-aggregation activity of Hsp90 for two different proteins.

Given the striking impact of deleting both charge-rich regions of Hsp90 on anti-aggregation activity, we wondered if  $\Delta$ CL $\Delta$ CX was itself mis-folded. To address this question we analyzed the secondary structure by circular dichroism (CD). We find that  $\Delta$ CL $\Delta$ CX contains secondary structure that is indistinguishable from wild-type Hsp90 and the individual  $\Delta$ CL and  $\Delta$ CX constructs (Figure 5.6A). We next considered the possibility that deleting both charge-rich regions thermodynamically destabilized Hsp90. Thermodynamic stability can be measured by monitoring the concentration of urea required to unfold the protein. We observed that similar concentrations of urea were required to unfold all of our constructs (Figure 5.6B). These results indicate that the folded domains of  $\Delta$ CL $\Delta$ CX are well-folded and thermodynamically stable compared to wild-type Hsp90. It is also possible that deletion of the CL and CX disrupts the Hsp90

**Figure 5.6. Deletion of charge-rich regions does not disrupt the Hsp90 dimer or essential function.**

(A) CD analysis indicated that all Hsp90 constructs have secondary structure content similar to wild-type. (B) All Hsp90 constructs unfold at similar concentrations of urea. The midpoint concentration ( $C_m$ ) of urea required to denature Hsp90 was unchanged by deletion of the CL and CX (Table 5.3). (C)  $\Delta CL\Delta CX$  Hsp90 behaves as a dimer during analytical ultracentrifugation. Single-species fit indicates that the molecular mass is 155 kDa (similar to the theoretical mass of a dimer: 151 kDa). The fit for a theoretical monomer is shown in grey for comparison. (D) Hsp90 constructs lacking the CL and CX were capable of hydrolyzing ATP similar to wild-type.

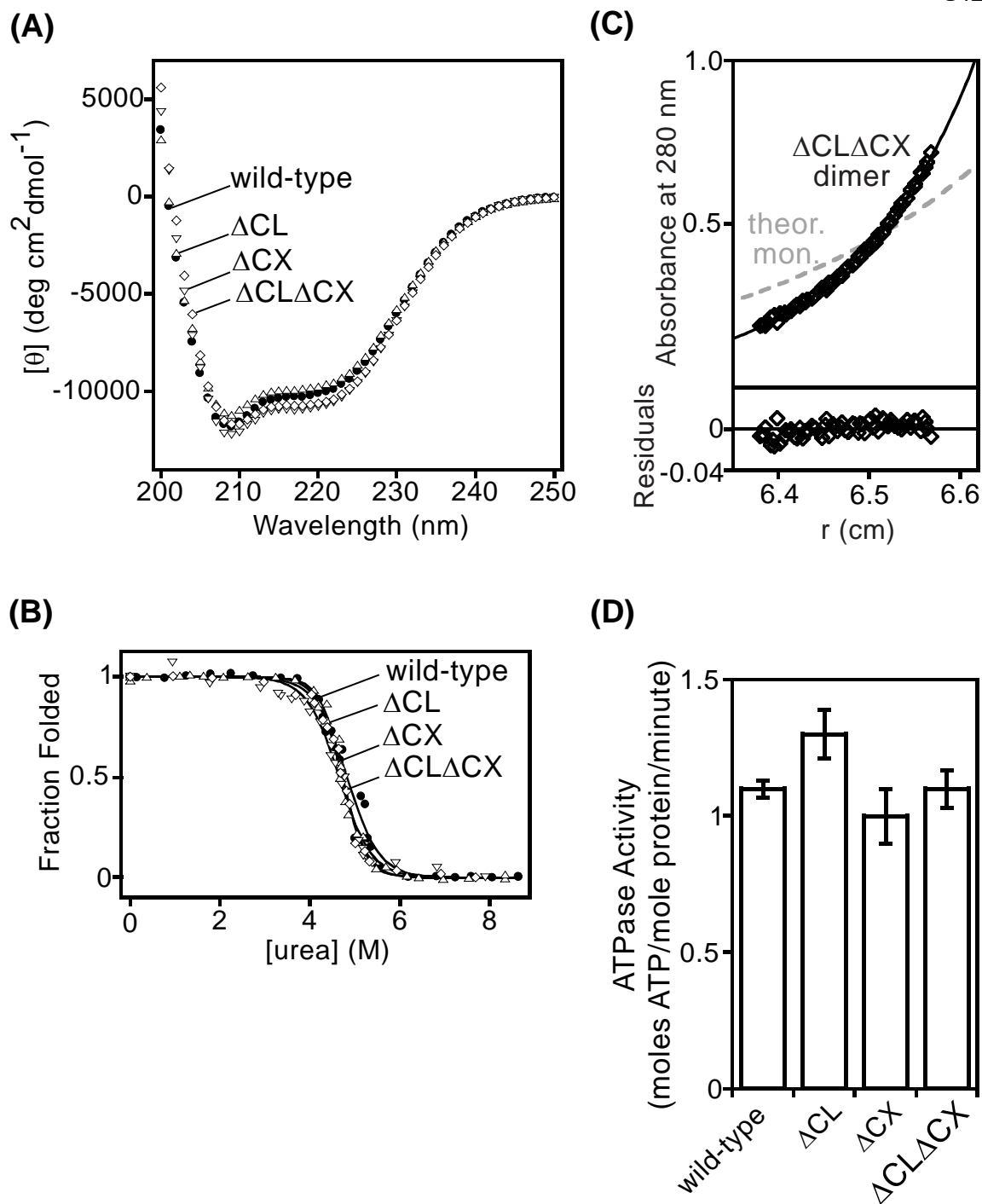


Figure 5.6

---

**Table 5.3.** Midpoint concentrations of urea required to denature Hsp90

---

Hsp90	Cm <sup>a</sup> (M)
Wild-type	4.8
ΔCL	4.7
ΔCX	4.6
ΔCLΔCX	4.7
CR	4.5

---

<sup>a</sup>Midpoint concentration (Cm) is the concentration of urea where half the protein is unfolded

---

dimer, resulting in a non-functional monomeric construct. However, analytical ultracentrifugation indicates that  $\Delta\text{CL}\Delta\text{CX}$  Hsp90 is dimeric (Figure 5.6C).

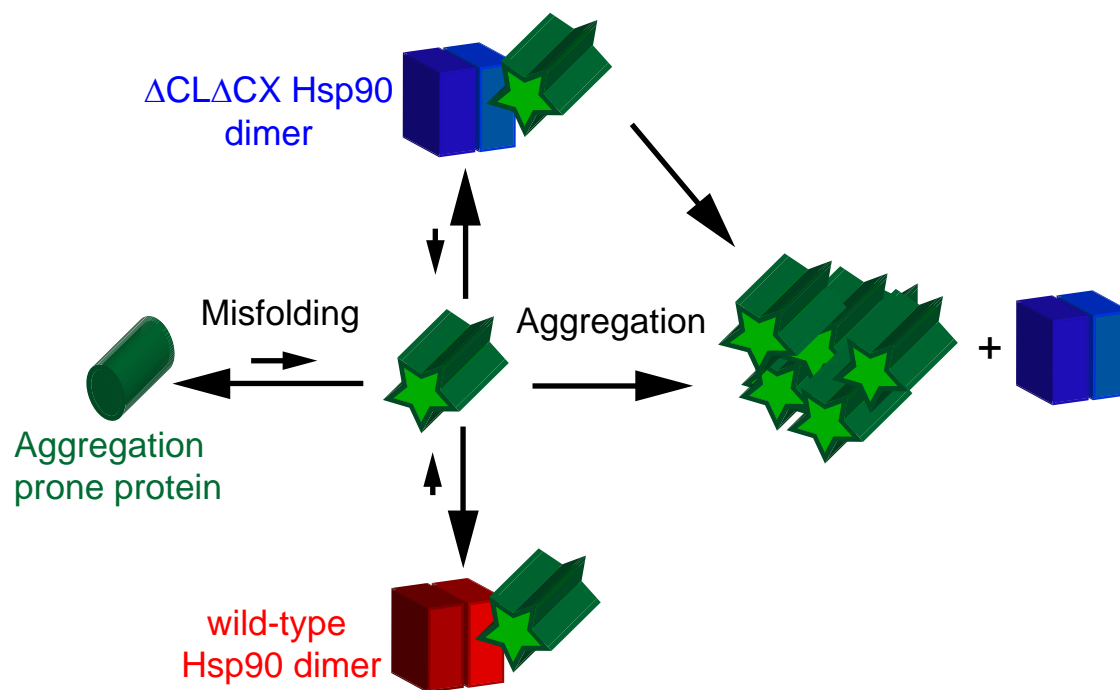
Because our  $\Delta\text{CL}$  constructs shorten the linker connecting the N-terminal and middle domains we wondered if interactions between these domains were perturbed. Communication between the N-terminal and middle domains is important for the inherent ATPase activity of Hsp90 (14). We tested ATPase activity and found that all of our constructs hydrolyze ATP at similar levels to wild-type Hsp90 (Figure 5.6D). This result indicates that our deletions do not compromise communication between the N-terminal and middle domains. By deleting only the acid-rich region of the CL, our constructs retain flexibility that was previously found to be important for proper communication between the N-terminal and middle domains (156, 160).

Our experimental observations are consistent with a model where both wild-type and  $\Delta\text{CL}\Delta\text{CX}$  Hsp90 are capable of forming complexes with mis-folded proteins, but only wild-type Hsp90 complexes effectively suppress the aggregation of mis-folded proteins (Figure 5.7). It is well established that the propensity of proteins to aggregate increases under conditions that promote mis-folding (85-88, 139). The ability of wild-type Hsp90 to suppress the temperature-induced aggregation of CFTR-NBD1 and CS indicates that it is capable of binding to these mis-folded proteins and reducing their propensity to aggregate. In our model,  $\Delta\text{CL}\Delta\text{CX}$  Hsp90 is also capable of binding to mis-



**Figure 5.7. Mechanistic model of charge-dependent anti-aggregation activity of Hsp90.**

Stress-induced mis-folding of an aggregation-prone protein leads to exposure of hydrophobic surfaces that cause non-specific aggregation in the absence of a chaperone. In our model, both wild-type and  $\Delta\text{CL}\Delta\text{CX}$  Hsp90 bind to the mis-folded state, but only wild-type complexes efficiently hinder aggregation. The deficient anti-aggregation activity of  $\Delta\text{CL}\Delta\text{CX}$  Hsp90 could also be caused by impaired binding to mis-folded protein.

**Figure 5.7**

folded conformations, but is unable to suppress the aggregation of the mis-folded proteins. However, our results are also consistent with a model where  $\Delta\text{CL}\Delta\text{CX}$  Hsp90 is defective for binding to mis-folded proteins.

We developed experiments to distinguish whether  $\Delta\text{CL}\Delta\text{CX}$  is deficient for binding to mis-folded proteins or deficient in reducing the aggregation of bound, mis-folded proteins. It is challenging to measure the binding of Hsp90 to mis-folded proteins because of the inherent technical challenge of aggregation. However, the two possible models make different and testable predictions regarding the anti-aggregation activity of mixtures of wild-type and  $\Delta\text{CL}\Delta\text{CX}$  Hsp90. If binding is the dominant defect of  $\Delta\text{CL}\Delta\text{CX}$  Hsp90, then mixtures of wild-type and  $\Delta\text{CL}\Delta\text{CX}$  Hsp90 should mimic the anti-aggregation activity of wild-type Hsp90 alone. If  $\Delta\text{CL}\Delta\text{CX}$  competes with wild-type Hsp90 for binding to mis-folded protein, but does not protect mis-folded protein from aggregating, then mixtures of wild-type and  $\Delta\text{CL}\Delta\text{CX}$  Hsp90 should exhibit intermediate anti-aggregation activity. Because Hsp90 is dimeric, there is the potential to form wild-type/ $\Delta\text{CL}\Delta\text{CX}$  Hsp90 heterodimers that would complicate the interpretation of these mixing experiments. To avoid this complication, we utilized a super-stabilized dimer wild-type Hsp90 (NMCcoil) that does not heterodimerize with non-superstabilized Hsp90 (110). We find that mixtures of NMCcoil and  $\Delta\text{CL}\Delta\text{CX}$  Hsp90 have anti-aggregation activity for both CFTR-NBD1 and CS that is intermediary to either Hsp90 construct alone (Figure 5.8A and B). These results indicate that both wild-type and  $\Delta\text{CL}\Delta\text{CX}$

**Figure 5.8. Charge-dependent anti-aggregation activity of Hsp90.**

(A and B) To determine whether  $\Delta\text{CL}\Delta\text{CX}$  is unable to bind mis-folded proteins or is deficient for suppressing the aggregation of bound protein, we monitored the ability of an equimolar mixed sample of  $\Delta\text{CL}\Delta\text{CX}$  and NMCcoil Hsp90 to suppress CFTR-NBD1 (A) or CS (B) aggregation. The intermediate anti-aggregation activity observed for the mixed sample indicates that both wild-type and  $\Delta\text{CL}\Delta\text{CX}$  Hsp90 compete for binding to mis-folded proteins. (C) Analysis of CFTR-NBD1 aggregates formed in the presence and absence of Hsp90 variants. Aggregates were collected by centrifugation and analyzed by western blotting for Hsp90 and CFTR-NBD1. We find that most  $\Delta\text{CL}\Delta\text{CX}$  Hsp90 remains soluble during the CFTR-NBD1 aggregation reaction.

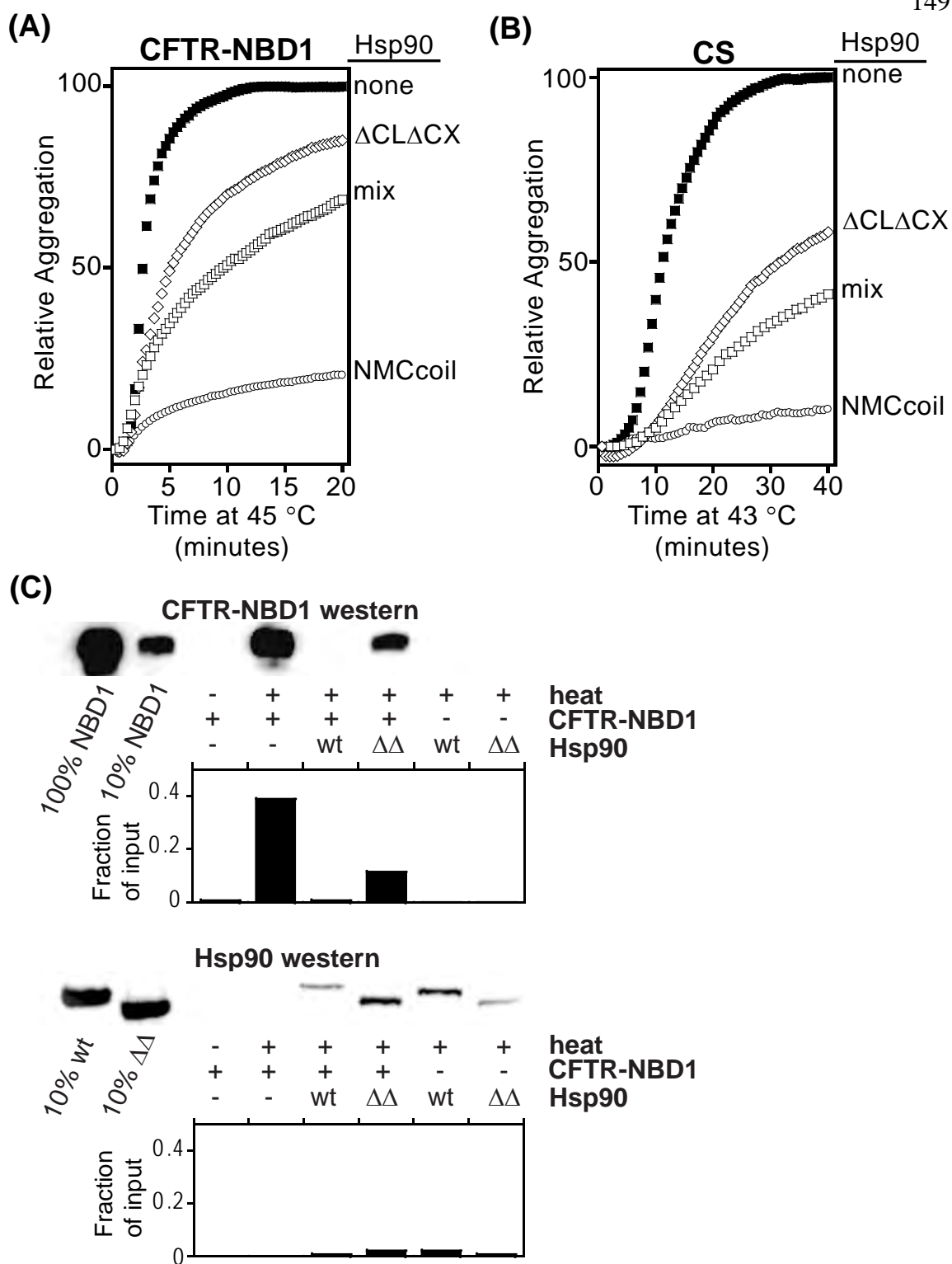


Figure 5.8

Hsp90 are capable of binding to mis-folded proteins but only wild-type Hsp90 complexes effectively suppress the aggregation of mis-folded proteins.

Having established that  $\Delta\text{CL}\Delta\text{CX}$  Hsp90 is capable of binding to mis-folded proteins, we next investigated if the  $\Delta\text{CL}\Delta\text{CX}$  Hsp90 in these complexes aggregates. The efficiency of  $\Delta\text{CL}\Delta\text{CX}$  Hsp90 aggregation from these complexes is likely to be influenced by the dynamics and mechanism of the aggregation process. Because  $\Delta\text{CL}\Delta\text{CX}$  Hsp90 in isolation is soluble under the conditions of these experiments (Figure 5.4), the relative amount of  $\Delta\text{CL}\Delta\text{CX}$  Hsp90 aggregation should be controlled by kinetic competition between aggregation and release from aggregating particles. To examine this issue, we monitored the content of aggregated particles formed by mis-folded CFTR-NBD1 in the presence and absence of  $\Delta\text{CL}\Delta\text{CX}$  Hsp90 (Figure 5.8C). Under the conditions of the experiment, we find that CFTR-NBD1 readily aggregates on its own and that this aggregation is efficiently rescued by wild-type Hsp90, but not  $\Delta\text{CL}\Delta\text{CX}$  Hsp90 consistent with our light-scattering experiments (Figure 5.6A). Aggregates formed in the presence of  $\Delta\text{CL}\Delta\text{CX}$  Hsp90 show background levels of the chaperone, indicating that most  $\Delta\text{CL}\Delta\text{CX}$  Hsp90 remains soluble. Thus, the mechanism and dynamics of the aggregation process permit  $\Delta\text{CL}\Delta\text{CX}$  Hsp90 release.

***The defective anti-aggregation activity of  $\Delta\text{CL}\Delta\text{CX}$  can be rescued by an exogenous acid-rich region.***

If removal of charge caused the anti-aggregation defects of  $\Delta\text{CL}\Delta\text{CX}$  Hsp90, adding charge back to the construct should rescue this activity. Alternatively, sequence-specific features of the CL and CX may have caused the loss of Hsp90 anti-aggregation activity. To distinguish these possibilities, we appended the human Hsp90 CL to the C-terminus of  $\Delta\text{CL}\Delta\text{CX}$  to generate a charge rescue (CR) Hsp90 construct (Figure 5.9 and 5.10). While the charge-rich nature of the CL is evolutionarily conserved, it is one of the most diverse regions of Hsp90 with respect to sequence. In addition, by appending the human CL to the C-terminus, we have dramatically altered its physical location relative to the rest of the Hsp90 domains. We found that CR Hsp90 efficiently reduces CFTR-NBD1 (Figure 5.9B) and CS (Figure 5.9C) aggregation indicating that charge modulates the anti-aggregation activity of Hsp90.

## **Discussion**




Our results clearly indicate that charge is important for the anti-aggregation activity of Hsp90. Hsp90 has been shown to reduce the aggregation propensity of numerous proteins (85-88). The aggregation propensity of many proteins, including CFTR and CS, increases under conditions that promote mis-folding. These observations are consistent with a widely recognized sequential model where natively-folded proteins transition to mis-folded states prior to aggregation (Figure 5.7). In this model, there are

**Figure 5.9. The anti-aggregation activity of  $\Delta\text{CL}\Delta\text{CX}$  Hsp90 was rescued by an exogenous acid-rich region.**

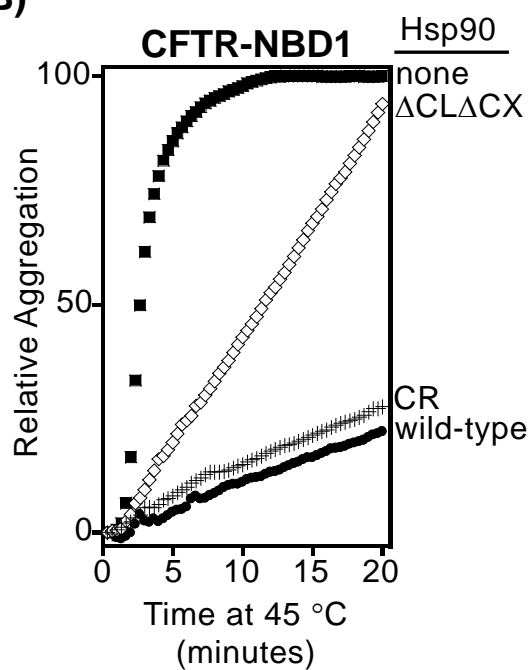
(A) The human Hsp90 CL was appended to the C-terminus of  $\Delta\text{CL}\Delta\text{CX}$  Hsp90 (black square) to generate a charge-rescue construct, CR. CR Hsp90 suppressed CFTR-NBD1 (B) and CS (C) aggregation at elevated temperature.



(A)

Hsp90 construct	net charge
wild-type	-37
	
$\Delta\text{CL}\Delta\text{CX}$	-14
	
CR	-30
	

(B)



(C)

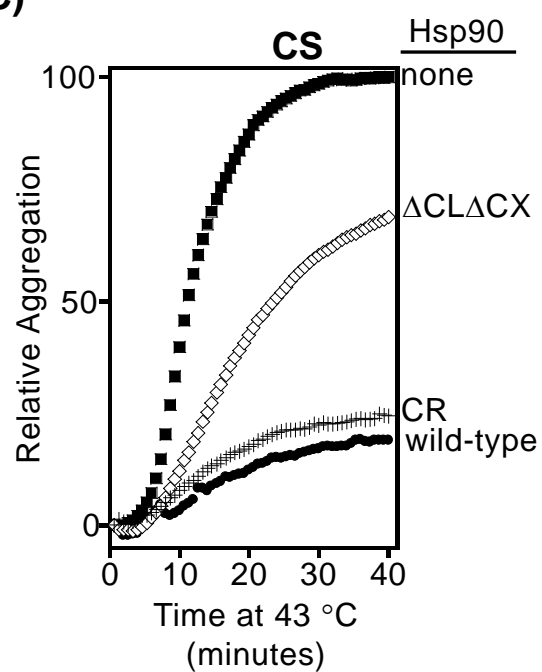
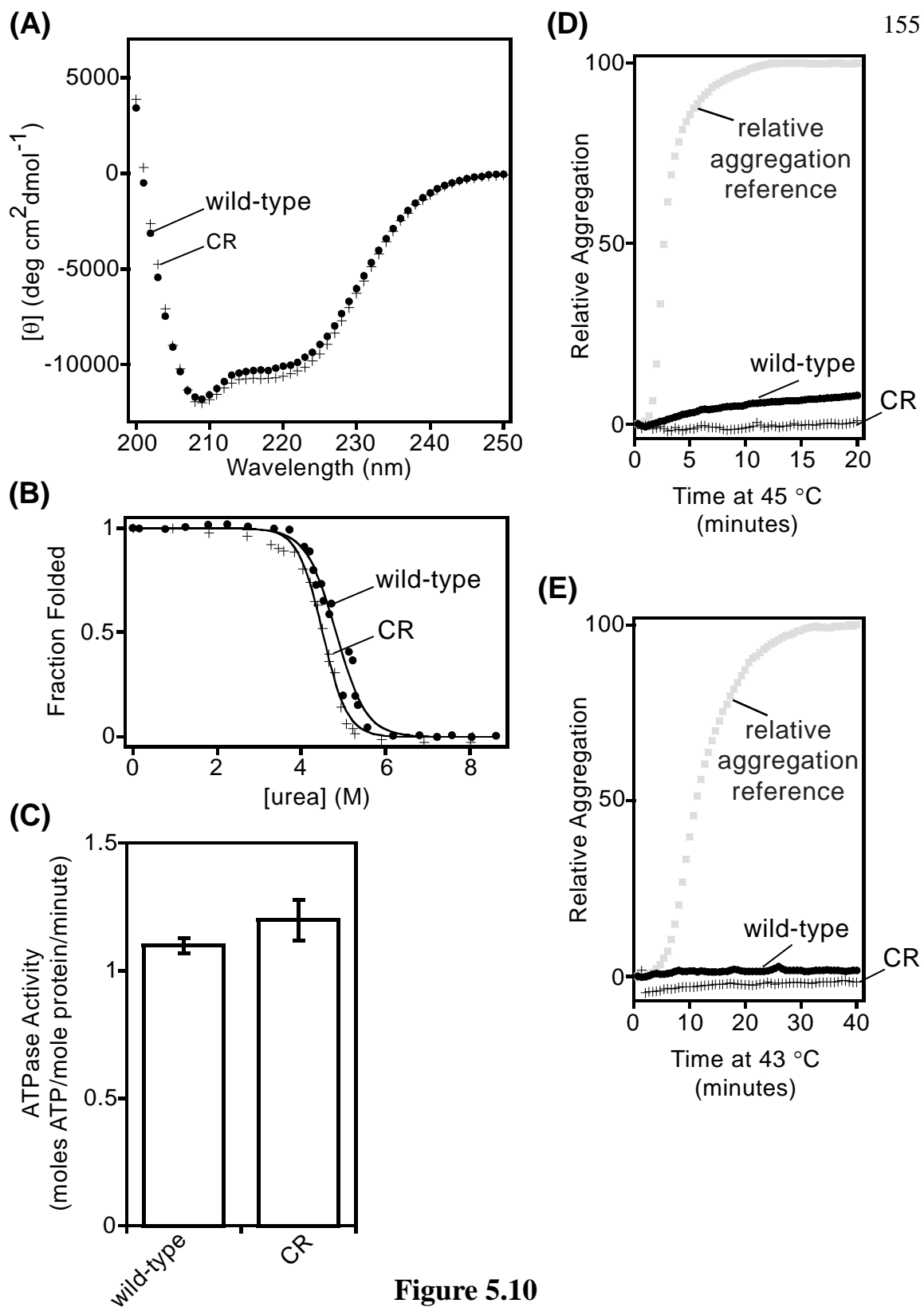


Figure 5.9

**Figure 5.10. Biochemical analysis of CR Hsp90.**

(A) Addition of the human Hsp90 CL to the C-terminus of  $\Delta\text{CL}\Delta\text{CX}$  Hsp90 does not affect secondary structure as monitored by CD. (B) The CR Hsp90 construct unfolds at a similar concentration of urea as wild-type Hsp90. The  $C_m$  of urea required to denature Hsp90 was unchanged by the addition of the human Hsp90 CL to the C-terminus of  $\Delta\text{CL}\Delta\text{CX}$  Hsp90 (Table 5.3). (C) CR Hsp90 was capable of hydrolyzing ATP similar to wild-type. (D) In the absence of CFTR-NBD1, CR Hsp90 maintained wild-type solubility at 45 °C. (E) In the absence of CS, CR Hsp90 maintained wild-type solubility at 43 °C.



**Figure 5.10**

three potential protein conformations (native, mis-folded, and aggregated) that may bind to Hsp90.

Hsp90 binding to proteins in a mis-folded conformation is consistent with our observation that charge-rich regions of Hsp90 modulate the aggregation process. In our experiments, CFTR-NBD1 and CS aggregation were initiated by temperature stress, a condition that promotes mis-folding (158). Mis-folded CFTR-NBD1 and CS are highly prone to aggregation, but this aggregation can be minimized by binding to Hsp90 (Figure 5.4). The anti-aggregation activity of Hsp90 is impaired by deletion of the charge-rich regions indicating that charge plays an important role in Hsp90 anti-aggregation activity. Importantly, deletion of the charge-rich regions does not prevent Hsp90 from binding to mis-folded proteins (Figure 5.8).

Although unable to prevent the aggregation of both CFTR-NBD1 and CS,  $\Delta\text{CL}\Delta\text{CX}$  Hsp90 alters the kinetics of the aggregation reaction for CFTR-NBD1 (Figure 5.4A) but not for CS (Figure 5.4B). This change in the aggregation kinetics is concentration-dependent as it is not observed with half the concentration of  $\Delta\text{CL}\Delta\text{CX}$  Hsp90 (Figure 5.8A). These observations are consistent with a model where  $\Delta\text{CL}\Delta\text{CX}$  Hsp90 slows the aggregation of mis-folded CFTR-NBD1 but the eventual accumulation of aggregated protein drives the equilibrium to a fully-aggregated state.

In bacterial Hsp90 (HtpG), the CL and CX regions are absent (159, 161). However, in *E. coli* HtpG the net charge remains highly negative due to the amino acid composition of the structured regions. The estimated charge per 100 amino acids on HtpG is -4.2 (compared to -2.2 for  $\Delta\text{CL}\Delta\text{CX}$ ). These findings suggest that net charge may also be valuable in bacterial Hsp90 for anti-aggregation activity though the location of the charge is distinct from eukaryotic Hsp90.

There are two well-established physical properties of charge-rich regions that are likely to reduce aggregation: favorable interactions between charged atoms and aqueous solvent, and Coulombic repulsion between like-charged complexes. Our results indicate that the charge-rich regions of Hsp90 enhance the solubility of Hsp90 complexes with mis-folded proteins through favorable solvent interactions and Coulombic self-repulsion with other like-charged complexes.

Net charge is a common characteristic of many chaperones and may influence their ability to prevent protein aggregation. We observe that net charge is a common characteristic of the Hsp33, Hsp70, and Hsp90 families of anti-aggregation chaperones. These chaperone families are also characterized by small hydrophobic patches capable of binding to exposed hydrophobic regions of mis-folded proteins. Our results with Hsp90 suggest that charge may be important in the function of these chaperones.

## **CHAPTER VI**

### **Investigating the role of Hsp90 anti-aggregation activity *in vivo***

## Abstract

The ATP-independent anti-aggregation activity of Hsp90 observed *in vitro* has been a long-standing puzzle. *In vitro*, Hsp90 clearly hinders the aggregation of many hard-to-fold proteins without ATP. In cells, however, all of the biologically important functions of Hsp90 identified to date, including the maturation of kinases and nuclear steroid hormone receptors, clearly require ATP hydrolysis by Hsp90. Why does Hsp90 robustly hinder the aggregation of hard-to-fold proteins without ATP *in vitro*, but *in vivo* uses ATP hydrolysis for all of its essential functions? By utilizing separation of function Hsp90 variants (that specifically lack *in vitro* anti-aggregation activity) we have begun to address this question. We find that anti-aggregation deficient Hsp90 is unable to support yeast growth under stressful conditions. Thus, the anti-aggregation activity of Hsp90 is important for its essential function *in vivo*. Interestingly, the ATP-independent anti-aggregation activity of Hsp90 is not sufficient for supporting cell function. Thus, hindering the aggregation of most hard-to-fold proteins by Hsp90 (independent of ATP hydrolysis) does not appear to be important for cell function. These results suggest a cellular model where the Hsp40/60/70 machinery is responsible for hindering the aggregation of most hard-to-fold proteins while Hsp90 assists in the maturation of a select set of clients in an ATP-dependent fashion, potentially aided by its inherent anti-aggregation properties.

## Introduction

Hsp90 is an essential molecular chaperone in eukaryotes where it is required for the maturation of a select group of signal transduction client proteins including numerous kinases and steroid hormone receptors (8, 91). Structurally, Hsp90 is a homodimeric chaperone consisting of an N-terminal domain that is the site of ATP binding and hydrolysis, a middle domain, and a C-terminal dimerization domain (10). Hsp90 mutants that are unable to bind or hydrolyze ATP fail to support yeast viability (11, 96) or mature Hsp90 client proteins *in vivo* (110) emphasizing the importance of ATP hydrolysis for Hsp90 function *in vivo*.

In contrast to the requirement for ATP binding and hydrolysis *in vivo*, Hsp90 has been shown to robustly hinder the aggregation of numerous hard-to-fold proteins *in vitro* in the absence of ATP (85, 86, 88-90). How can essential Hsp90 function *in vivo* absolutely require ATP while *in vitro* Hsp90 can function as an anti-aggregation chaperone independent of ATP binding and hydrolysis?

Interestingly, while Hsp90 has been shown to be a promiscuous anti-aggregation chaperone *in vitro*, it does not appear to be important for the proper folding of most cellular proteins (84). To investigate this apparent discrepancy, we tested the function of anti-aggregation deficient Hsp90 in yeast cells. In our previous work, we determined that deletion of the acidic charged linker and C-terminal extension of Hsp90 ( $\Delta$ CLACX)



significantly impaired the anti-aggregation activity of Hsp90 *in vitro* (162).  $\Delta\text{CL}\Delta\text{CX}$  Hsp90 maintains wild-type ATP hydrolysis levels allowing us to investigate Hsp90 anti-aggregation activity *in vivo* as well as investigate the role of ATP hydrolysis in this activity.

## Results

### ***Hsp90 anti-aggregation activity is required for yeast growth under stressful conditions.***

Hsp90 is an essential gene in eukaryotes (4, 115, 116). Hsp90 mutants described in Chapter 5 that lack *in vitro* anti-aggregation activity (162) were used to investigate the role of anti-aggregation activity in Hsp90 function *in vivo*. We first tested whether anti-aggregation deficient Hsp90 mutants can support yeast viability as the sole copy of Hsp90. Each mutant was introduced into a yeast strain whose other source of Hsp90 was encoded on a *URA3* plasmid that can be swapped out using 5-FOA (126). Anti-aggregation deficient Hsp90 mutants were able to support yeast growth in the presence and absence of wild-type Hsp90 (Figure 6.1A) and were found to accumulate to wild-type levels in yeast cells grown at room temperature (Figure 6.1B).

Yeast cells express numerous cellular chaperones in addition to Hsp90, including Hsp110, Hsp70, Hsp60, and Hsp40 (163, 164). Under non-stress conditions, other cellular chaperones may be able to compensate for the defective anti-aggregation activity of Hsp90 allowing for normal growth. Anti-aggregation deficient Hsp90s may be unable

**Figure 6.1. Hsp90 anti-aggregation activity is not required for the essential function of Hsp90 in yeast.**

(A) All Hsp90 mutants support yeast viability when expressed as the sole copy of Hsp90 in yeast cells at 25 °C. (B) Hsp90 mutants accumulate to wild-type levels in yeast grown at 25 °C.

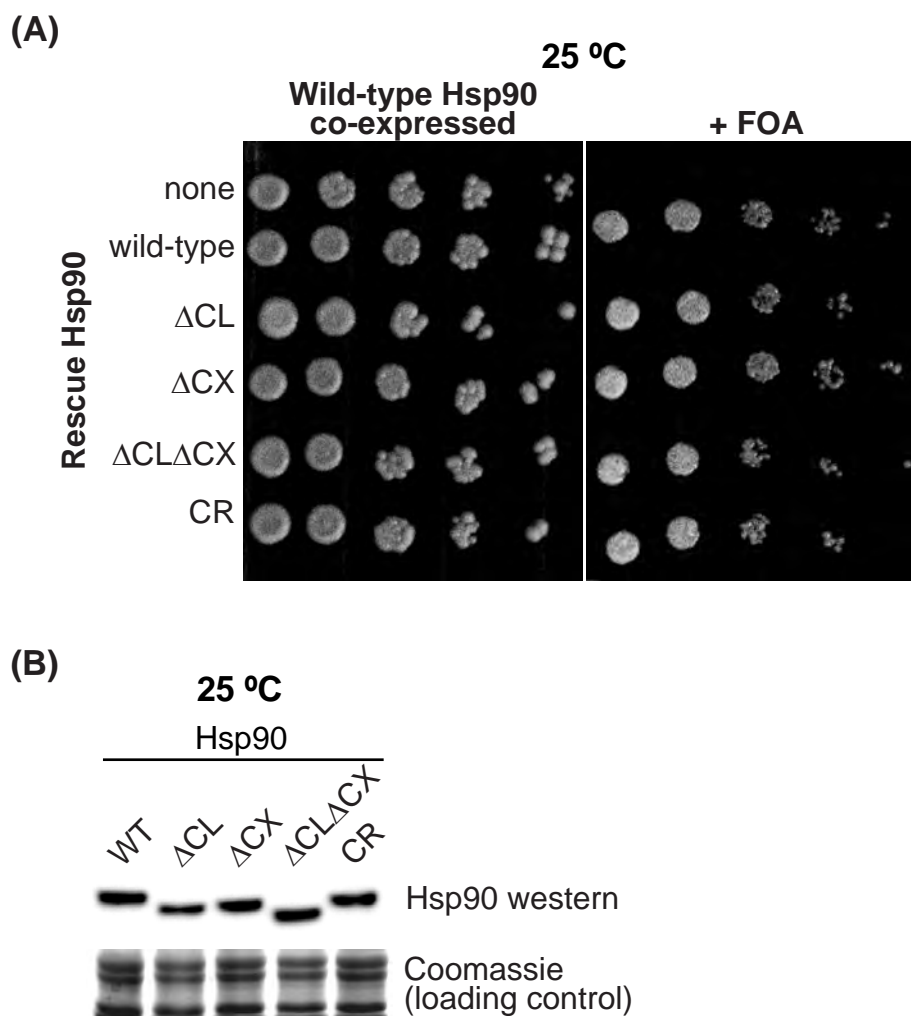


Figure 6.1

to support yeast growth under stressful conditions where aggregation poses a greater challenge to the cell. In fact, yeast strains expressing anti-aggregation deficient Hsp90 as the sole copy of Hsp90 were unable to grow at elevated temperature (Figure 6.2A&B).

The failure to support yeast growth at elevated temperature may be due to reduced expression levels of anti-aggregation deficient Hsp90. To test this possibility, we analyzed the cellular expression levels of each Hsp90 anti-aggregation mutant in yeast lysates by western blotting (Figure 6.2C). The anti-aggregation deficient Hsp90 mutants  $\Delta CL$  and  $\Delta CL\Delta CX$  which were unable to support yeast growth under stressful conditions displayed reduced cellular expression levels when grown at elevated temperature for an extended period of time.

Previous studies showed that reduced Hsp90 levels results in decreased growth at elevated temperatures (4). To determine whether the growth defect observed for anti-aggregation deficient Hsp90 at elevated temperature is due to reduced expression, we engineered wild-type Hsp90 constructs with reduced cellular expression levels. Expression of wild-type Hsp90 can be reduced by changing the promoter controlling expression from the plasmid system (108). We first monitored the ability of two promoters to reduce the cellular expression of wild-type Hsp90 compared to the GPD-expressed construct by analyzing Hsp90 levels in yeast lysates by quantitative western blotting (Figure 6.3A). Importantly, the GPD promoter has previously been shown to

**Figure 6.2. Hsp90 anti-aggregation activity is required for yeast growth under stressful conditions.**

Yeast expressing anti-aggregation deficient Hsp90 as the sole copy are unable to support yeast growth at elevated temperature on (A) plates or (B) in liquid culture. Error bars represent SD, n=3. (C) Cellular expression levels of Hsp90 anti-aggregation mutants are reduced compared to wild-type Hsp90 after 48 hours growth at 37 °C.

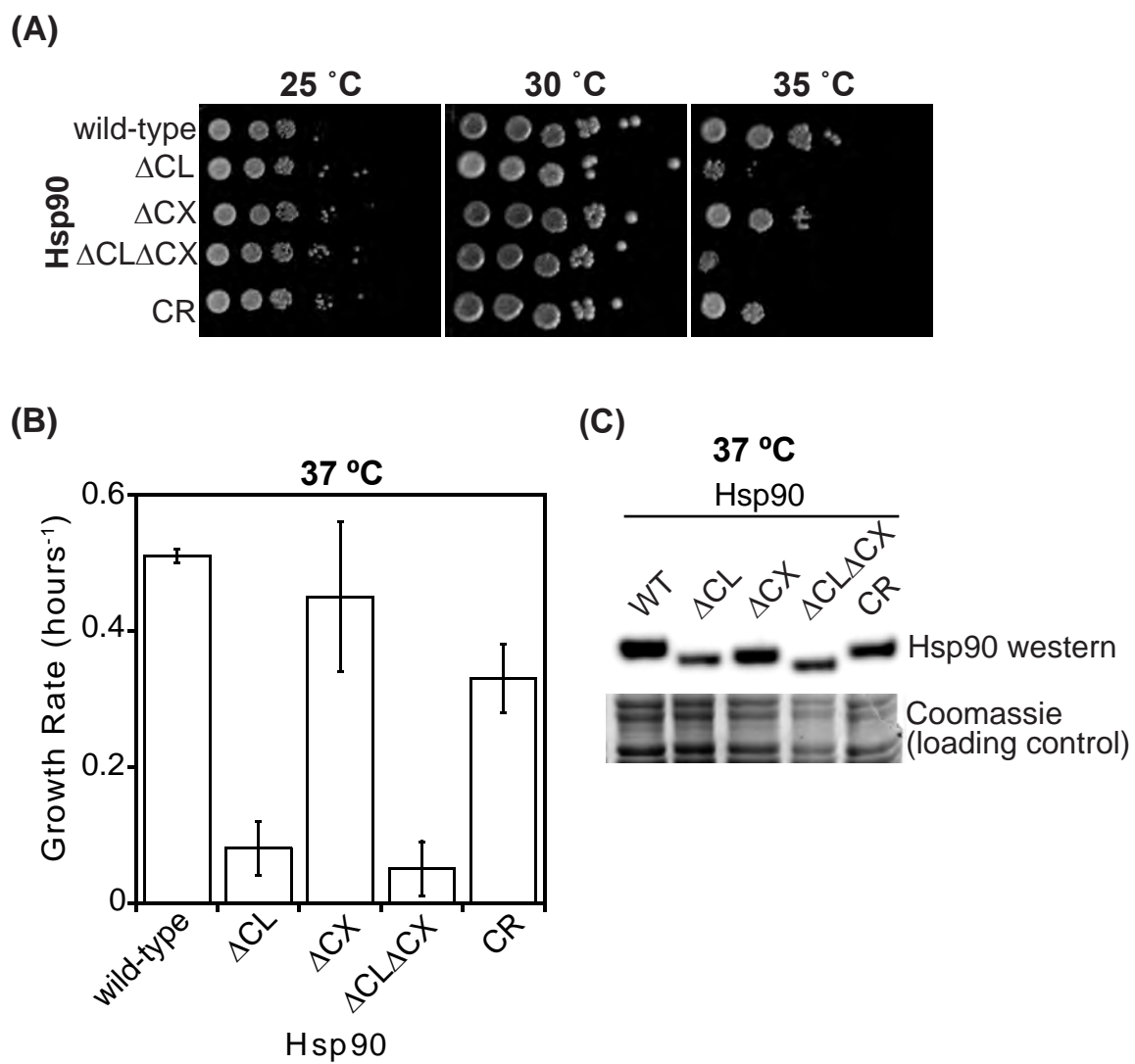


Figure 6.2

**Figure 6.3. Reducing cellular expression levels of Hsp90 impairs cell function.**

(A) Cellular expression levels of Hsp90 were reduced by expressing Hsp90 under the control of 3 promoters: GPD (wild-type), *TEF1*, or *ADHI*. Expression levels in yeast were determined by quantitative western blotting. Intervening lanes were removed for presentation purposes where indicated by grey lines. (B) Yeast expressing 15 % of wild-type Hsp90 protein (*ADHI*-expressed) showed reduced viability when expressed as the sole copy of Hsp90 at 25 °C. (C) Reducing cellular expression of Hsp90 results in a decreased growth rate at 37 °C. Error bars represent SD, n=3.

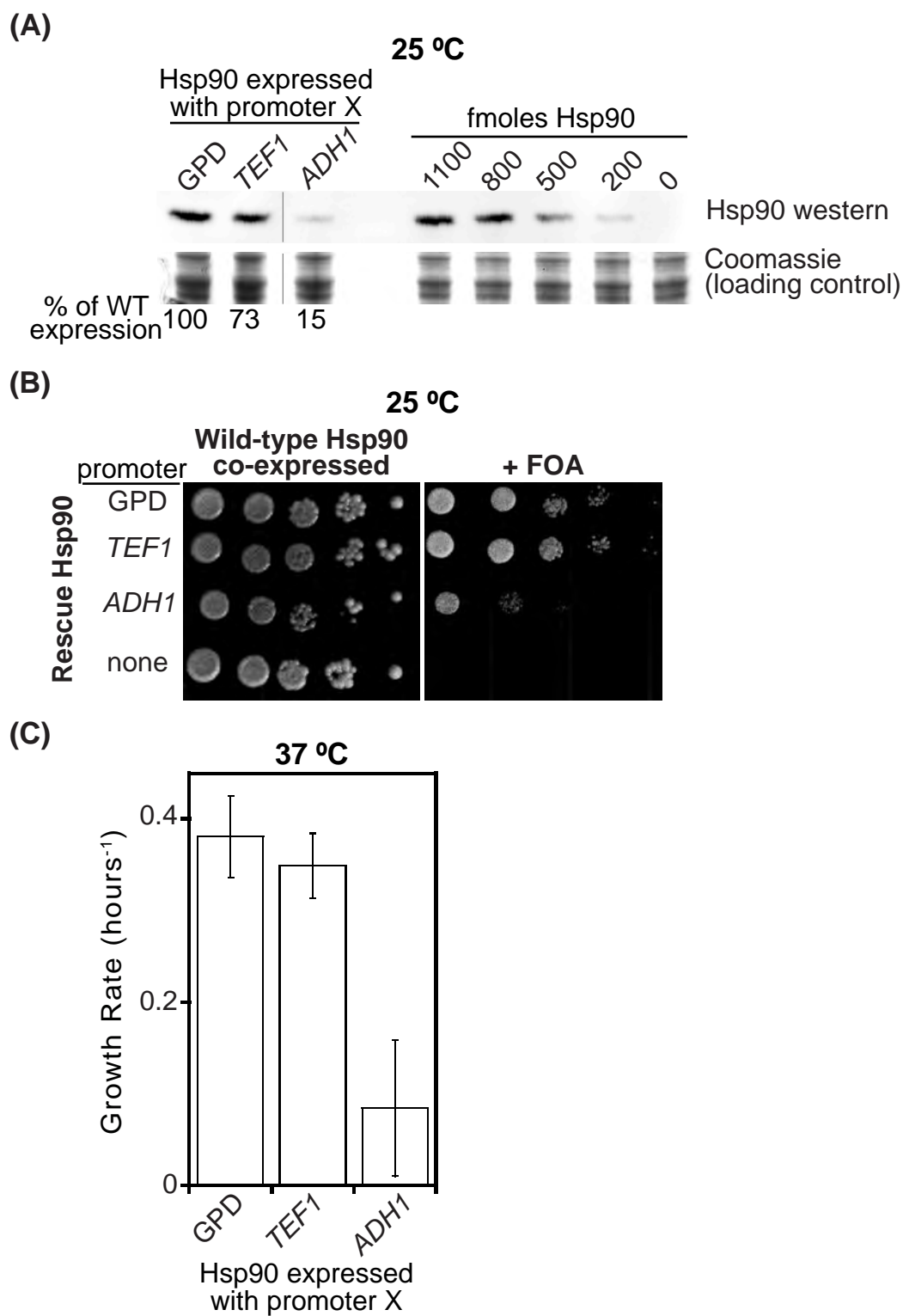


Figure 6.3

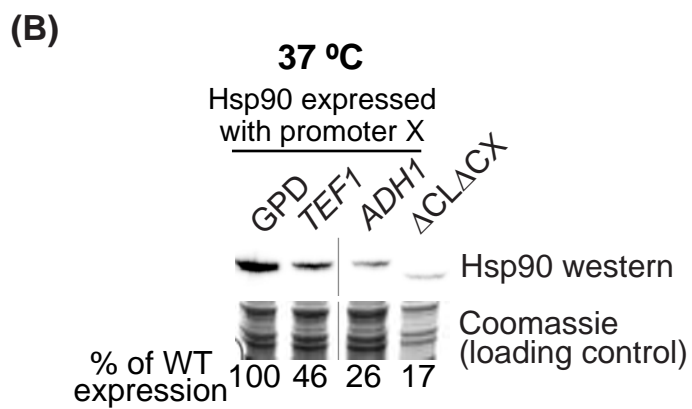
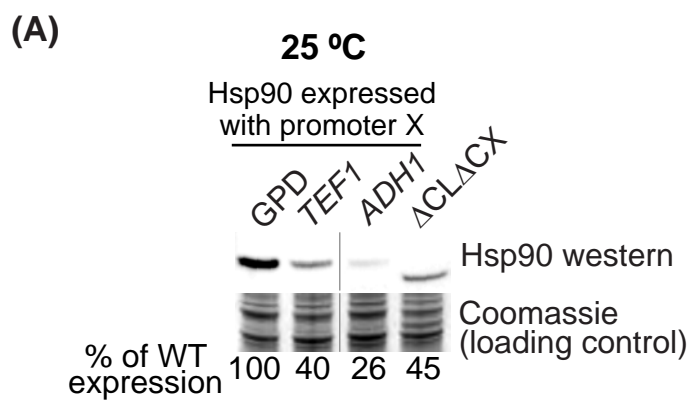


express Hsp90 at endogenous levels (117). We find that expression of wild-type Hsp90 from both the *TEF1* and *ADH1* promoters significantly reduces the cellular expression level of Hsp90. When grown under conditions that select for *TEF1*- or *ADH1*-expressed Hsp90 as the sole copy of Hsp90, we find that moderate reduction (*TEF1*) of Hsp90 levels does not impair yeast growth but further reduction (*ADH1*) impairs the ability of Hsp90 to support yeast growth under non-stress conditions (Figure 6.3B). When grown at 37 °C for an extended period of time *TEF1*-expressed Hsp90 was able to support yeast growth similar to wild-type but *ADH1*-expressed Hsp90 was significantly impaired for growth (Figure 6.3C) confirming that reducing Hsp90 levels leads to decreased growth at elevated temperatures.

We next compared the cellular expression level of anti-aggregation deficient  $\Delta\text{CL}\Delta\text{CX}$  Hsp90 to our three wild-type Hsp90 constructs with modified expression levels by western blotting of yeast lysates. Under non-stress conditions, we find that  $\Delta\text{CL}\Delta\text{CX}$  accumulates to the level of *TEF1*-expressed wild-type Hsp90 (Figure 6.4A). However, growth under stressful conditions results in  $\Delta\text{CL}\Delta\text{CX}$  expression levels resembling *ADH1*-expressed wild-type Hsp90 (Figure 6.4B). Reducing the expression levels of wild-type Hsp90 does not allow us to differentiate between anti-aggregation and expression level defects for  $\Delta\text{CL}\Delta\text{CX}$  under stressful conditions.

**Figure 6.4. How does the expression level of  $\Delta\text{CL}\Delta\text{CX}$  Hsp90 compare to different expression levels of wild-type Hsp90?**

Expression levels in yeast were determined by western blotting. Intervening lanes were removed for presentation purposes where indicated by grey lines. (A) At 25 °C, the expression level of  $\Delta\text{CL}\Delta\text{CX}$  Hsp90 is similar to that of *TEF1*-expressed Hsp90. (B) After 9 hours at 37 °C, the expression level of  $\Delta\text{CL}\Delta\text{CX}$  Hsp90 more closely resembles that of *ADH1*-expressed Hsp90.

**Figure 6.4**

Wild-type and anti-aggregation deficient Hsp90 proteins were expressed from 414GPD low-copy plasmids in yeast cells.  $\Delta\text{CL}\Delta\text{CX}$  Hsp90 expression was next increased by utilizing a high-copy yeast expression plasmid. By expressing  $\Delta\text{CL}\Delta\text{CX}$  Hsp90 from the 424GPD and 424TEF1 plasmids, we observed expression levels comparable to that of wild-type Hsp90 under non-stress (Figure 6.5A) and stressful conditions (Figure 6.5B). When all wild-type and  $\Delta\text{CL}\Delta\text{CX}$  Hsp90 constructs with modified expression levels were grown at 37 °C for an extended period of time  $\Delta\text{CL}\Delta\text{CX}$  Hsp90 expressed from the 424GPD plasmid accumulated to wild-type levels (Figure 6.5B) but was unable to support yeast growth (Figure 6.6) at 37 °C. Therefore, the reduced cellular expression of  $\Delta\text{CL}\Delta\text{CX}$  Hsp90 does not result in the growth defect observed at 37 °C and the anti-aggregation activity of Hsp90 is required for its essential function *in vivo*.

***ATP-independent anti-aggregation activity of Hsp90 is not sufficient for cell function.***

If the anti-aggregation activity of Hsp90 is truly ATP-independent, we should be able to rescue the growth defect of  $\Delta\text{CL}\Delta\text{CX}$  Hsp90 under stressful conditions with an otherwise non-functional Hsp90 mutant that maintains anti-aggregation activity *in vitro*. We co-expressed the ATP-binding deficient D79N Hsp90 mutant which was previously shown to maintain *in vitro* anti-aggregation activity (110) with  $\Delta\text{CL}\Delta\text{CX}$  Hsp90 and monitored yeast growth at elevated temperature. To prevent heterodimer formation, our D79N construct contained a C-terminal coiled-coil dimerization domain as described in

**Figure 6.5.  $\Delta\text{CL}\Delta\text{CX}$  Hsp90 can be expressed at wild-type levels.**

Expression levels in yeast were determined by western blotting. (A) At 25 °C, the expression level of  $\Delta\text{CL}\Delta\text{CX}$  424TEF1 is similar to that of wild-type Hsp90. (B) After 8 hours at 37 °C, expression of  $\Delta\text{CL}\Delta\text{CX}$  Hsp90 from the 424GPD plasmid is similar to that of wild-type Hsp90.

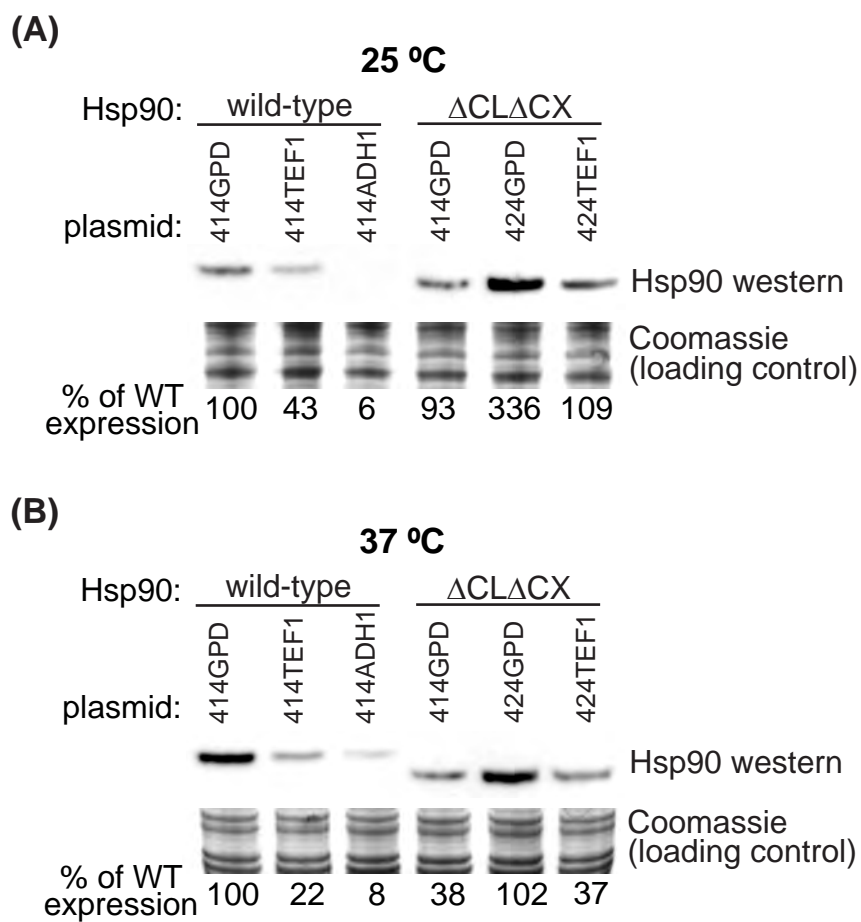
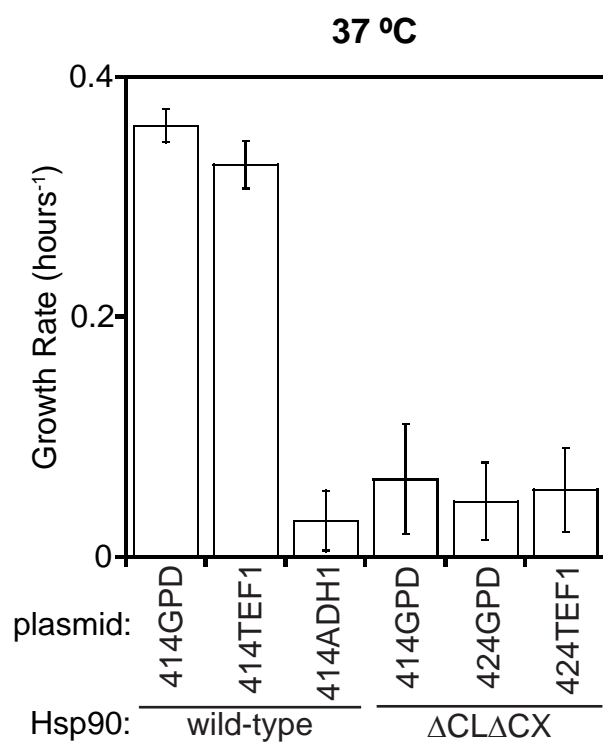


Figure 6.5

**Figure 6.6. Reduced expression of anti-aggregation deficient  $\Delta\text{CL}\Delta\text{CX}$  Hsp90 is not responsible for the growth defect observed at 37 °C.**

Increasing the expression of  $\Delta\text{CL}\Delta\text{CX}$  Hsp90 to the level of wild-type Hsp90 using the 424GPD and 424TEF1 plasmids does not rescue the growth defect observed for  $\Delta\text{CL}\Delta\text{CX}$  Hsp90 expressed from the 414GPD plasmid at 37 °C. Error bars represent SD, n=3.

**Figure 6.6**



Chapter 4. D79N Hsp90 was unable to rescue the growth defect of  $\Delta\text{CL}\Delta\text{CX}$  Hsp90 (Figure 6.7), indicating that the ATP-independent anti-aggregation activity of Hsp90 is not sufficient for cell function.

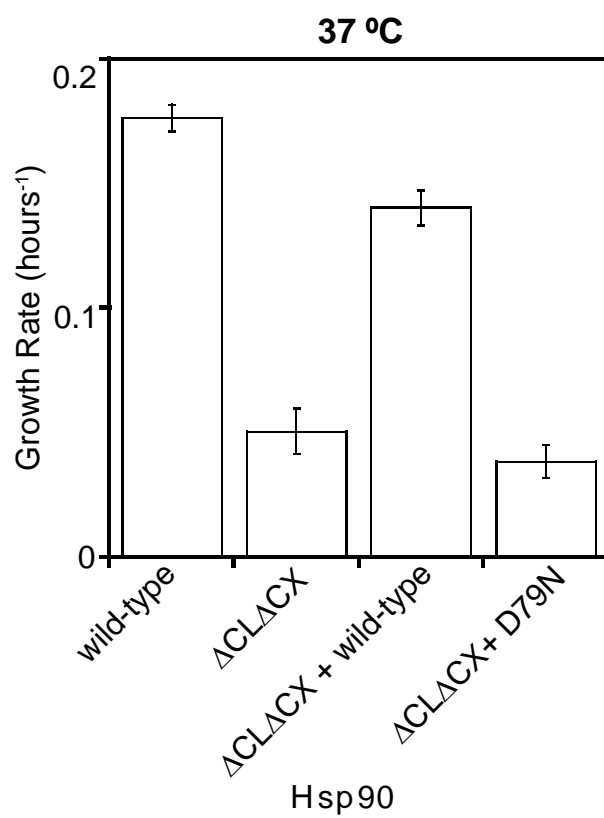
Our results are also consistent with a model where the growth defect observed for  $\Delta\text{CL}\Delta\text{CX}$  Hsp90 is a dominant defect where D79N Hsp90 is drawn into aggregates rendering it unable to function. To address this concern, we co-expressed wild-type Hsp90 (with the C-terminal coiled-coil dimerization domain) with  $\Delta\text{CL}\Delta\text{CX}$  and monitored growth under stressful conditions (Figure 6.7). We find that wild-type Hsp90 is able to effectively rescue the growth defect observed for  $\Delta\text{CL}\Delta\text{CX}$  indicating that it is not a dominant growth defect and supporting a model where ATP-independent anti-aggregation activity is not sufficient for Hsp90 function in cells.

## Discussion

Hsp90 efficiently suppresses the aggregation of hard-to-fold proteins *in vitro* in the absence of ATP yet all known functions of Hsp90 *in vivo* strictly require ATP hydrolysis. To investigate this discrepancy, we tested the function of Hsp90 separation of function mutants that lack anti-aggregation activity but maintain ATPase activity in yeast cells. While anti-aggregation deficient Hsp90 mutants were able to support yeast viability as the sole Hsp90 under non-stress conditions (Figure 6.1) they were unable to support yeast growth under stressful conditions (Figure 6.2). We found that after extended growth

**Figure 6.7. The ATP-independent anti-aggregation activity of Hsp90 is not sufficient for cell function.**

The growth defect of  $\Delta\text{CL}\Delta\text{CX}$  Hsp90 observed under stressful conditions (37 °C) could not be rescued by co-expression of ATPase-deficient D79N Hsp90 but was rescued by co-expression of wild-type Hsp90. Wild-type and D79N Hsp90 contained C-terminal coiled-coil dimerization domains to inhibit heterodimer formation. Error bars represent SD, n=3.

**Figure 6.7**

at elevated temperatures, expression of anti-aggregation deficient Hsp90 was significantly reduced compared to wild-type Hsp90.

Reducing cellular levels of Hsp90 has previously been shown to lead to growth defects at elevated temperature (4). When the cellular expression level of wild-type Hsp90 was reduced by changing the promoter on the plasmid system, significantly reducing Hsp90 levels resulted in impaired yeast growth at elevated temperatures (Figure 6.3). When we compared the expression of  $\Delta\text{CL}\Delta\text{CX}$  Hsp90 to that of *TEF1*- and *ADH1*-expressed Hsp90 under non-stress conditions,  $\Delta\text{CL}\Delta\text{CX}$  Hsp90 expression resembled *TEF1*-expressed Hsp90 (Figure 6.4A) which was able to efficiently support yeast growth. However, under stressful conditions,  $\Delta\text{CL}\Delta\text{CX}$  expression resembled *ADH1*-expressed Hsp90 (Figure 6.4B), which was unable to support efficient yeast growth under stressful conditions.

To explore this issue further, we changed the expression system for  $\Delta\text{CL}\Delta\text{CX}$  Hsp90 to a high-copy expression plasmid in yeast. Expression of  $\Delta\text{CL}\Delta\text{CX}$  Hsp90 from the 424GPD and 424TEF1 high-copy expression plasmids was comparable to expression of wild-type Hsp90 under non-stress and stressful conditions (Figure 6.5). We found that after extended growth at 37 °C,  $\Delta\text{CL}\Delta\text{CX}$  Hsp90 constructs that accumulate to wild-type levels (Figure 6.5B) were unable to efficiently support yeast growth under stressful conditions (Figure 6.6). Therefore, the reduced cellular expression of  $\Delta\text{CL}\Delta\text{CX}$  Hsp90

does not cause the growth defect observed at 37 °C. These results indicate that the anti-aggregation activity of Hsp90 is required for its essential function *in vivo*.

Our observation that  $\Delta\text{CL}\Delta\text{CX}$  Hsp90 can support yeast growth at 25 °C (Figure 6.1) but not at 37 °C (Figures 6.2) is also consistent with an Hsp90 defect in the cell integrity signaling pathway. Perturbations in the cell wall caused by various cell-stresses including heat induces the cell integrity signaling pathway (165). Mutations of components of the cell integrity signaling pathway share common phenotypes including temperature-sensitive growth at 37 °C (165). Hsp90 is known to bind to one stress-activated MAP kinase, Slt2, of the cell integrity signaling pathway allowing Slt2 to activate downstream targets (8, 166). An inability of  $\Delta\text{CL}\Delta\text{CX}$  Hsp90 to activate Slt2 at 37 °C could also explain the observed growth defect.

To differentiate between anti-aggregation and heat-induced cell integrity signaling pathway defects, we plan to monitor  $\Delta\text{CL}\Delta\text{CX}$  Hsp90 function in yeast cells with decreased levels of other cellular chaperones such as Hsp40, Hsp70, or Hsp110. Three of the four Hsp70 genes in *S. cerevisiae* can be deleted without compromising viability (strain: *ssa1 ssa2 ssa3* or *ssa1 ssa3 ssa4*) (167). Either Hsp110 gene can be deleted (strain: *sse1* or *sse2*) but the combined deletion of both is non-viable (168-170). The Hsp70 co-chaperone Hsp40 (*YDJ1*) could also be deleted (171, 172). By reducing the

abundance of other anti-aggregation chaperones, we can then monitor  $\Delta\text{CL}\Delta\text{CX}$  Hsp90 function at 25 °C where the cell integrity signaling pathway plays a less prominent role.

To further probe the role of the ATP-independent anti-aggregation activity of Hsp90 observed *in vitro* in yeast cells, we co-expressed the ATPase-deficient D79N Hsp90 mutant with  $\Delta\text{CL}\Delta\text{CX}$  in an effort to rescue the growth defect observed at elevated temperature. D79N Hsp90 was unable to rescue the growth defect of  $\Delta\text{CL}\Delta\text{CX}$  Hsp90 at elevated temperature (Figure 6.7) indicating that any ATP-independent function of Hsp90 does not have a measurable impact on cell function. Importantly, the growth defect of  $\Delta\text{CL}\Delta\text{CX}$  is not a dominant defect as wild-type Hsp90 was able to efficiently rescue the growth defect of  $\Delta\text{CL}\Delta\text{CX}$  Hsp90 (Figure 6.7).

In the future, we hope to further probe the role of Hsp90 anti-aggregation activity *in vivo*. The inability of an ATPase-deficient Hsp90 mutant with intact anti-aggregation functions to rescue the growth defect of anti-aggregation deficient Hsp90 suggests that hindering the aggregation of most hard-to-fold proteins by Hsp90 (independent of ATP hydrolysis) is not sufficient for cell function. This hypothesis is further supported by preliminary results from cadmium-stress experiments with anti-aggregation deficient Hsp90 mutants. Exposure to heavy metals provides an oxidative stress that induces the formation of reactive oxygen species and damaged proteins (173). Growth of yeast expressing anti-aggregation deficient Hsp90 mutants was not affected by the addition of

cadmium chloride at 25 or 37 °C (data not shown) confirming that Hsp90 is not required for proper maintenance of most cellular proteins. These results suggests a possible cellular model where the Hsp40/60/70 machinery is responsible for hindering the aggregation of most hard-to-fold proteins while Hsp90 primarily assists in the maturation of a select set of clients in an ATP-dependent fashion, potentially aided by its inherent anti-aggregation properties.

## **CHAPTER VII**

### **Discussion and Future Directions**



In this thesis, I provide a thorough evaluation of how dimerization of Hsp90 contributes to its function in cells and the role of ATP binding and hydrolysis in client protein activation by Hsp90. I also show how the net charge of Hsp90 modulates its anti-aggregation activity *in vitro* and provide some initial insights into the role of Hsp90 anti-aggregation activity *in vivo*. Previous studies suggested that the ATPase activity of Hsp90 is required for its essential function *in vivo* but the details of this activity remained to be elucidated. I provide evidence that Hsp90 ATPase activity requires a functional Hsp90 dimer and that this ATPase activity is required for client protein activation in cells by Hsp90. I also discovered that Hsp90 anti-aggregation activity is regulated by negative charge and began investigating the role of Hsp90 anti-aggregation activity in cells.

Previous studies showed that Hsp90 monomers have significantly reduced ATPase activity (93). However, given the large network of Hsp90 co-chaperone and client protein interactions (8), it is essential that the role of Hsp90 monomers be studied in cells. We created a monomeric Hsp90 construct, NMCC, and showed that dimerization is required for Hsp90 function in yeast cells (Chapter 3). Hsp90 monomers have significantly reduced ATPase activity *in vitro*, are unable to support yeast viability, and are unable to activate the Hsp90 client proteins v-src and GR *in vivo*. NMCC Hsp90 provides a useful tool for studying the potential role of monomers in the Hsp90 conformational cycle and to study possible interactions of Hsp90 monomers with co-chaperones and substrate proteins.

To further understand the precise mechanism of ATP-binding and hydrolysis by Hsp90 and its implications for Hsp90 function, we explored the role of Hsp90 ATPase activity in client protein maturation in yeast cells. Hsp90 ATPase mutants E33A and D79N are unable to support yeast viability (11, 96) but the role of Hsp90 ATPase activity in client protein maturation was previously unknown. Our work in Chapter 4 showed that ATP binding and hydrolysis by Hsp90 are necessary for proper maturation of the Hsp90 clients v-src and GR *in vivo*.

Interestingly, the R380A ATP-hydrolysis mutant which is non-viable (14) was unable to mature v-src but was able to activate GR to a significant level (Figure 7.1). To explore this further, I would next like to test whether this activity is specific for activation of GR or whether R380A Hsp90 is able to activate other hormone receptors such as the androgen or progesterone receptors. In order to explore this mechanism in greater depth, I can also use the previously described system for reconstituting hormone receptor activation *in vitro* (62) to determine if the chaperone system is altered for activation of hormone receptors by R380A Hsp90 compared to wild-type.

Numerous Hsp90 client proteins have been identified and studied extensively *in vivo*. Hsp90 has also been shown to suppress the *in vitro* aggregation of a number of hard-to-fold proteins. However, the mechanism of Hsp90 anti-aggregation activity is not

**Figure 7.1. R380A Hsp90 can activate GR but not v-src in yeast.**

(A) As was observed for the Hsp90 ATPase mutants in Chapter 4, the R380A mutation to Hsp90 which inhibits ATP hydrolysis leads to reduced v-src accumulation and background levels of tyrosine kinase activity in yeast. (B) Unlike the inability of E33A and D79N Hsp90 to activate GR observed in Chapter 4, R380A Hsp90 showed reporter activity levels significantly greater than background using a single-tailed student T-test. Error bars represent SEM. (C) Expression level of GR analyzed by Western blots of yeast lysates. (D) Dose response to varying DOCS concentration for R380A and wild-type Hsp90.

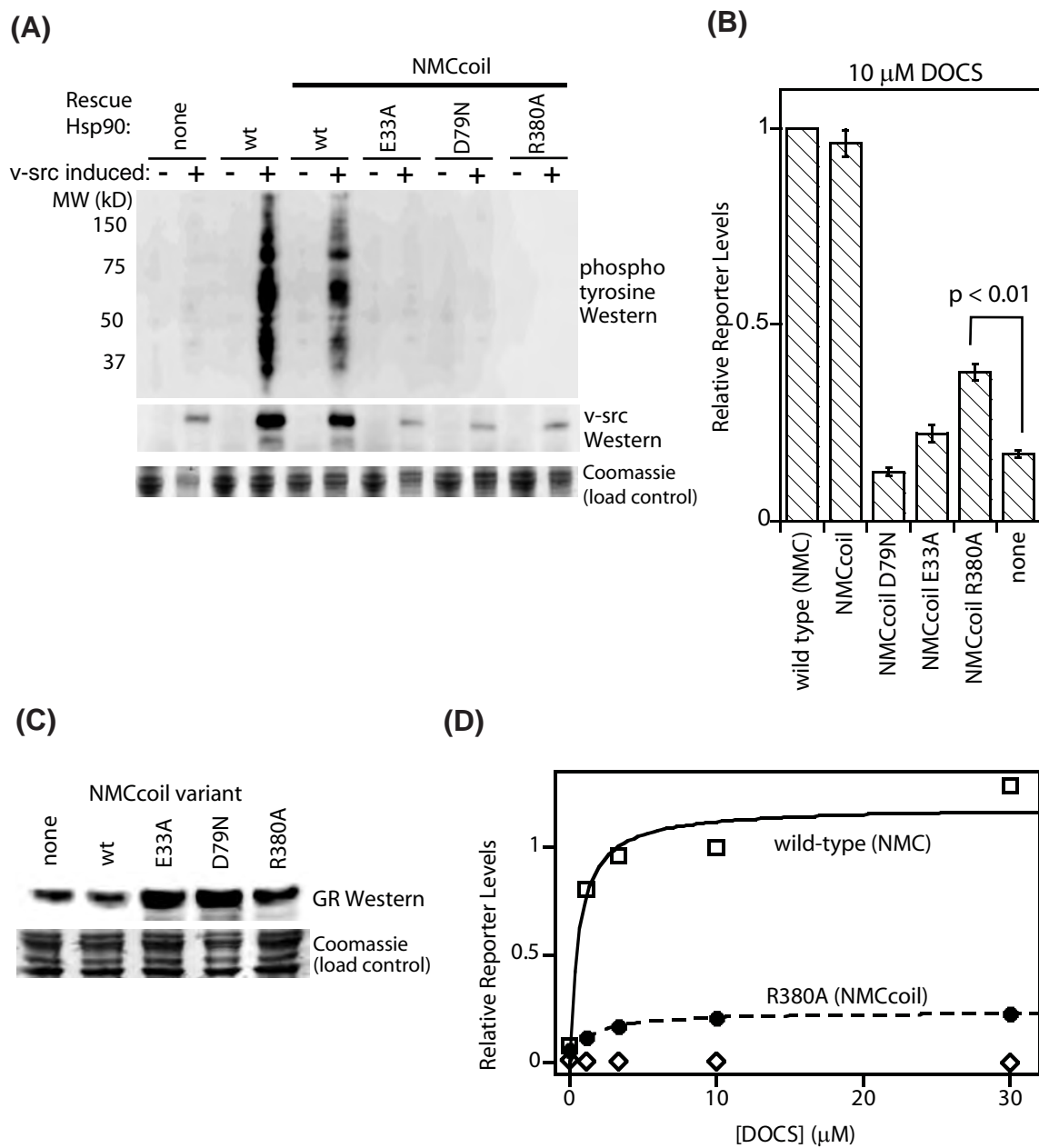


Figure 7.1

well understood. Unlike all other known functions of Hsp90, the ability of Hsp90 to suppress the aggregation of these hard-to-fold proteins often occurs in the absence of ATP. But what is promoting the solubility of complexes between Hsp90 and mis-folded proteins was largely unknown.

In Chapter 5, we showed that the negative charge of Hsp90 modulates its anti-aggregation activity. Specifically, the highly charged CL and CX of Hsp90 provide the negative charge to Hsp90 required to modulate its anti-aggregation activity. The addition of an exogenous charge-rich region to an Hsp90 construct lacking both the CL and CX rescued the observed anti-aggregation defect confirming the importance of charge for Hsp90 anti-aggregation activity.

One question that arises from these results is how the charge of hard-to-fold proteins affects their interaction with Hsp90. Full-length CFTR protein is positively charged (Table 7.1). Several highly charged motifs in CFTR have been identified including negatively charged motifs in the N- and C-terminal tails and three positively charged motifs in the R-domain (174). The NBD1 region of CFTR used in the aggregation experiments is negatively charged. In contrast, CS is positively charged (Table 7.1) suggesting that the interaction of Hsp90 with mis-folded proteins is not dependent on the charge of the mis-folded protein. To confirm this observation, charge-reversal mutations could be made to CFTR-NBD1 and CS and the ability of Hsp90 to

**Table 7.1.** Protein charge analysis of select Hsp90 anti-aggregation substrates

Human Protein	GenBank accession number	net charge <sup>a</sup>	number of amino acids	charge per 100 amino acids
CFTR	NP 000483	22.5	1480	1.5
CS	AF053631	4.8	466	1.0

<sup>a</sup>Predicted net charge at pH 7, determined with the program SEDNTERP.

prevent the aggregation of these mis-folded proteins tested.

Our charge analysis of other cytoplasmic proteins (Table 5.1) suggests a potential shared mechanism of anti-aggregation activity among chaperones that utilize hydrophobic patches. Analysis of the charge properties of the yeast small heat shock proteins Hsp26 and Hsp42 as well as  $\alpha$ A-crystallin, the closest mammalian homolog to Hsp26 (175), indicates they are also highly negatively charged (Table 7.2). The Hsp110 chaperone is negatively charged and its charge is evolutionarily conserved (Table 7.3). To investigate this potential shared mechanism of anti-aggregation activity further, I could mutate regions of surface exposed charge on these other negatively charged chaperones and determine if net charge is important for their anti-aggregation activity.

In addition to cellular chaperones, other cellular molecules are also highly charged which may play a role in their solubility and function. For example, both DNA and RNA are highly negatively charged. In the case of RNA, this negative charge has been shown to play a role in the solubility of partner proteins (120). To explore the anti-aggregation characteristics of these highly charged cellular molecules, I could test the ability of DNA and RNA to suppress the *in vitro* aggregation of hard-to-fold proteins such as CFTR-NBD1 and CS. Studying the role of charge in general solubility in the cell could increase our understanding of why charge is so often evolutionarily conserved and how cells control general protein aggregation problems. Given the interest in developing

**Table 7.2.** Protein charge analysis of small heat shock proteins

Chaperone	GenBank accession number	net charge <sup>a</sup>	number of amino acids	charge per 100 amino acids
Hsp26 ( <i>S. cerevisiae</i> )	CAA85016	-4.8	214	-2.3
$\alpha$ A-crystallin ( <i>H. sapiens</i> )	AAA97523	-4.3	173	-2.5
Hsp42 ( <i>S. cerevisiae</i> )	NP 010456	-21.5	375	-5.7

<sup>a</sup>Predicted net charge at pH 7, determined with the program SEDNTERP.



**Table 7.3.** Protein charge analysis of Hsp110 chaperone

Species	GenBank accession number	net charge <sup>a</sup>	number of amino acids	charge per 100 amino acids
<i>Homo sapiens</i>	Q92598	-24.0	858	-2.8
<i>Mus musculus</i>	NP 038587	-22.6	858	-2.6
<i>Saccharomyces cerevisiae</i>	3D2F_A	-16.4	658	-2.5

<sup>a</sup>Predicted net charge at pH 7, determined with the program SEDNTERP.

treatments for aggregation-based diseases, understanding how cells regulate protein aggregation has important therapeutic implications.

All known Hsp90 functions in cells identified to date are ATP-dependent yet Hsp90 efficiently suppresses protein aggregation *in vitro* in the absence of ATP. Interestingly, in Chapter 4 we found that the ATPase-deficient E33A and D79N Hsp90 mutants were able to efficiently suppress the aggregation of CFTR-NBD1 (Figure 4.5) further suggesting that Hsp90 anti-aggregation activity is an ATP-independent process. This left us wondering whether there is an unidentified Hsp90 anti-aggregation function in cells that does not require ATP or if the *in vitro* ATP-independent activity of Hsp90 is an artifact. This question was examined more closely in Chapter 6.

Using the Hsp90 charge mutants described in Chapter 5 that lack anti-aggregation activity but maintain ATPase activity (Figures 5.4 and 5.6), we tested the role of Hsp90 anti-aggregation activity in cells. Our results suggest that the anti-aggregation activity of Hsp90 is required for cell growth under stressful conditions (Figure 6.2). We also found that any ATP-independent function of Hsp90 that exists is not sufficient for cell function (Figure 6.7). This leads us to a preliminary model where the anti-aggregation activity of Hsp90 is important for growth under stressful conditions where it contributes to an ATP-dependent function of Hsp90.

Hsp90 has been implicated in the maturation of many kinases and hormone receptors but there is little evidence that the anti-aggregation activity of Hsp90 is required for the proper activation of these clients. However, my results in Chapter 6 suggest that Hsp90 anti-aggregation activity is important for cell function. In the future, yeast strains expressing anti-aggregation deficient  $\Delta\text{CL}\Delta\text{CX}$  Hsp90 can be used to identify endogenous anti-aggregation substrates of Hsp90. The protein composition of soluble and insoluble fractions of yeast lysates prepared from cells collected during growth under various stress conditions such as elevated temperature, heavy metal exposure, or reduced cellular chaperone levels can be analyzed by mass spectrometry analysis. These experiments would provide further evidence for the role of Hsp90 anti-aggregation activity *in vivo*.

Future experiments will be designed to establish a clearer picture of how the ATPase activity of Hsp90 is coordinated within the dimeric structure of Hsp90 and how this regulates the function of Hsp90 in cells. Using our new understanding of Hsp90 anti-aggregation activity, the role of Hsp90 anti-aggregation activity *in vivo* can be further investigated and used to identify novel Hsp90 anti-aggregation substrates. This information can then be used to elucidate the mechanism(s) of client protein activation by Hsp90 and determine how its anti-aggregation activity contributes to client protein activation.

## Conclusion

In this thesis, I have extensively studied the function of Hsp90 *in vitro* and *in vivo*. I have shown that Hsp90 monomers are non-functional and that ATPase activity is required for Hsp90 function *in vivo*. I have also shown that negative charge modulates Hsp90 anti-aggregation activity *in vitro* and that this anti-aggregation activity is required for Hsp90 function in yeast under stressful conditions. While I have learned a lot about the requirement for ATPase activity for Hsp90 function *in vivo* and about Hsp90 anti-aggregation activity, there are many questions left to be answered to truly understand Hsp90 function. The molecular mechanism by which Hsp90 catalyzes the maturation of any client is an open and active area of research. Current structural models indicate that Hsp90 undergoes dramatic rearrangements in response to ATP binding and hydrolysis (10, 19, 20). However, how these structural rearrangements lead to client maturation is not clear. In the coming years, research will help to reveal the molecular mechanism by which Hsp90 binds to client proteins and along with co-chaperones and ATP catalyzes the maturation of these clients to active states.

## **APPENDIX I**

### **Chaperoning of yeast kinases by Hsp90**

## Introduction

Hsp90 is important for the activation and cellular stability of many kinases including then non-receptor tyrosine kinases c-src and v-src, serine/threonine kinases, such as Raf and Akt, and tyrosine kinases such as ErbB-1 and ErbB-2 (42, 71, 93, 176-181). Recent large-scale screening efforts have identified many novel Hsp90 client kinases that warrant further investigation (8, 166).

The chaperoning of protein kinases by Hsp90 occurs almost exclusively in cooperation with Cdc37, a co-chaperone known to protect nascent kinase chains from rapid degradation during or immediately following translation and promote kinase maturation to the folded state (75). A recent study found that more than 50 % of the *S. cerevisiae* kinome was affected by the loss of active Cdc37 (75) demonstrating the importance of the Hsp90:Cdc37 complex in kinase stability and activation.

The majority of Hsp90-dependent kinases have been identified primarily by changes in cellular accumulation upon Hsp90 inactivation. In this work, we set out to distinguish whether Hsp90 client kinases require Hsp90 for stability, for activation, or for both.

## Results

### *Hsp90 is important for kinase accumulation in yeast cells.*

In order to compare changes in cellular kinase accumulation to changes in kinase activity upon Hsp90 inactivation we studied ten *S. cerevisiae* kinases (Table A.1). Where known, the dependence of the kinases on Cdc37 for stability is noted (75). GST-tagged kinases were expressed in a yeast strain expressing a temperature-sensitive Hsp90 mutant as the sole copy of Hsp90. Kinases were expressed at the non-permissive temperature in the presence and absence of a rescue copy of Hsp90 and kinase accumulation measured by western blotting (Figure A.1A). Eight out of ten of the kinases were found to have more than a 50 % reduction in cellular accumulation upon Hsp90 inactivation indicating that their steady-state levels in yeast cells are dependent on Hsp90.

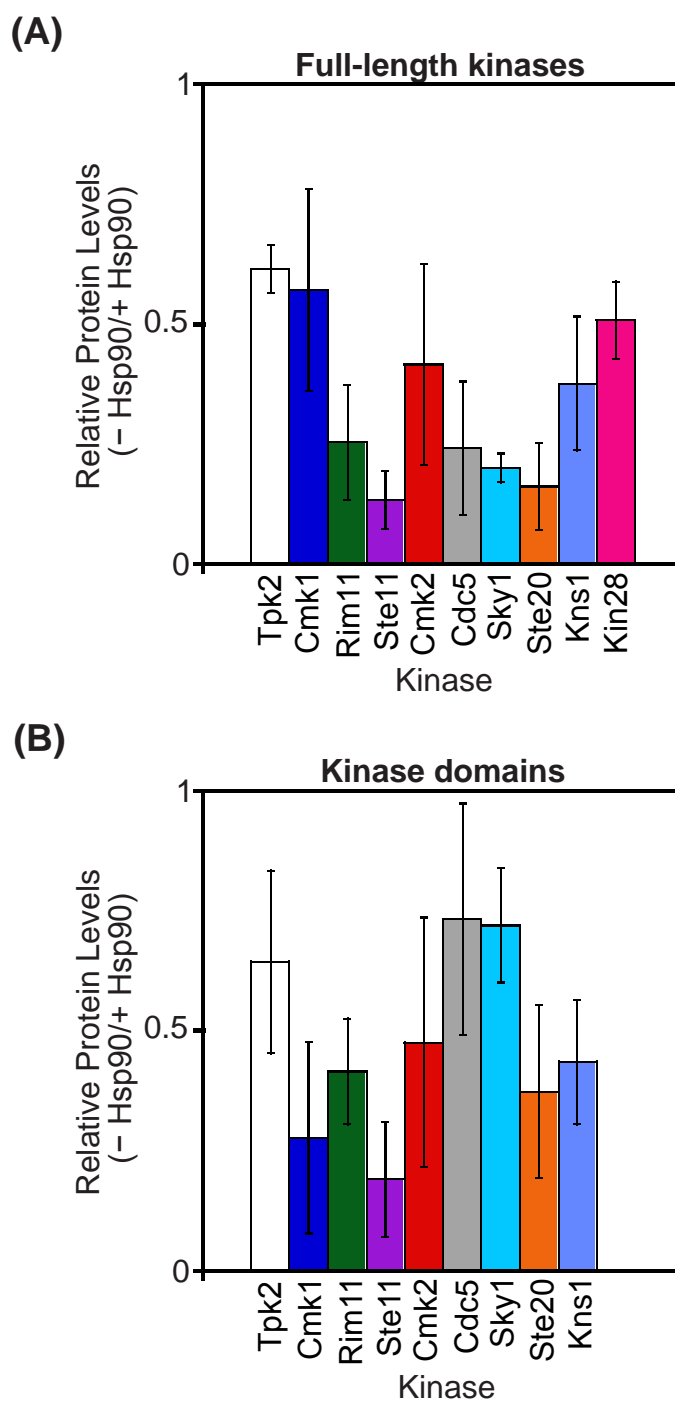
For the hormone receptor GR, Hsp90 is required for opening the ligand-binding cleft allowing access of to the steroid and subsequent GR activation (182). Some kinases have distinct kinase and regulatory domains that bind to each other in the inactive form (183). We propose a model where Hsp90 is required for the displacement of regulatory domains from the kinase domain of client kinases leading to activation similar to the opening of the hormone receptor structure to allow steroid binding.

**Table A.1.** Yeast kinases used in this study.

Kinase	Cdc37 Dependent?(75)	Substrate
Tpk2	yes	YFR017C
Cmk1	yes	YDL006W (Ptc1)
Rim11	yes	YPL077C
Ste11	yes	YOL016C (Cmk2)
Cmk2	no	YER064C
Cdc5	no	YDR360W
Sky1	no	YGL105W (Arc1)
Ste20	no	YBR071W
Kns1	unknown	MBP
Kin28	unknown	



**Figure A.1. Hsp90 influences the cellular accumulation of numerous yeast kinases.** Cellular accumulation of (A) full-length kinases and (B) isolated kinase domain constructs measured in the presence (+) or absence (-) of active Hsp90. Error bars represent SD, n=3.




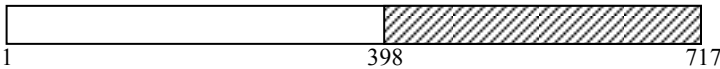
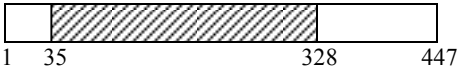
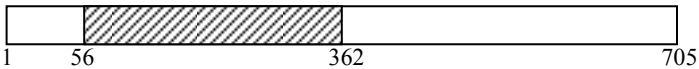
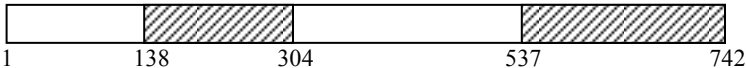
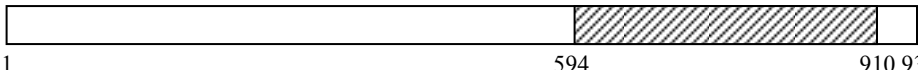


**Figure A.1**

If Hsp90 is required for the displacement of regulatory domains from the kinase domain of client kinases, isolated kinase domain constructs would not require Hsp90 for activation. We generated isolated kinase domain constructs (Table A.2) for nine out of the ten kinases tested (Kin28 does not have a regulatory domain) and monitored the accumulation of the kinase domains in the absence of active Hsp90 (Figure A.1B). Interestingly, the isolated kinase domains for Sky1 and Cdc5 were far less dependent on Hsp90 for cellular accumulation than their full-length counterparts.

#### ***Role of Hsp90 in kinase activation.***

In order to monitor changes in kinase activity upon Hsp90 inactivation, we set out to identify peptide substrates for each kinase. Ptacek et al. identified *in vitro* substrates of most yeast protein kinases using proteome chip technology (184). Using substrates identified for each of our kinases (Table A.1), we designed eleven amino acid peptides surrounding every serine or threonine in the substrate protein. Peptides were synthesized on amino-PEG cellulose membranes (MIT Biopolymers Laboratory). To identify peptide substrates, cellulose membranes were incubated with purified yeast proteins and  $^{32}\text{P}$ -ATP. As a control for non-specific phosphorylation by contaminating yeast kinases in the purified samples, a non-kinase GST-tagged control protein was purified from yeast and incubated with the cellulose membranes and  $^{32}\text{P}$ -ATP first. Any peptide phosphorylated by the non-kinase control sample was considered background. The cellulose membranes were then incubated with the corresponding kinase and  $^{32}\text{P}$ -ATP (Figures A.2 and A.3).

**Table A.2.** Yeast kinase domain constructs

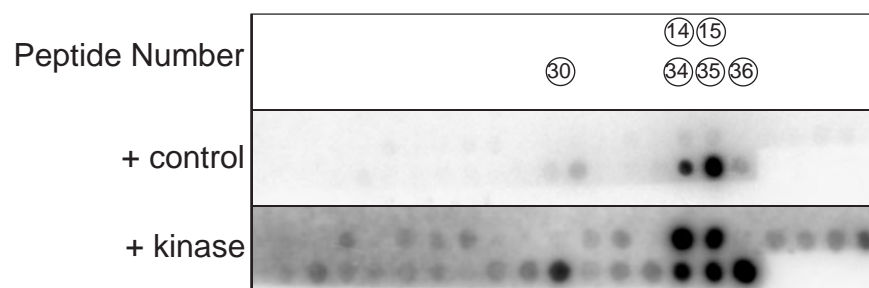
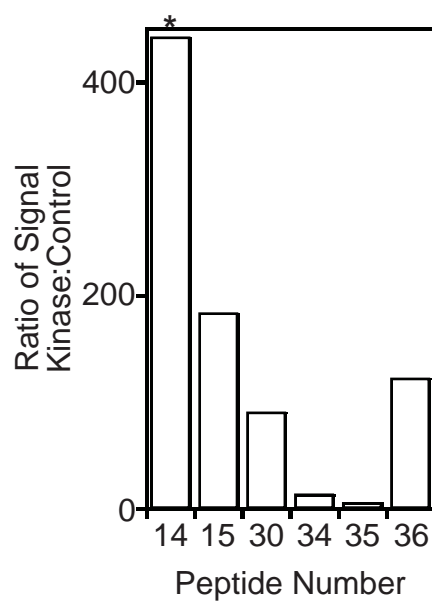
Kinase	Kinase Domain <sup>a</sup>
Tpk2	
Cmk1	
Rim11	
Ste11	
Cmk2	
Cdc5	
Sky1	
Ste20	
Kns1	
Kin28 <sup>b</sup>	

<sup>a</sup>Shaded region is the predicted kinase domain based on BLAST search.

<sup>b</sup>Kin28 was primarily predicted to be a kinase domain. No isolated kinase domain construct was made.

**Figure A.2. Identification of peptide substrates for yeast kinases.**

Example of peptide substrate identification for the yeast kinase Tpk2. (A) 11-mer peptides were synthesized on cellulose membranes. Peptides were first incubated with a non-kinase control protein purified from yeast and  $^{32}\text{P}$ -ATP to determine background from purification procedure. Peptides were then de-phosphorylated and incubated with purified kinase and  $^{32}\text{P}$ -ATP. (B) Signal from spots was quantified using Multi Gauge and the signal was normalized for background phosphorylation. Peptide selected for further investigation is indicated (\*).

**(A)****(B)**

Peptide Number	Peptide Sequence	Ratio of Signal Kinase:Control
14	MIRRRSTNYMD	442
15	IRRRSTNYMDA	183
30	PIFKNSYLDNN	90
34	PPQLGTRRKSS	13
35	GTRRKSSFKEYE	5
36	TRRKSSFKEYED	122

**Figure A.2**

**Figure A.3. Phosphorylation of select peptide substrates for yeast kinases.**

Potential peptide substrates for four additional kinases were phosphorylated more than three times greater than background in the presence of kinase. Graphs illustrate the ratio of specific:non-specific activity for (A) Rim11, (B) Ste11, (C) Cmk2, and (D) Sky1. The sequences for the selected peptides (\*) are shown in Table A.3.

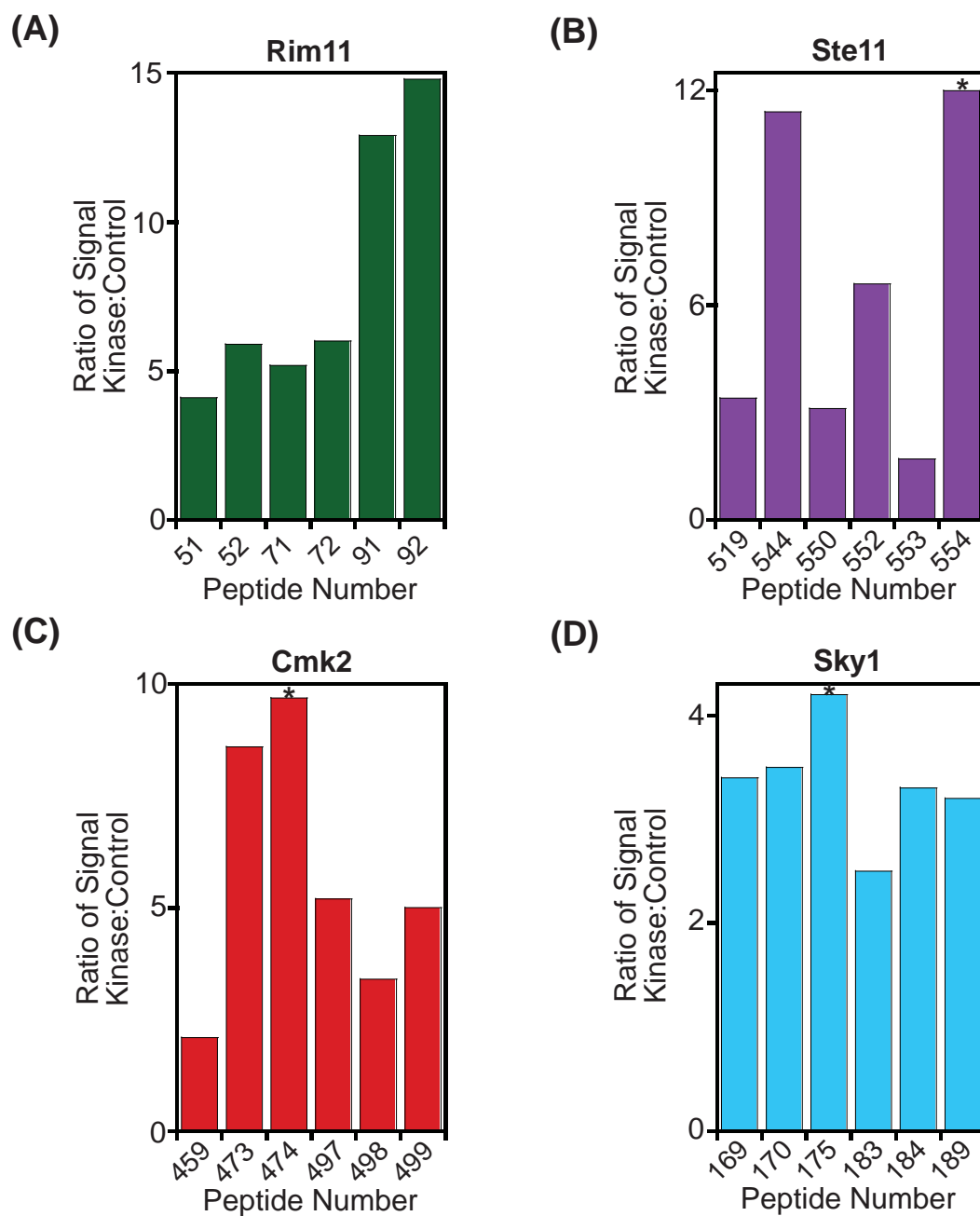


Figure A.3



Peptide substrates were identified for four kinases: Tpk2, Sky1, Cmk2, Ste11 (Table A.3).

A recent study used a rapid peptide screening approach to determine consensus phosphorylation site motifs for 61 out of 122 kinases in *S. cerevisiae* (185). Using these results, we generated ideal peptide substrates for Tpk2 and Cmk2 to complement our experimentally-derived peptides. We also tested a previously reported myelin basic protein (MBP) peptide for the kinase Kns1 (186) and a commercially available peptide sequence for Tpk2 (Promega). All peptides were synthesized with an N-terminal fluorophore, 5CF, followed by a 7 amino acid peptide solubility tag (109) to enhance peptide solubility.

Fluorescently-labeled peptides were incubated with purified kinases and  $^{32}\text{P}$ -ATP. Phosphorylation was measured by gel shift on Native-PAGE (Figure A.4). Unfortunately, we were not able to detect significant phosphorylation of any of our peptide substrates. One possibility is that our kinases require a co-factor for full activity that is not present. This is unlikely given that the purification was completed in the same manner for the initial peptide substrate identification. To test this possibility, we monitored peptide phosphorylation following incubation with yeast lysates over-expressing the kinase of interest. We are able to see a gel shift for 3 of the peptides when incubated with the lysates, however, the shift is larger than expected for a single phosphorylation event and

**Table A.3.** Potential peptide substrates for select *S. cerevisiae* kinases.

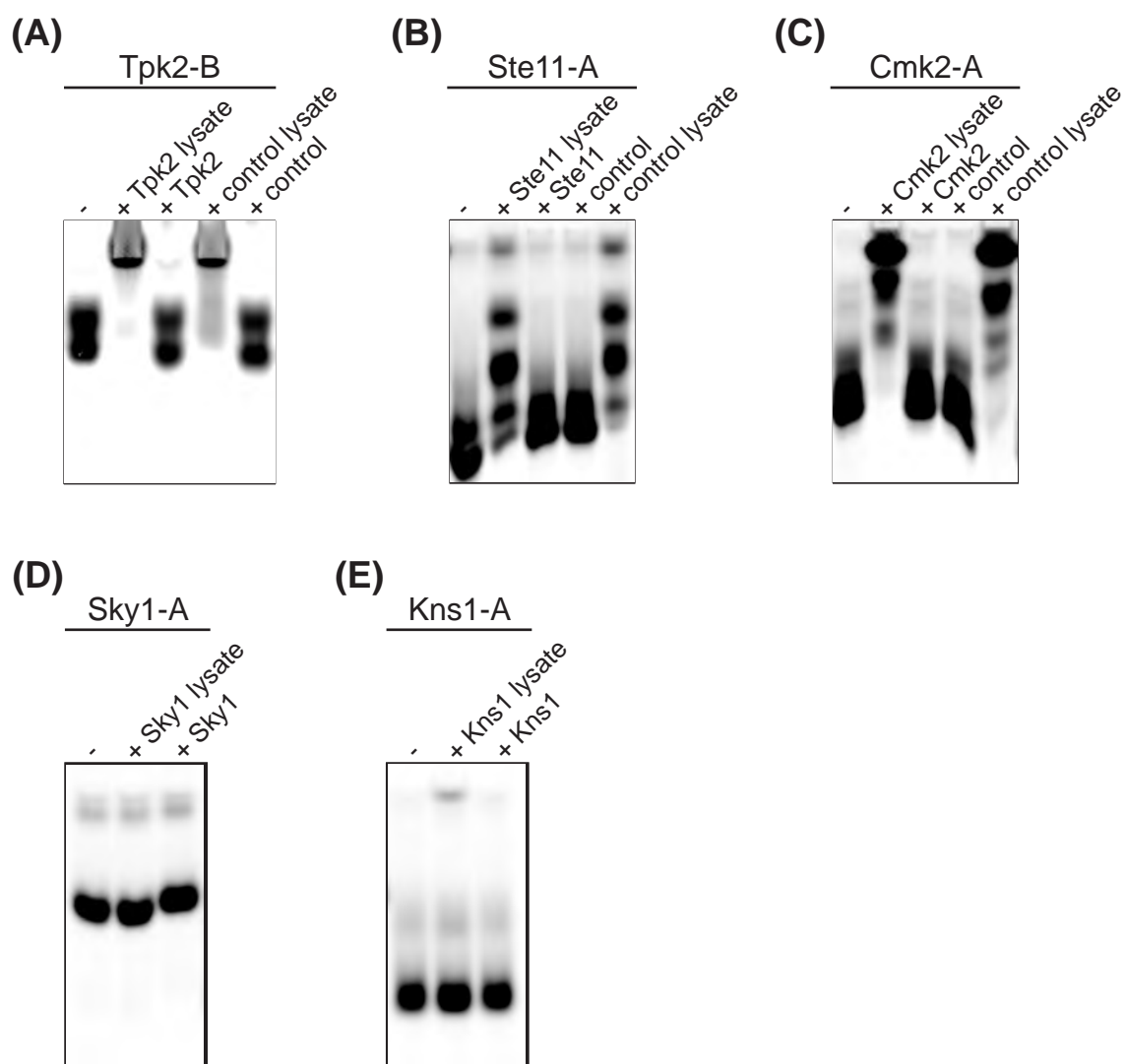
Kinase	Peptide Name	Peptide Sequence <sup>a</sup>	Peptide Source
Tpk2	Tpk2-A	5CF-NKKGRHGMIRRRSTNYMD	this work
Tpk2	Tpk2-B	5CF-NKKGRHGLRRASLG	Promega <sup>b</sup>
Tpk2	Tpk2-C	5CF-NKKGRHGRRRRPSQDDD	(185)
Cmk2	Cmk2-A	5CF-NKKGRHGKKLLDSKKKIA	this work
Cmk2	Cmk2-B	5CF-NKKGRHGLRRRRTFYYY	(185)
Sky1	Sky1-A	5CF-NKKGRHGADEDVSKKAKK	this work
Kns1	Kns1-A	5CF-NKKGRHGS GSPMARR	(186)

<sup>a</sup>Peptides have an N-terminal 7 amino acid solubility tag: NKKGRHG (109).

<sup>b</sup>Kemptide is a synthetic peptide substrate for cAMP-dependent protein kinase known to be phosphorylated by Tpk2 (75).

**Figure A.4. Example gel shift experiments to monitor peptide phosphorylation.**

Peptides were incubated alone, in the presence of yeast lysates or the in the presence of protein (kinase or control) purified from yeast lysates for 30-60 minutes at 30 °C then separated on 6 % Hepes/Imidazole Native gels. Peptides (A) Tpk2-B, (B) Ste11-A, and (C) Cmk2-A show reduced mobility in yeast lysates independent of kinase over-expression. Reduced mobility may indicate phosphorylation or degradation. Peptides (D) Sky1-A and (E) Kns1-A do not show any shift in the presence of kinase.

**Figure A.4**

not specific for over-expression of the kinase of interest (Figure A.4A,B&C). For Skyl and Kns1 peptide substrates, no shift was observed when incubated with purified kinase or yeast lysates (Figure A.4D&E).

## Discussion and Future Directions

Comparison of kinase steady-state levels identified potential Hsp90 client yeast kinases (Figure A.1A). Interestingly, all kinases tested accumulated at reduced levels in the absence of active Hsp90 suggesting a general regulatory role for Hsp90 in kinase stability. To explore this further, we plan to monitor changes in cellular accumulation of a known Hsp90 client kinase (v-src) and a non-Hsp90 client protein (SspB) to determine if this defect is specific to kinase clients or is the result of a general protein stability defect upon Hsp90 inactivation. However, the cellular levels of eight of the ten kinases tested were more than 50 % lower in the absence of active Hsp90 identifying them as potential Hsp90 client kinases.

Although numerous Hsp90 client kinases have been identified previously, there is little information available about the mechanism of kinase activation by Hsp90. Recent evidence suggests that kinases bind to Cdc37 and this complex then binds to Hsp90 (21, 24). But what happens once the Cdc37:kinase complex is bound to Hsp90? We propose a model where Hsp90 promotes the opening of the kinase structure to separate the regulatory domain from the kinase domain allowing activation of the kinase. To test this

model, we generated isolated kinase domain constructs and monitored changes in cellular accumulation upon Hsp90 inactivation (Figure A.1B). When compared to cellular levels of full-length kinases, we found that the accumulation of two isolated kinase domain constructs was less dependent on Hsp90 than the full-length kinases. These two kinase domain constructs, Sky1 and Cdc5, accumulate to a similar level as their full-length counterparts expressed in the presence of active Hsp90 even when Hsp90 is inactivated. This suggests these kinases may require Hsp90 to separate the regulatory domain from the kinase domain promoting activation and enhanced cellular stability.

To really understand the mechanism of kinase activation by Hsp90, we need to test kinase activity in the absence of active Hsp90 in addition to monitoring changes in cellular accumulation. Our initial attempts to identify peptide substrates for our panel of yeast kinases yielded peptide substrates for four kinases (Figure A.2). However, initial efforts to develop activity assays using these peptide substrates have been unsuccessful (Figure A.4). One possible explanation is that the substantial fraction of peptide required to observe a gel shift is not being phosphorylated whereas the experiments using  $^{32}\text{P}$ -ATP are more sensitive to smaller populations of phosphorylated peptide.

A possible explanation for the observed non-specific potential phosphorylation of the peptides is that they are being degraded during incubation in yeast lysates. Yeast lysates were prepared in the presence of the serine protease inhibitor PMSF but there are

many other proteases and peptidases present in yeast lysates. To test this, we obtained two additional peptides with C-terminal amide protecting groups. Combined with additional protease inhibitors, we hope that the degradation of the peptides will be reduced and the activity of the kinases can be assayed in yeast lysates.

In the event that kinase activity assays cannot be worked out with our peptide substrates, there are other potential activity assays that could be developed. One option would be to use a traditional non-specific kinase substrate such as MBP. Another option would be to purify the full-length substrate proteins and monitor phosphorylation when incubated with kinase and  $^{32}\text{P}$ -ATP.

With an activity assay for our kinases, we hope to be able to compare changes in cellular accumulation to changes in activity upon Hsp90 inactivation. By comparing full-length and isolated kinase domain constructs, we can hopefully gain more information about the mechanism of kinase activation by Hsp90.

## References

- (1) Ritossa, F. (1962) A new puffing pattern induced by temperature shock and DNP in drosophila. *Experientia* 18, 571-573.
- (2) McKenzie, S. L., Henikoff, S., and Meselson, M. (1975) Localization of RNA from heat-induced polysomes at puff sites in *Drosophila melanogaster*. *Proc Natl Acad Sci U S A* 72, 1117-21.
- (3) Lindquist, S. (1986) The heat-shock response. *Annu Rev Biochem* 55, 1151-91.
- (4) Borkovich, K. A., Farrelly, F.W., Finkelstein, D.B., Taulien, J., Lindquist, S. (1989) hsp82 Is an Essential Protein That Is Required in Higher Concentrations for Growth of Cells at Higher Temperatures. *Molecular and Cellular Biology* 9, 3919-3930.
- (5) Howson, R., Huh, W. K., Ghaemmaghami, S., Falvo, J. V., Bower, K., Belle, A., Dephoure, N., Wykoff, D. D., Weissman, J. S., and O'Shea, E. K. (2005) Construction, verification and experimental use of two epitope-tagged collections of budding yeast strains. *Comp Funct Genomics* 6, 2-16.
- (6) Bardwell, J. C., and Craig, E. A. (1988) Ancient heat shock gene is dispensable. *J Bacteriol* 170, 2977-83.
- (7) Picard, D., Khursheed, B., Garabedian, M. J., Fortin, M. G., Lindquist, S., and Yamamoto, K. R. (1990) Reduced levels of hsp90 compromise steroid receptor action in vivo. *Nature* 348, 166-8.
- (8) Zhao, R., Davey, M., Hsu, Y. C., Kaplanek, P., Tong, A., Parsons, A. B., Krogan, N., Cagney, G., Mai, D., Greenblatt, J., Boone, C., Emili, A., and Houry, W. A. (2005) Navigating the chaperone network: an integrative map of physical and genetic interactions mediated by the hsp90 chaperone. *Cell* 120, 715-27.
- (9) Prodromou, C., Roe, S.M., O'Brien, R., Ladbury, J.E., Piper, P.W., Pearl, L.H. (1997) Identification and Structural Characterization of the ATP/ADP-Binding Site in the Hsp90 Molecular Chaperone *Cell* 90, 65-75.
- (10) Ali, M. M., Roe, S. M., Vaughan, C. K., Meyer, P., Panaretou, B., Piper, P. W., Prodromou, C., and Pearl, L. H. (2006) Crystal structure of an Hsp90-nucleotide-p23/Sba1 closed chaperone complex. *Nature* 440, 1013-7.



- (11) Panaretou, B., Prodromou, C., Roe, S. M., O'Brien, R., Ladbury, J. E., Piper, P. W., and Pearl, L. H. (1998) ATP binding and hydrolysis are essential to the function of the Hsp90 molecular chaperone in vivo. *Embo J* 17, 4829-36.
- (12) Taipale, M., Jarosz, D. F., and Lindquist, S. (2010) HSP90 at the hub of protein homeostasis: emerging mechanistic insights. *Nat Rev Mol Cell Biol* 11, 515-28.
- (13) Johnson, B. D., Chadli, A., Felts, S.J., Bouhouche, I., Catelli, M.G., Toft, D.O. (2000) Hsp90 Chaperone Activity Requires the Full-length Protein and Interaction among Its Multiple Domains. *The Journal of Biological Chemistry* 275, 32499-32507.
- (14) Meyer, P., Prodromou, C., Hu, B., Vaughan, C., Roe, S. M., Panaretou, B., Piper, P. W., and Pearl, L. H. (2003) Structural and functional analysis of the middle segment of hsp90: implications for ATP hydrolysis and client protein and cochaperone interactions. *Mol Cell* 11, 647-58.
- (15) Minami, Y., Kimura, Y., Kawasaki, H., Suzuki, K., and Yahara, I. (1994) The carboxy-terminal region of mammalian HSP90 is required for its dimerization and function in vivo. *Mol Cell Biol* 14, 1459-64.
- (16) Prodromou, C., Panaretou, B., Chohan, S., Siligardi, G., O'Brien, R., Ladbury, J. E., Roe, S. M., Piper, P. W., and Pearl, L. H. (2000) The ATPase cycle of Hsp90 drives a molecular 'clamp' via transient dimerization of the N-terminal domains. *Embo J* 19, 4383-92.
- (17) Hessling, M., Richter, K., and Buchner, J. (2009) Dissection of the ATP-induced conformational cycle of the molecular chaperone Hsp90. *Nat Struct Mol Biol* 16, 287-93.
- (18) Ratzke, C., Mickler, M., Hellenkamp, B., Buchner, J., and Hugel, T. (2010) Dynamics of heat shock protein 90 C-terminal dimerization is an important part of its conformational cycle. *Proc Natl Acad Sci U S A* 107, 16101-6.
- (19) Southworth, D. R., and Agard, D. A. (2008) Species-dependent ensembles of conserved conformational states define the Hsp90 chaperone ATPase cycle. *Mol Cell* 32, 631-40.
- (20) Shiau, A. K., Harris, S. F., Southworth, D. R., and Agard, D. A. (2006) Structural Analysis of E. coli hsp90 reveals dramatic nucleotide-dependent conformational rearrangements. *Cell* 127, 329-40.

- (21) Vaughan, C. K., Gohlke, U., Sobott, F., Good, V. M., Ali, M. M., Prodromou, C., Robinson, C. V., Saibil, H. R., and Pearl, L. H. (2006) Structure of an Hsp90-Cdc37-Cdk4 complex. *Mol Cell* 23, 697-707.
- (22) Zhang, W., Hirshberg, M., McLaughlin, S. H., Lazar, G. A., Grossmann, J. G., Nielsen, P. R., Sobott, F., Robinson, C. V., Jackson, S. E., and Laue, E. D. (2004) Biochemical and structural studies of the interaction of Cdc37 with Hsp90. *J Mol Biol* 340, 891-907.
- (23) Panaretou, B., Siligardi, G., Meyer, P., Maloney, A., Sullivan, J. K., Singh, S., Millson, S. H., Clarke, P. A., Naaby-Hansen, S., Stein, R., Cramer, R., Mollapour, M., Workman, P., Piper, P. W., Pearl, L. H., and Prodromou, C. (2002) Activation of the ATPase activity of hsp90 by the stress-regulated cochaperone aha1. *Mol Cell* 10, 1307-18.
- (24) Roe, S. M., Ali, M. M., Meyer, P., Vaughan, C. K., Panaretou, B., Piper, P. W., Prodromou, C., and Pearl, L. H. (2004) The Mechanism of Hsp90 regulation by the protein kinase-specific cochaperone p50(cdc37). *Cell* 116, 87-98.
- (25) Trepel, J., Mollapour, M., Giaccone, G., and Neckers, L. (2010) Targeting the dynamic HSP90 complex in cancer. *Nat Rev Cancer* 10, 537-49.
- (26) Johnson, J. L., and Toft, D. O. (1995) Binding of p23 and hsp90 during assembly with the progesterone receptor. *Mol Endocrinol* 9, 670-8.
- (27) Fang, Y., Fliss, A. E., Rao, J., and Caplan, A. J. (1998) SBA1 encodes a yeast hsp90 cochaperone that is homologous to vertebrate p23 proteins. *Mol Cell Biol* 18, 3727-34.
- (28) Sullivan, W., Stensgard, B., Caucutt, G., Bartha, B., McMahon, N., Alnemri, E. S., Litwack, G., and Toft, D. (1997) Nucleotides and two functional states of hsp90. *J Biol Chem* 272, 8007-12.
- (29) McLaughlin, S. H., Smith, H. W., and Jackson, S. E. (2002) Stimulation of the weak ATPase activity of human hsp90 by a client protein. *J Mol Biol* 315, 787-98.
- (30) Richter, K., Walter, S., and Buchner, J. (2004) The Co-chaperone Sba1 connects the ATPase reaction of Hsp90 to the progression of the chaperone cycle. *J Mol Biol* 342, 1403-13.

- (31) Pratt, W. B., and Dittmar, K. D. (1998) Studies with Purified Chaperones Advance the Understanding of the Mechanism of Glucocorticoid Receptor-hsp90 Heterocomplex Assembly. *Trends Endocrinol Metab* 9, 244-52.
- (32) Young, J. C., and Hartl, F. U. (2000) Polypeptide release by Hsp90 involves ATP hydrolysis and is enhanced by the co-chaperone p23. *Embo J* 19, 5930-40.
- (33) Siligardi, G., Hu, B., Panaretou, B., Piper, P. W., Pearl, L. H., and Prodromou, C. (2004) Co-chaperone regulation of conformational switching in the Hsp90 ATPase cycle. *J Biol Chem* 279, 51989-98.
- (34) Prodromou, C., Siligardi, G., O'Brien, R., Woolfson, D. N., Regan, L., Panaretou, B., Ladbury, J. E., Piper, P. W., and Pearl, L. H. (1999) Regulation of Hsp90 ATPase activity by tetratricopeptide repeat (TPR)-domain co-chaperones. *Embo J* 18, 754-62.
- (35) Richter, K., Muschler, P., Hainzl, O., Reinstein, J., and Buchner, J. (2003) Sti1 is a non-competitive inhibitor of the Hsp90 ATPase. Binding prevents the N-terminal dimerization reaction during the atpase cycle. *J Biol Chem* 278, 10328-33.
- (36) Siligardi, G., Panaretou, B., Meyer, P., Singh, S., Woolfson, D. N., Piper, P. W., Pearl, L. H., and Prodromou, C. (2002) Regulation of Hsp90 ATPase activity by the co-chaperone Cdc37p/p50cdc37. *J Biol Chem* 277, 20151-9.
- (37) Lotz, G. P., Lin, H., Harst, A., and Obermann, W. M. (2003) Aha1 binds to the middle domain of Hsp90, contributes to client protein activation, and stimulates the ATPase activity of the molecular chaperone. *J Biol Chem* 278, 17228-35.
- (38) Meyer, P., Prodromou, C., Liao, C., Hu, B., Roe, S. M., Vaughan, C. K., Vlasic, I., Panaretou, B., Piper, P. W., and Pearl, L. H. (2004) Structural basis for recruitment of the ATPase activator Aha1 to the Hsp90 chaperone machinery. *Embo J* 23, 1402-10.
- (39) Vaughan, C. K., Neckers, L., and Piper, P. W. (2010) Understanding of the Hsp90 molecular chaperone reaches new heights. *Nat Struct Mol Biol* 17, 1400-4.
- (40) Li, J., Richter, K., and Buchner, J. (2011) Mixed Hsp90-cochaperone complexes are important for the progression of the reaction cycle. *Nat Struct Mol Biol* 18, 61-6.

- (41) Retzlaff, M., Hagn, F., Mitschke, L., Hessling, M., Gugel, F., Kessler, H., Richter, K., and Buchner, J. (2010) Asymmetric activation of the hsp90 dimer by its cochaperone aha1. *Mol Cell* 37, 344-54.
- (42) Whitesell, L., Mimnaugh, E. G., De Costa, B., Myers, C. E., and Neckers, L. M. (1994) Inhibition of heat shock protein HSP90-pp60v-src heteroprotein complex formation by benzoquinone ansamycins: essential role for stress proteins in oncogenic transformation. *Proc Natl Acad Sci U S A* 91, 8324-8.
- (43) Stebbins, C. E., Russo, A. A., Schneider, C., Rosen, N., Hartl, F. U., and Pavletich, N. P. (1997) Crystal structure of an Hsp90-geldanamycin complex: targeting of a protein chaperone by an antitumor agent. *Cell* 89, 239-50.
- (44) Whitesell, L., and Lindquist, S. L. (2005) Hsp90 and the Chaperoning of Cancer. *Nature Reviews* 5, 761-772.
- (45) Pratt, W. B., and Toft, D. O. (2003) Regulation of signaling protein function and trafficking by the hsp90/hsp70-based chaperone machinery. *Exp Biol Med (Maywood)* 228, 111-33.
- (46) Arlander, S. J., Felts, S. J., Wagner, J. M., Stensgard, B., Toft, D. O., and Karnitz, L. M. (2006) Chaperoning checkpoint kinase 1 (Chk1), an Hsp90 client, with purified chaperones. *J Biol Chem* 281, 2989-98.
- (47) Loo, M. A., Jensen, T. J., Cui, L., Hou, Y., Chang, X. B., and Riordan, J. R. (1998) Perturbation of Hsp90 interaction with nascent CFTR prevents its maturation and accelerates its degradation by the proteasome. *Embo J* 17, 6879-87.
- (48) Wang, X., Venable, J., LaPointe, P., Hutt, D. M., Koulov, A. V., Coppinger, J., Gurkan, C., Kellner, W., Matteson, J., Plutner, H., Riordan, J. R., Kelly, J. W., Yates, J. R., and Balch, W. E. (2006) Hsp90 Cochaperone Aha1 Downregulation Rescues Misfolding of CFTR in Cystic Fibrosis. *Cell* 127, 803-815.
- (49) Sun, F., Mi, Z., Condliffe, S. B., Bertrand, C. A., Gong, X., Lu, X., Zhang, R., Latoche, J. D., Pilewski, J. M., Robbins, P. D., and Frizzell, R. A. (2008) Chaperone displacement from mutant cystic fibrosis transmembrane conductance regulator restores its function in human airway epithelia. *Faseb J* 22, 3255-63.
- (50) Grandin, N., and Charbonneau, M. (2001) Hsp90 levels affect telomere length in yeast. *Mol Genet Genomics* 265, 126-34.

- (51) Binder, R. J., Blachere, N. E., and Srivastava, P. K. (2001) Heat shock protein-chaperoned peptides but not free peptides introduced into the cytosol are presented efficiently by major histocompatibility complex I molecules. *J Biol Chem* 276, 17163-71.
- (52) Rajagopal, D., Bal, V., Mayor, S., George, A., and Rath, S. (2006) A role for the Hsp90 molecular chaperone family in antigen presentation to T lymphocytes via major histocompatibility complex class II molecules. *Eur J Immunol* 36, 828-41.
- (53) Joab, I., Radanyi, C., Renoir, M., Buchou, T., Catelli, M. G., Binart, N., Mester, J., and Baulieu, E. E. (1984) Common non-hormone binding component in non-transformed chick oviduct receptors of four steroid hormones. *Nature* 308, 850-3.
- (54) Sanchez, E. R., Toft, D. O., Schlesinger, M. J., and Pratt, W. B. (1985) Evidence that the 90-kDa phosphoprotein associated with the untransformed L-cell glucocorticoid receptor is a murine heat shock protein. *J Biol Chem* 260, 12398-401.
- (55) Dalman, F. C., Koenig, R. J., Perdew, G. H., Massa, E., and Pratt, W. B. (1990) In contrast to the glucocorticoid receptor, the thyroid hormone receptor is translated in the DNA binding state and is not associated with hsp90. *J Biol Chem* 265, 3615-8.
- (56) Dalman, F. C., Sturzenbecker, L. J., Levin, A. A., Lucas, D. A., Perdew, G. H., Petkovitch, M., Chambon, P., Grippo, J. F., and Pratt, W. B. (1991) Retinoic acid receptor belongs to a subclass of nuclear receptors that do not form "docking" complexes with hsp90. *Biochemistry* 30, 5605-8.
- (57) Redeuilh, G., Moncharmont, B., Secco, C., and Baulieu, E. E. (1987) Subunit composition of the molybdate-stabilized "8-9 S" nontransformed estradiol receptor purified from calf uterus. *J Biol Chem* 262, 6969-75.
- (58) Veldscholte, J., Berrevoets, C. A., Zegers, N. D., van der Kwast, T. H., Grootegeed, J. A., and Mulder, E. (1992) Hormone-induced dissociation of the androgen receptor-heat-shock protein complex: use of a new monoclonal antibody to distinguish transformed from nontransformed receptors. *Biochemistry* 31, 7422-30.
- (59) Denis, M., Wikstrom, A. C., and Gustafsson, J. A. (1987) The molybdate-stabilized nonactivated glucocorticoid receptor contains a dimer of Mr 90,000 non-hormone-binding protein. *J Biol Chem* 262, 11803-6.

- (60) Smith, D. F., Schowalter, D. B., Kost, S. L., and Toft, D. O. (1990) Reconstitution of progesterone receptor with heat shock proteins. *Mol Endocrinol* 4, 1704-11.
- (61) Smith, D. F., and Toft, D. O. (1992) Composition, assembly and activation of the avian progesterone receptor. *J Steroid Biochem Mol Biol* 41, 201-7.
- (62) Kosano, H., Stensgard, B., Charlesworth, M. C., McMahon, N., and Toft, D. (1998) The assembly of progesterone receptor-hsp90 complexes using purified proteins. *J Biol Chem* 273, 32973-9.
- (63) Wagner, R. L., Apriletti, J. W., McGrath, M. E., West, B. L., Baxter, J. D., and Fletterick, R. J. (1995) A structural role for hormone in the thyroid hormone receptor. *Nature* 378, 690-7.
- (64) Williams, S. P., and Sigler, P. B. (1998) Atomic structure of progesterone complexed with its receptor. *Nature* 393, 392-6.
- (65) Stancato, L. F., Silverstein, A. M., Gitler, C., Groner, B., and Pratt, W. B. (1996) Use of the thiol-specific derivatizing agent N-iodoacetyl-3-[125I]iodotyrosine to demonstrate conformational differences between the unbound and hsp90-bound glucocorticoid receptor hormone binding domain. *J Biol Chem* 271, 8831-6.
- (66) Grenert, J. P., Johnson, B. D., and Toft, D. O. (1999) The importance of ATP binding and hydrolysis by hsp90 in formation and function of protein heterocomplexes. *J Biol Chem* 274, 17525-33.
- (67) Brugge, J. S., Erikson, E., and Erikson, R. L. (1981) The specific interaction of the Rous sarcoma virus transforming protein, pp60src, with two cellular proteins. *Cell* 25, 363-72.
- (68) An, W. G., Schulte, T. W., and Neckers, L. M. (2000) The heat shock protein 90 antagonist geldanamycin alters chaperone association with p210bcr-abl and v-src proteins before their degradation by the proteasome. *Cell Growth Differ* 11, 355-60.
- (69) Reed, S. I. (1980) The selection of *S. cerevisiae* mutants defective in the start event of cell division. *Genetics* 95, 561-77.
- (70) Dey, B., Lightbody, J. J., and Boschelli, F. (1996) CDC37 is required for p60v-src activity in yeast. *Mol Biol Cell* 7, 1405-17.

- (71) Xu, Y., and Lindquist, S. (1993) Heat-shock protein hsp90 governs the activity of pp60v-src kinase. *Proc Natl Acad Sci U S A* 90, 7074-8.
- (72) Cutforth, T., and Rubin, G. M. (1994) Mutations in Hsp83 and cdc37 impair signaling by the sevenless receptor tyrosine kinase in *Drosophila*. *Cell* 77, 1027-36.
- (73) Dai, K., Kobayashi, R., and Beach, D. (1996) Physical interaction of mammalian CDC37 with CDK4. *J Biol Chem* 271, 22030-4.
- (74) Citri, A., Harari, D., Shohat, G., Ramakrishnan, P., Gan, J., Lavi, S., Eisenstein, M., Kimchi, A., Wallach, D., Pietrokovski, S., and Yarden, Y. (2006) Hsp90 recognizes a common surface on client kinases. *J Biol Chem* 281, 14361-9.
- (75) Mandal, A. K., Lee, P., Chen, J. A., Nillegoda, N., Heller, A., DiStasio, S., Oen, H., Victor, J., Nair, D. M., Brodsky, J. L., and Caplan, A. J. (2007) Cdc37 has distinct roles in protein kinase quality control that protect nascent chains from degradation and promote posttranslational maturation. *J Cell Biol* 176, 319-28.
- (76) Dittmar, K. D., Banach, M., Galigniana, M. D., and Pratt, W. B. (1998) The role of DnaJ-like proteins in glucocorticoid receptor.hsp90 heterocomplex assembly by the reconstituted hsp90.p60.hsp70 foldosome complex. *J Biol Chem* 273, 7358-66.
- (77) Holt, S. E., Aisner, D. L., Baur, J., Tesmer, V. M., Dy, M., Ouellette, M., Trager, J. B., Morin, G. B., Toft, D. O., Shay, J. W., Wright, W. E., and White, M. A. (1999) Functional requirement of p23 and Hsp90 in telomerase complexes. *Genes Dev* 13, 817-26.
- (78) DeZwaan, D. C., Toogun, O. A., Echtenkamp, F. J., and Freeman, B. C. (2009) The Hsp82 molecular chaperone promotes a switch between unextendable and extendable telomere states. *Nat Struct Mol Biol* 16, 711-6.
- (79) Toogun, O. A., Dezwaan, D. C., and Freeman, B. C. (2008) The hsp90 molecular chaperone modulates multiple telomerase activities. *Mol Cell Biol* 28, 457-67.
- (80) Prehn, R. T., and Main, J. M. (1957) Immunity to methylcholanthrene-induced sarcomas. *J Natl Cancer Inst* 18, 769-78.
- (81) DuBois, G. C., Law, L. W., and Appella, E. (1982) Purification and biochemical properties of tumor-associated transplantation antigens from methylcholanthrene-induced murine sarcomas. *Proc Natl Acad Sci U S A* 79, 7669-73.

- (82) Srivastava, P. K., DeLeo, A. B., and Old, L. J. (1986) Tumor rejection antigens of chemically induced sarcomas of inbred mice. *Proc Natl Acad Sci U S A* 83, 3407-11.
- (83) Riordan, J. R. (2005) Assembly of functional CFTR chloride channels. *Annu Rev Physiol* 67, 701-18.
- (84) Nathan, D. F., Vos, M. H., and Lindquist, S. (1997) In vivo functions of the *Saccharomyces cerevisiae* Hsp90 chaperone. *Proc Natl Acad Sci U S A* 94, 12949-56.
- (85) Jakob, U., Lilie, H., Meyer, I., and Buchner, J. (1995) Transient interaction of Hsp90 with early unfolding intermediates of citrate synthase. Implications for heat shock in vivo. *J Biol Chem* 270, 7288-94.
- (86) Evans, C. G., Wisen, S., and Gestwicki, J. E. (2006) Heat shock proteins 70 and 90 inhibit early stages of amyloid beta-(1-42) aggregation in vitro. *J Biol Chem* 281, 33182-91.
- (87) Muller, L., Schaupp, A., Walerych, D., Wegele, H., and Buchner, J. (2004) Hsp90 regulates the activity of wild type p53 under physiological and elevated temperatures. *J Biol Chem* 279, 48846-54.
- (88) Youker, R. T., Walsh, P., Beilharz, T., Lithgow, T., and Brodsky, J. L. (2004) Distinct roles for the Hsp40 and Hsp90 molecular chaperones during cystic fibrosis transmembrane conductance regulator degradation in yeast. *Mol Biol Cell* 15, 4787-97.
- (89) Wiech, H., Buchner, J., Zimmermann, R., and Jakob, U. (1992) Hsp90 chaperones protein folding in vitro. *Nature* 358, 169-70.
- (90) Yonehara, M., Minami, Y., Kawata, Y., Nagai, J., and Yahara, I. (1996) Heat-induced chaperone activity of HSP90. *J Biol Chem* 271, 2641-5.
- (91) Pratt, W. B., and Toft, D. O. (1997) Steroid receptor interactions with heat shock protein and immunophilin chaperones. *Endocr Rev* 18, 306-60.
- (92) Murata, S., Chiba, T., and Tanaka, K. (2003) CHIP: a quality-control E3 ligase collaborating with molecular chaperones. *Int J Biochem Cell Biol* 35, 572-8.



- (93) Richter, K., and Buchner, J. (2001) Hsp90: chaperoning signal transduction. *J Cell Physiol* 188, 281-90.
- (94) Louvion, J. F., Warth, R., and Picard, D. (1996) Two eukaryote-specific regions of Hsp82 are dispensable for its viability and signal transduction functions in yeast. *Proc Natl Acad Sci U S A* 93, 13937-42.
- (95) Wegele, H., Muschler, P., Bunck, M., Reinstein, J., and Buchner, J. (2003) Dissection of the contribution of individual domains to the ATPase mechanism of Hsp90. *J Biol Chem* 278, 39303-10.
- (96) Obermann, W. M., Sonderrmann, H., Russo, A. A., Pavletich, N. P., and Hartl, F. U. (1998) In vivo function of Hsp90 is dependent on ATP binding and ATP hydrolysis. *J Cell Biol* 143, 901-10.
- (97) Zhang, Y., Howitt, J., McCorkle, S., Lawrence, P., Springer, K., and Freimuth, P. (2004) Protein aggregation during overexpression limited by peptide extensions with large net negative charge. *Protein Expression and Purification* 36, 207-216.
- (98) Havranek, J. J., and Harbury, P. B. (2003) Automated design of specificity in molecular recognition. *Nat Struct Biol* 10, 45-52.
- (99) Zhu, H., Klemic, J. F., Chang, S., Bertone, P., Casamayor, A., Klemic, K. G., Smith, D., Gerstein, M., Reed, M. A., and Snyder, M. (2000) Analysis of yeast protein kinases using protein chips. *Nat Genet* 26, 283-9.
- (100) Bowie, J. U., and Sauer, R. T. (1989) Equilibrium dissociation and unfolding of the Arc repressor dimer. *Biochemistry* 28, 7139-43.
- (101) Santoro, M. M., and Bolen, D. W. (1988) Unfolding free energy changes determined by the linear extrapolation method. 1. Unfolding of phenylmethanesulfonyl alpha-chymotrypsin using different denaturants. *Biochemistry* 27, 8063-8.
- (102) Cantor, C. R., and Schimmel, P. R. (1980) *Biophysical Chemistry*, W. H. Freeman and Company, New York, NY.
- (103) Norby, J. G. (1988) Coupled assay of Na<sup>+</sup>,K<sup>+</sup>-ATPase activity. *Methods Enzymol* 156, 116-9.

- (104) Llauger-Bufi, L., Felts, S. J., Huezo, H., Rosen, N., and Chiosis, G. (2003) Synthesis of novel fluorescent probes for the molecular chaperone Hsp90. *Bioorg Med Chem Lett* 13, 3975-8.
- (105) Lakowicz, J. R. (1999) *Principles of Fluorescence Spectroscopy*, Second ed., Kluwer Academic/Plenum Publishers, Boston, MA.
- (106) Maroney, A. C., Marugan, J. J., Mezzasalma, T. M., Barnakov, A. N., Garrabrant, T. A., Weaner, L. E., Jones, W. J., Barnakova, L. A., Koblish, H. K., Todd, M. J., Masucci, J. A., Deckman, I. C., Galembo, R. A., Jr., and Johnson, D. L. (2006) Dihydroquinone ansamycins: toward resolving the conflict between low in vitro affinity and high cellular potency of geldanamycin derivatives. *Biochemistry* 45, 5678-85.
- (107) Nathan, D. F., Lindquist, S. (1995) Mutation analysis of Hsp90 function: interactions with a steroid receptor and a protein kinase. *Molecular and Cellular Biology* 15, 3917-3925.
- (108) Mumberg, D., Muller, R., and Funk, M. (1995) Yeast vectors for the controlled expression of heterologous proteins in different genetic backgrounds. *Gene* 156, 119-22.
- (109) Wah, D. A., Levchenko, I., Baker, T. A., and Sauer, R. T. (2002) Characterization of a specificity factor for an AAA+ ATPase: assembly of SspB dimers with ssrA-tagged proteins and the ClpX hexamer. *Chem Biol* 9, 1237-45.
- (110) Wayne, N., Lai, Y., Pullen, L., and Bolon, D. N. (2010) Modular control of cross-oligomerization: analysis of superstabilized Hsp90 homodimers in vivo. *J Biol Chem* 285, 234-41.
- (111) Bornberg-Bauer, E., and Chan, H. S. (1999) Modeling evolutionary landscapes: mutational stability, topology, and superfunnels in sequence space. *Proc Natl Acad Sci U S A* 96, 10689-94.
- (112) Robinson, C. R., and Sauer, R. T. (1998) Optimizing the stability of single-chain proteins by linker length and composition mutagenesis. *Proc Natl Acad Sci U S A* 95, 5929-34.
- (113) Martin, A., Baker, T. A., and Sauer, R. T. (2005) Rebuilt AAA + motors reveal operating principles for ATP-fuelled machines. *Nature* 437, 1115-20.

- (114) Plescia, J., Salz, W., Xia, F., Pennati, M., Zaffaroni, N., Daidone, M. G., Meli, M., Dohi, T., Fortugno, P., Nefedova, Y., Gabrilovich, D. I., Colombo, G., and Altieri, D. C. (2005) Rational design of shepherdin, a novel anticancer agent. *Cancer Cell* 7, 457-68.
- (115) Birnby, D. A., Link, E. M., Vowels, J. J., Tian, H., Colacurcio, P. L., and Thomas, J. H. (2000) A transmembrane guanylyl cyclase (DAF-11) and Hsp90 (DAF-21) regulate a common set of chemosensory behaviors in *Caenorhabditis elegans*. *Genetics* 155, 85-104.
- (116) Kimura, Y., Rutherford, S. L., Miyata, Y., Yahara, I., Freeman, B. C., Yue, L., Morimoto, R. I., and Lindquist, S. (1997) Cdc37 is a molecular chaperone with specific functions in signal transduction. *Genes Dev* 11, 1775-85.
- (117) Chang, H. C., and Lindquist, S. (1994) Conservation of Hsp90 macromolecular complexes in *Saccharomyces cerevisiae*. *J Biol Chem* 269, 24983-8.
- (118) Johnston, G. C., Ehrhardt, C.W., Lorincz, A., Carter, B.L.A. (1979) Regulation of Cell Size in the Yeast *Saccharomyces cerevisiae*. *Journal of Bacteriology* 137, 1-5.
- (119) Larabell, C. A. a. L. G., M.A. (2004) X-ray Tomography Generates 3-D Reconstructions of the Yeast, *Saccharomyces cerevisiae*, at 60-nm Resolution. *Molecular Biology of the Cell* 15, 957-962.
- (120) Choi, S. I., Han, K. S., Kim, C. W., Ryu, K. S., Kim, B. H., Kim, K. H., Kim, S. I., Kang, T. H., Shin, H. C., Lim, K. H., Kim, H. K., Hyun, J. M., and Seong, B. L. (2008) Protein solubility and folding enhancement by interaction with RNA. *PLoS One* 3, e2677.
- (121) Bolon, D. N., Wah, D. A., Hersch, G. L., Baker, T. A., and Sauer, R. T. (2004) Bivalent tethering of SspB to ClpXP is required for efficient substrate delivery: a protein-design study. *Mol Cell* 13, 443-9.
- (122) Nemoto, T., Ohara-Nemoto, Y., Ota, M., Takagi, T., and Yokoyama, K. (1995) Mechanism of dimer formation of the 90-kDa heat-shock protein. *Eur J Biochem* 233, 1-8.
- (123) Riggs, D. L., Cox, M. B., Tardif, H. L., Hessling, M., Buchner, J., and Smith, D. F. (2007) Noncatalytic role of the FKBP52 peptidyl-prolyl isomerase domain in the regulation of steroid hormone signaling. *Mol Cell Biol* 27, 8658-69.

- (124) Wandinger, S. K., Richter, K., and Buchner, J. (2008) The Hsp90 chaperone machinery. *J Biol Chem* 283, 18473-7.
- (125) Bolon, D. N., Grant, R. A., Baker, T. A., and Sauer, R. T. (2005) Specificity versus stability in computational protein design. *Proc Natl Acad Sci U S A* 102, 12724-9.
- (126) Wayne, N., and Bolon, D. N. (2007) Dimerization of Hsp90 is required for in vivo function. Design and analysis of monomers and dimers. *J Biol Chem* 282, 35386-95.
- (127) Floer, M., Bryant, G. O., and Ptashne, M. (2008) HSP90/70 chaperones are required for rapid nucleosome removal upon induction of the GAL genes of yeast. *Proc Natl Acad Sci U S A* 105, 2975-80.
- (128) Wu, Y., Vadrevu, R., Kathuria, S., Yang, X., and Matthews, C. R. (2007) A tightly packed hydrophobic cluster directs the formation of an off-pathway sub-millisecond folding intermediate in the alpha subunit of tryptophan synthase, a TIM barrel protein. *J Mol Biol* 366, 1624-38.
- (129) Kathuria, S. V., Day, I. J., Wallace, L. A., and Matthews, C. R. (2008) Kinetic traps in the folding of beta alpha-repeat proteins: CheY initially misfolds before accessing the native conformation. *J Mol Biol* 382, 467-84.
- (130) Krukenberg, K. A., Forster, F., Rice, L. M., Sali, A., and Agard, D. A. (2008) Multiple conformations of E. coli Hsp90 in solution: insights into the conformational dynamics of Hsp90. *Structure* 16, 755-65.
- (131) Pratt, W. B., Morishima, Y., Murphy, M., and Harrell, M. (2006) Chaperoning of glucocorticoid receptors. *Handb Exp Pharmacol*, 111-38.
- (132) DeLano, W. L., and Brunger, A. T. (1994) Helix packing in proteins: prediction and energetic analysis of dimeric, trimeric, and tetrameric GCN4 coiled coil structures. *Proteins* 20, 105-23.
- (133) Ozbek, S., Engel, J., and Stetefeld, J. (2002) Storage function of cartilage oligomeric matrix protein: the crystal structure of the coiled-coil domain in complex with vitamin D(3). *Embo J* 21, 5960-8.
- (134) Ross, C. A., and Poirier, M. A. (2004) Protein aggregation and neurodegenerative disease. *Nat Med* 10 Suppl, S10-7.

- (135) Powers, E. T., Morimoto, R. I., Dillin, A., Kelly, J. W., and Balch, W. E. (2009) Biological and chemical approaches to diseases of proteostasis deficiency. *Annu Rev Biochem* 78, 959-91.
- (136) Chaudhuri, T. K., and Paul, S. (2006) Protein-misfolding diseases and chaperone-based therapeutic approaches. *Febs J* 273, 1331-49.
- (137) Gao, X., and Hu, H. (2008) Quality control of the proteins associated with neurodegenerative diseases. *Acta Biochim Biophys Sin (Shanghai)* 40, 612-8.
- (138) Chiti, F., and Dobson, C. M. (2006) Protein misfolding, functional amyloid, and human disease. *Annu Rev Biochem* 75, 333-66.
- (139) Gregersen, N., Bolund, L., and Bross, P. (2005) Protein misfolding, aggregation, and degradation in disease. *Mol Biotechnol* 31, 141-50.
- (140) Dill, K. A. (1990) Dominant forces in protein folding. *Biochemistry* 29, 7133-55.
- (141) Dobson, C. M. (2004) Principles of protein folding, misfolding and aggregation. *Semin Cell Dev Biol* 15, 3-16.
- (142) Schmittschmitt, J. P., and Scholtz, J. M. (2003) The role of protein stability, solubility, and net charge in amyloid fibril formation. *Protein Sci* 12, 2374-8.
- (143) Lawrence, M. S., Phillips, K. J., and Liu, D. R. (2007) Supercharging proteins can impart unusual resilience. *J Am Chem Soc* 129, 10110-2.
- (144) Hartl, F. U., and Hayer-Hartl, M. (2009) Converging concepts of protein folding in vitro and in vivo. *Nat Struct Mol Biol* 16, 574-81.
- (145) Liberek, K., Lewandowska, A., and Zietkiewicz, S. (2008) Chaperones in control of protein disaggregation. *Embo J* 27, 328-35.
- (146) Lee, S., and Tsai, F. T. (2005) Molecular chaperones in protein quality control. *J Biochem Mol Biol* 38, 259-65.
- (147) Young, J. C., Agashe, V. R., Siegers, K., and Hartl, F. U. (2004) Pathways of chaperone-mediated protein folding in the cytosol. *Nat Rev Mol Cell Biol* 5, 781-91.

- (148) Feder, M. E., and Hofmann, G. E. (1999) Heat-shock proteins, molecular chaperones, and the stress response: evolutionary and ecological physiology. *Annu Rev Physiol* 61, 243-82.
- (149) Xu, Z., Horwich, A. L., and Sigler, P. B. (1997) The crystal structure of the asymmetric GroEL-GroES-(ADP)<sub>7</sub> chaperonin complex. *Nature* 388, 741-50.
- (150) Sigler, P. B., Xu, Z., Rye, H. S., Burston, S. G., Fenton, W. A., and Horwich, A. L. (1998) Structure and function in GroEL-mediated protein folding. *Annu Rev Biochem* 67, 581-608.
- (151) Pearl, L. H., and Prodromou, C. (2006) Structure and mechanism of the Hsp90 molecular chaperone machinery. *Annu Rev Biochem* 75, 271-94.
- (152) Mayer, M. P., and Bukau, B. (2005) Hsp70 chaperones: cellular functions and molecular mechanism. *Cell Mol Life Sci* 62, 670-84.
- (153) Kumsta, C., and Jakob, U. (2009) Redox-regulated chaperones. *Biochemistry* 48, 4666-76.
- (154) Scheibel, T., and Buchner, J. (1998) The Hsp90 Complex - A Super-Chaperone Machine as a Novel Drug Target. *Biochemical Pharmacology* 56, 675-682.
- (155) Freeman, B. C., and Morimoto, R. I. (1996) The human cytosolic molecular chaperones hsp90, hsp70 (hsc70) and hsc70 have distinct roles in recognition of a non-native protein and protein refolding. *Embo J* 15, 2969-79.
- (156) Hainzl, O., Lapina, M. C., Buchner, J., and Richter, K. (2009) The charged linker region is an important regulator of Hsp90 function. *J Biol Chem*.
- (157) Gasteiger, E., Gattiker, A., Hoogland, C., Ivanyi, I., Appel, R. D., and Bairoch, A. (2003) ExPASy: The proteomics server for in-depth protein knowledge and analysis. *Nucleic Acids Res* 31, 3784-8.
- (158) Qu, B. H., and Thomas, P. J. (1996) Alteration of the cystic fibrosis transmembrane conductance regulator folding pathway. *J Biol Chem* 271, 7261-4.
- (159) Scheibel, T., Siegmund, H.I., Jaenicke, R., Ganz, P., Lilie, H., Buchner, J. (1999) The charged region of Hsp90 modulates the function of the N-terminal domain. *Proc. Natl. Acad. Sci.* 96, 1297-1302.

- (160) Tsutsumi, S., Mollapour, M., Graf, C., Lee, C. T., Scroggins, B. T., Xu, W., Haslerova, L., Hessling, M., Konstantinova, A. A., Trepel, J. B., Panaretou, B., Buchner, J., Mayer, M. P., Prodromou, C., and Neckers, L. (2009) Hsp90 charged-linker truncation reverses the functional consequences of weakened hydrophobic contacts in the N domain. *Nat Struct Mol Biol* 16, 1141-7.
- (161) Bardwell, J. C., and Craig, E. A. (1987) Eukaryotic Mr 83,000 heat shock protein has a homologue in Escherichia coli. *Proc Natl Acad Sci U S A* 84, 5177-81.
- (162) Wayne, N., and Bolon, D. N. (2010) Charge-rich regions modulate the anti-aggregation activity of Hsp90. *J Mol Biol* 401, 931-9.
- (163) Mosser, D. D., and Morimoto, R. I. (2004) Molecular chaperones and the stress of oncogenesis. *Oncogene* 23, 2907-18.
- (164) Easton, D. P., Kaneko, Y., and Subject, J. R. (2000) The hsp110 and Grp1 70 stress proteins: newly recognized relatives of the Hsp70s. *Cell Stress Chaperones* 5, 276-90.
- (165) Levin, D. E. (2005) Cell wall integrity signaling in Saccharomyces cerevisiae. *Microbiol Mol Biol Rev* 69, 262-91.
- (166) Millson, S. H., Truman, A. W., King, V., Prodromou, C., Pearl, L. H., and Piper, P. W. (2005) A two-hybrid screen of the yeast proteome for Hsp90 interactors uncovers a novel Hsp90 chaperone requirement in the activity of a stress-activated mitogen-activated protein kinase, Slt2p (Mpk1p). *Eukaryot Cell* 4, 849-60.
- (167) Werner-Washburne, M., Stone, D.E., Craig, E.A. (1987) Complex Interactions among Members of an Essential Subfamily of hsp70 Genes in Saccharomyces cerevisiae. *Molecular and Cellular Biology* 7, 2568-2577.
- (168) Liu, X. D., Morano, K. A., and Thiele, D. J. (1999) The yeast Hsp110 family member, Sse1, is an Hsp90 cochaperone. *J Biol Chem* 274, 26654-60.
- (169) Shaner, L., Trott, A., Goeckeler, J. L., Brodsky, J. L., and Morano, K. A. (2004) The function of the yeast molecular chaperone Sse1 is mechanistically distinct from the closely related hsp70 family. *J Biol Chem* 279, 21992-2001.
- (170) Mukai, H., Kuno, T., Tanaka, H., Hirata, D., Miyakawa, T., and Tanaka, C. (1993) Isolation and characterization of SSE1 and SSE2, new members of the yeast HSP70 multigene family. *Gene* 132, 57-66.

- (171) Caplan, A. J., and Douglas, M. G. (1991) Characterization of YDJ1: a yeast homologue of the bacterial dnaJ protein. *J Cell Biol* 114, 609-21.
- (172) Fan, C. Y., Ren, H. Y., Lee, P., Caplan, A. J., and Cyr, D. M. (2005) The type I Hsp40 zinc finger-like region is required for Hsp70 to capture non-native polypeptides from Ydj1. *J Biol Chem* 280, 695-702.
- (173) Brennan, R. J., and Schiestl, R. H. (1996) Cadmium is an inducer of oxidative stress in yeast. *Mutat Res* 356, 171-8.
- (174) Chen, J. M., Cutler, C., Jacques, C., Boeuf, G., Denamur, E., Lecointre, G., Mercier, B., Cramb, G., and Ferec, C. (2001) A combined analysis of the cystic fibrosis transmembrane conductance regulator: implications for structure and disease models. *Mol Biol Evol* 18, 1771-88.
- (175) Kashlan, O. B., Mueller, G. M., Qamar, M. Z., Poland, P. A., Ahner, A., Rubenstein, R. C., Hughey, R. P., Brodsky, J. L., and Kleyman, T. R. (2007) Small heat shock protein alphaA-crystallin regulates epithelial sodium channel expression. *J Biol Chem* 282, 28149-56.
- (176) Jakob, U. (1996) HSP90--news from the front. *Front Biosci* 1, d309-17.
- (177) Xu, Y., Singer, M. A., and Lindquist, S. (1999) Maturation of the tyrosine kinase c-src as a kinase and as a substrate depends on the molecular chaperone Hsp90. *Proc Natl Acad Sci U S A* 96, 109-14.
- (178) Basso, A. D., Solit, D. B., Chiosis, G., Giri, B., Tsiichlis, P., and Rosen, N. (2002) Akt forms an intracellular complex with heat shock protein 90 (Hsp90) and Cdc37 and is destabilized by inhibitors of Hsp90 function. *J Biol Chem* 277, 39858-66.
- (179) Xu, W., Mimnaugh, E., Rosser, M. F., Nicchitta, C., Marcu, M., Yarden, Y., and Neckers, L. (2001) Sensitivity of mature ErbB2 to geldanamycin is conferred by its kinase domain and is mediated by the chaperone protein Hsp90. *J Biol Chem* 276, 3702-8.
- (180) Citri, A., Alroy, I., Lavi, S., Rubin, C., Xu, W., Grammatikakis, N., Patterson, C., Neckers, L., Fry, D. W., and Yarden, Y. (2002) Drug-induced ubiquitylation and degradation of ErbB receptor tyrosine kinases: implications for cancer therapy. *Embo J* 21, 2407-17.



- (181) Pratt, W. B., Morishima, Y., and Osawa, Y. (2008) The Hsp90 chaperone machinery regulates signaling by modulating ligand binding clefts. *J Biol Chem* 283, 22885-9.
- (182) Grad, I., and Picard, D. (2007) The glucocorticoid responses are shaped by molecular chaperones. *Mol Cell Endocrinol* 275, 2-12.
- (183) Engen, J. R., Wales, T. E., Hochrein, J. M., Meyn, M. A., 3rd, Banu Ozkan, S., Bahar, I., and Smithgall, T. E. (2008) Structure and dynamic regulation of Src-family kinases. *Cell Mol Life Sci* 65, 3058-73.
- (184) Ptacek, J., Devgan, G., Michaud, G., Zhu, H., Zhu, X., Fasolo, J., Guo, H., Jona, G., Breitkreutz, A., Sopko, R., McCartney, R. R., Schmidt, M. C., Rachidi, N., Lee, S. J., Mah, A. S., Meng, L., Stark, M. J., Stern, D. F., De Virgilio, C., Tyers, M., Andrews, B., Gerstein, M., Schweitzer, B., Predki, P. F., and Snyder, M. (2005) Global analysis of protein phosphorylation in yeast. *Nature* 438, 679-84.
- (185) Mok, J., Kim, P. M., Lam, H. Y., Piccirillo, S., Zhou, X., Jeschke, G. R., Sheridan, D. L., Parker, S. A., Desai, V., Jwa, M., Cameroni, E., Niu, H., Good, M., Remenyi, A., Ma, J. L., Sheu, Y. J., Sassi, H. E., Sopko, R., Chan, C. S., De Virgilio, C., Hollingsworth, N. M., Lim, W. A., Stern, D. F., Stillman, B., Andrews, B. J., Gerstein, M. B., Snyder, M., and Turk, B. E. Deciphering protein kinase specificity through large-scale analysis of yeast phosphorylation site motifs. *Sci Signal* 3, ra12.
- (186) Lee, K., Du, C., Horn, M., and Rabinow, L. (1996) Activity and autophosphorylation of LAMMER protein kinases. *J Biol Chem* 271, 27299-303.